

Aus dem Biomedizinischen Centrum  
Lehrstuhl Physiologische Chemie  
Institut der Ludwig-Maximilians-Universität München

Vorstand: Prof. Andreas Ladurner

**Deciphering the role of the sugar-induced  
transcription factor, Mondo in *Drosophila*  
*Melanogaster***

Dissertation  
zum Erwerb des Doktorgrades der Naturwissenschaften  
an der Medizinischen Fakultät der  
Ludwig-Maximilians-Universität zu München

vorgelegt von  
Hui-Lan Huang

aus  
Taichung, Taiwan

2020

**Mit Genehmigung der Medizinischen Fakultät  
der Universität München**

Betreuer: Prof. Andreas Ladurner, Ph.D.

Zweitgutachter(in): Prof. Dr. John Parsch, Ph.D.

Dekan: Prof. Dr. med. dent. Reinhard Hickel

Tag der mündlichen Prüfung: 17. 11. 2020

## **Eidesstattliche Versicherung**

Huang, Hui-Lan

Ich erkläre hiermit an Eides statt,  
dass ich die vorliegende Dissertation mit dem Thema

**Deciphering the role of the sugar-induced transcription factor, Mondo in  
*Drosophila Melanogaster***

selbständig verfasst, mich außer der angegebenen keiner weiteren Hilfsmittel bedient und alle Erkenntnisse, die aus dem Schrifttum ganz oder annähernd übernommen sind, als solche kenntlich gemacht und nach ihrer Herkunft unter Bezeichnung der Fundstelle einzeln nachgewiesen habe.

Ich erkläre des Weiteren, dass die hier vorgelegte Dissertation nicht in gleicher oder in ähnlicher Form bei einer anderen Stelle zur Erlangung eines akademischen Grades eingereicht wurde.

Taipei, 26.02.2021

Ort, Datum

Hui-Lan Huang

Unterschrift Doktorandin

# Acknowledgement

I want to acknowledge my supervisor Dr. Carla Margulies. Firstly, for supervising my PhD project and showing me the importance of being critical and analytical in doing research. Secondly, for providing me the chance to have various training that sharpened both of my soft and hard skills. Last but not the least, I thank Carla for not only helping me with my working progress, but also for caring for my physical and mental states during my time in Germany. I thank Prof. Andreas Ladurner for taking me through IMPRS program and being my official supervisor. Thank him for providing me a nice working environment, and allowing me to do exciting research. I thank my TAC members Dr. Nicolas Gompel, Dr. Catherine Postic and Dr. Ann Classen for the advice to my project. I thank IMPRS-LS program and of course the wonderful program coordinators, Dr. Hans-Joerg Schaeffer, Dr. Ingrid Wolf, and Ms. Maximiliane Reif. I eventually realized what I want to pursue in the future after attending the great career events supported by IMPRS-LS program.

I thank Teresa Burrell and Sandra Esser. Thank them for supporting me from the very beginning to the end. It was my honor to work with them and have them as friends! I thank Dr. Ava Handley and Dr. Tamas Schauer for sharing their experiences with me. I thank Thomas Pysik and Mehera Emrich, who also work on other Mondo/ChREBP projects. It is fun to learn more about this protein from different aspects. A great appreciation goes to Dr. Rupa Banerjee. Only with her support, I did not lose myself and was able to be persistent to the end of my PhD life. I also thank my friends Shao-Yen Kao, Annie Yim, Valerie Goh, Julia Preißer, Flavia Söllner, Umut Günsel, Giuliana Möller, Gopal Jarajee, Jun Chen, and Roman Pritulyak. I thank lovely Christine Werner for her kind support. Undoubtedly, their companies enrich my life in Germany.

I thank my father for encouraging me throughout my PhD. A great thank goes to my mother for always caring about me and reminding me to be humble and grateful in life. I thank my brother for sharing his inspiring experiences in career and life with me. In the end, I thank those countless nervous breakdowns in the last two years of my PhD. They were indeed unbearable. Nevertheless, I have learned how bitter life could be, and I was eventually able to face it. What didn't defeat me only makes me stronger. It is learning progress, and we all aim to become a better one, don't we?

# Summary

Overconsumption of sugar promotes the occurrence of metabolic disorders. Therefore, studying the mechanisms underlying our physiological responses to sugar helps identify the underlying molecular mechanisms and potential therapeutic targets. Mondo family transcription factors are evolutionarily conserved across a number of species including *Drosophila melanogaster*, and they are known as the key “sugar sensor” in our body. Lines of evidence indicate that this component is misregulated in insulin resistance and diabetes.

The aims of my PhD thesis are to determine the function of fly Mondo and its interacting partner Mlx during different stages and in different nutrition states, and to globally identify its direct target genes and regulated pathways. A deficiency in Mondo and Mlx causes sugar inviability in flies fed on a high sugar diet. Furthermore, Mondo is essential for survival during starvation after sugar deprivation, which brings our attention to the involvement of Mondo in the regulation of nutrient usage and metabolic adaptation during starvation.

The chromatin Mondo-Mlx binding profile reveals several known sugar-dependent Mondo target sites and potential new targets. The identified target genes are functionally clustered in metabolic pathways regarding sugar, lipid, and amino acids, which supports the concept that Mondo is a master metabolic regulator. Importantly, the data indicates that Mondo-Mlx is at the top of a regulatory network composed of abundant secondary transcriptional effectors. Motif searching analysis shows some interesting findings: in addition to the canonical ChoRE motif, a putative novel Mondo binding motif was also identified. Finally, our RNA Pol II ChIP-seq data provides the first direct evidence indicating that Mondo acts as both a transcriptional activator and repressor for different target genes and regulates gene transcription via influencing Pol II recruitment or elongation.

Less is known about the role of Mondo family proteins in the nervous system, although Mondo expression has previously been observed in this metabolically active organ system. Here, I provide evidence of Mondo’s role in the central nervous system’s metabolism of sugar, lipids, and amino acids, specifically in the amino acids serine, glycine, and glutamine. Interestingly, the metabolism of lipid and serine in the fly brain has been shown to determine sleeping behaviors, though further

investigation is necessary to test whether Mondo has a systemic role in controlling sleeping behaviors.

## Zusammenfassung

Der vermehrte Konsum von Zucker fördert die Entstehung metabolischer Erkrankungen. Die Erforschung der grundlegenden Mechanismen der physiologischen Antwort auf Zucker ist hilfreich, um die zugrundeliegenden molekularen Mechanismen und mögliche therapeutische Targets zu identifizieren. Die Familie der Mondo Transkriptionsfaktoren ist evolutionär über Spezies hinweg, inklusive *Drosophila melanogaster*, konserviert und sie werden als „Zucker Sensoren“ unseres Körpers bezeichnet. Mehrere Beweislinien zeigen, dass diese Komponente in Diabetes und der Insulinresistenz falsch reguliert ist.

Die Ziele meiner Promotion sind sowohl die Bestimmung der Funktion von Mondo sowie seines Interaktionspartners Mlx während der verschiedenen Entwicklungsstadien der Fliege und unter unterschiedlicher Nahrungsbedingungen, als auch die globale Identifizierung der Zielgene und der regulierten Stoffwechselwege. Ein Mangel an Mondo und Mlx führt zu einer Zucker-Lebensunfähigkeit der Fliege, wenn diese unter einer Diät mit hoher Zuckerzufuhr gefüttert wurde. Des Weiteren ist Mondo essentiell für das Überleben während des Hungerns nach einer Zuckerreduktion. Dies lenkt unsere Aufmerksamkeit auf die Beteiligung von Mondo in der Regulation von Nährstoffverwendung und der metabolischen Anpassung während des Hungers.

Das Mondo-Mlx Chromatin-Bindeprofil offenbart einige bekannte Zucker-abhängige Mondo-Zielgene, sowie potentiell neue Zielgene. Die identifizierten Gene sind funktionell nach metabolischem Weg in Bezug auf Zucker, Lipide und Aminosäuren gruppiert, was die Rolle von Mondo als einen metabolischen Master-Regulator hervorhebt. Die Daten zeigen, dass Mondo-Mlx an der Spitze eines regulatorischen Netzwerkes aus den zahlreichen sekundären Transkriptionsregulatoren steht. Die Motif-Analyse für Mondo-Mlx Bindestellen zeigen ein weiteres interessantes Ergebnis: zusätzlich zum kanonischen ChoRE Motif konnte ein neues Bindemotif beschrieben werden. Zu guter Letzt liefern unsere RNA

## SUMMARY

---

Pol II ChIP-seq Daten erstmalig eine direkte Evidenz, dass Mondo einerseits sowohl als Aktivator als auch als Repressor für unterschiedliche Zielgene agiert und darüber hinaus die Transkription von Genen durch die Beeinflussung der Pol II Rekrutierung und Elongation reguliert.

Weniger ist über Rolle der Mondo-Proteinfamilie im Nervensystem bekannt, dies obwohl die Expression von Mondo in diesem metabolisch aktiven Organsystem gezeigt wurde. In dieser Arbeit liefere ich Hinweise für eine Rolle von Mondo im Zentralen Nervensystem für die Metabolisierung von Zucker, Lipiden und Aminosäuren, im Speziellen für Serin, Glycin und Glutamin. Interessanterweise zeigten Studien im Fliegenhirn bereits eine Rolle des Serin- und des Lipidmetabolismus bei der Bestimmung des Schlafverhaltens. Ob Mondo eine systemische Rolle bei der Kontrolle des Schlafverhaltens hat, muss durch weiterführende Studien erforscht werden.

# Contents

## 1. Introduction

1.1. Nutrient sensing and metabolism.....	1
1.1.1. Sugar-sensing pathways .....	2
1.1.2. Lipid-sensing pathways.....	4
1.1.3. Amino acid-sensing pathways.....	4
1.1.4. The metabolic organ system and nutrient sensing in the fly .....	6
1.2. Transcription regulation in response to different nutrients.....	8
1.2.1. Transcriptional regulation of carbohydrate metabolism .....	8
1.2.2. Transcriptional regulation of lipid metabolism.....	9
1.2.3. Transcriptional regulation of amino acid metabolism.....	10
1.3. The Mondo protein family as major sugar sensors.....	11
1.3.1. The Mondo protein family belongs to the basic helix-loop-helix leucine zipper (bHLH/LZ) class of transcription factors .....	11
1.3.2. Functional protein domains are conserved in the Mondo protein family .....	13
1.3.3. Regulatory mechanisms of ChREBP activity .....	17
1.3.4. ChREBP is at the center of interlinked transcription networks in response to different nutrition states.....	20
1.4. Metabolic adjustment in the fasting-refeeding cycle.....	24
1.4.1. Metabolism of the fed state .....	24
1.4.2. Metabolism of the starvation state .....	24
1.4.3. Metabolism of the refeed state .....	25
1.5. Dynamic functions of ChREBP/Mondo protein in different tissues .....	26
1.5.1. ChREBP regulates sugar-induced <i>de novo</i> lipogenesis in the liver ...	27
1.5.2. ChREBP controls adipocyte differentiation and systemic insulin sensitivity .....	27
1.5.3. ChREBP promotes the proliferation of $\beta$ cells.....	28
1.5.4. Intestinal ChREBP is required for fructose tolerance .....	29
1.5.5. ChREBP in the brain may mediate feeding behavior .....	29

## 2. Investigating sugar- and starvation-induced phenotypes of the Mondo-Mlx-deficient fly .....

2.1. Summary.....	31
2.2. Introduction.....	32
2.3. Methods .....	34
2.4. Results.....	39

2.4.1. <i>Drosophila</i> requires Mondo/Mlx to develop on high-sugar food .....	39
2.4.2. Mondo is required for the fly to develop on both high-glucose and high-fructose diets .....	44
2.4.3. Does Mondo have a different role in the adult than in the developing organism? .....	45
2.4.4. Flies deprived of sugar are more sensitive to starvation .....	46
2.4.5. Mondo is most highly expressed in the fat body .....	48
2.4.6. Investigating the cell type-specific role of Mondo in sugar tolerance .....	50
2.5. Discussion and future directions .....	52
<b>3. Genome-wide identification of target genes for the Mondo-Mlx complex in the fly .....</b>	<b>55</b>
3.1. Summary .....	55
3.2. Introduction .....	56
3.3. Methods .....	58
3.4. Results .....	70
3.4.1. The time-course of sugar-induced transcriptome reveals the dynamics of sugar responses .....	70
3.4.2. <i>Drosophila</i> Mondo antibodies show specificity to recombinant and endogenous Mondo protein .....	74
3.4.3. Mondo is most active at the early sugar-refeeding time point .....	80
3.4.4. Identification of Mondo direct targets in the adult fly head .....	80
3.4.5. Mondo-Mlx binds primarily to promoters and intronic regions .....	86
3.4.6. Motif-searching analysis reveals the canonical ChoRE motif and A novel “GATAA” motif within putative Mondo-Mlx target sites ...	87
3.4.7. Mondo-Mlx’s target genes are functionally clustered in metabolic pathways .....	88
3.4.8. Mondo-Mlx is on the top of a transcription cascade that targets several transcription factor genes .....	89
3.4.9. Mondo regulates the recruitment and elongation of Pol II at the direct target genes .....	94
3.4.10. Correlation of Mondo binding and Mondo-dependent Pol II occupancy with RNA expression .....	97
3.4.11. The comparison of Mondo-Mlx binding data with RNA expression data supports the role of Mondo as either a transcription activator or repressor .....	99
3.5. Discussion and future directions .....	101
3.6. Appendix .....	103
<b>4. Investigating Mondo function in the central nervous system of the fly .....</b>	<b>108</b>
4.1. Summary .....	108

## CONTENTS

---

4.2. Introduction.....	109
4.3. Methods .....	110
4.4. Results.....	111
4.4.1. Evidence indicating Mondo expression in the fly brain.....	111
4.4.2. RNA-seq data confirm Mondo’s expression and regulatory role on known target effector genes in the CNS.....	113
4.4.3. Comparison of sugar-induced transcriptome from the brain and whole head.....	115
4.4.4. Comparison of Mondo-dependent transcriptome in the brain with Mondo-Mlx target genes .....	115
4.4.5. Functional clustering of DEGs suggests that CNS-Mondo may be involved in the oxidation-reduction process, metabolic pathways, and sleep behavior.....	117
4.4.6. CNS-Mondo regulates the expression of sugar transporters in the brain.....	119
4.4.7. The metabolism of glycine, serine, glutamine, and purine may be regulated in a Mondo-dependent manner in the fly brain upon starvation .....	121
4.5. Discussion and future directions.....	125
<b>5. Perspectives .....</b>	<b>127</b>
<b>Abbreviations .....</b>	<b>131</b>
<b>List of figures and tables .....</b>	<b>135</b>
<b>Bibliography .....</b>	<b>138</b>
<b>Curriculum vitae.....</b>	<b>157</b>

# Chapter 1

## Introduction

### 1.1 Nutrient sensing and metabolism

Nutrients are macromolecules such as carbohydrates, lipids, and amino acids that can be utilized to produce energy, and they serve as the building blocks of biomass in organisms. Organisms acquire the ability to sense and respond to the abundance of essential nutrients for survival under the selective pressure derived from food scarcity. Meanwhile, as different nutrients are required for specific cellular and physiological processes, evolutionarily conserved nutrient-sensing pathways built in organisms enable them to choose different types of food based on the nutrition content (1,2). Moreover, nutrient-sensing pathways integrate external nutrition inputs and internal satiation signals to maintain a balanced nutrient homeostasis and to facilitate the coordination of cellular processes (3,4). Overly high or low nutrient levels both cause adverse effects for survival. For example, high blood glucose levels can result in glucotoxicity and negatively affect the function of  $\beta$  cells and insulin secretion, subsequently leading to diabetes. Therefore, nutrient-sensing pathways have evolved into complex networks for organisms to adapt to fluctuations in nutrition states.

Nutrient metabolism can be classified into two primary categories: catabolism, the decomposition of organic matters, and anabolism, the assembly of cellular components such as proteins, nucleic acids, and lipids. For example, during prolonged starvation, fatty acids are catabolized in the  $\beta$ -oxidation pathway to provide energy for the maintenance of cellular functions. In contrast, when food is available, the anabolic processes are activated to promote cellular growth and energy storage.

In general, specialized sensors sense particular types of nutrients, and they activate specific downstream signaling pathways and stimulate corresponding output signals. At the same time, each nutrient-sensing pathway is connected through sensors that can respond to multiple nutrients. This crosstalk allows efficient metabolic switches when the nutrition state changes and promotes the holistic maintenance of the energy balance. In the following sessions, I review the sensors and signaling

pathways that sense each type of nutrient and discuss how these pathways are delicately interlinked in response to a dynamic environment.

### **1.1.1 Sugar-sensing pathways**

Sugar is an important fuel for most of the cells in organisms, and it is essential for organs such as the brain and red blood cells (RBCs) because they mainly rely on it as an energy source. Sugar-sensing pathways have evolved to ensure effective sugar utilization in organisms; they are conserved across species but have adapted divergences in each.

In mammals, sugar sensing first starts in oral taste buds with G-protein-coupled taste receptors T1R2-T1R3 (5). These receptors bind sugars at a high concentration and trigger the downstream signal cascades, leading to the neurotransmission of taste information to the brain. Sugar is then absorbed in the small intestine. As in the taste buds, the intestinal epithelium also senses sugars via T1R2-T1R3 receptors. Glucose and galactose are transported from the intestinal lumen into enterocytes by the Na<sup>+</sup>/glucose cotransporter (SGLT1) (6), while fructose is transported by GLUT5, which is the specific transporter for fructose but not for glucose or galactose. Instead, flies sense sugars with the gustatory system. In contrast to mammals which use a widely tuned heterodimeric receptor, the fly genome harbors a subset of nine gustatory receptor (Gr) genes, Gr5a, Gr43a, Gr61a, and Gr64a–Gr64f, which have been shown to mediate the sensing of various types of sugar and even regulate feeding behaviors (7-9).

While sugar is taken up, it is of critical importance in both mammals and flies that sugar levels are maintained within a narrow range for normal cellular functions (10,11). In order to ensure an efficient clearance/release of glucose from/into the blood/hemolymph upon the fed or fasting state, glucose uptake, glucose storage, and metabolism are tightly regulated at different levels by different mechanisms, including hormonal regulation, glucose transporter regulation, and sugar-induced signaling. Insulin and glucagon are the two major hormonal regulators that systemically regulate sugar sensing in mammals, and a homologous hormonal system also exists in the fly (12-14). After food consumption, the pancreas senses elevated blood glucose levels and secretes insulin, which accelerates the uptake of blood

glucose into the liver, adipose tissues, and muscle. Conversely, while blood glucose levels decrease, the pancreas produces and secretes glucagon, which signals liver and muscle cells to convert stored glycogen into glucose or glucose metabolites that are again released into bloodstream.

In addition to hormonal regulation, several intracellular “glucose sensors” play a critical role in glucose-sensing pathways. One group of such sensors is sugar transporters, through which cells uptake sugars. In humans, the glucose transporter family is comprised of 14 isoforms, of which the GLUTs 1-4 are the most characterized (15). Different sugar binding affinity contributes to particular physiological properties of GLUTs 1-4. The  $K_m$  value for GLUT1 is approximately 1 mM; thus, it is close to saturation even during fasting. This high affinity of GLUT1 to glucose enables basal glucose uptake, which explains the high expression in the blood-brain barrier and RBCs, where sustained glucose supply is required. GLUT4 has a  $K_m$  value of around 5 mM and is predominantly expressed in the muscle and adipose tissues. GLUT2 has a higher  $K_m$  (20 mM) value than other glucose transporters of the same family, and this kinetic parameter makes it a glucose sensor that promotes glucose flux. Similar to human GLUT2, fly GLUT1 has been shown to regulate glucose levels rather than trehalose levels in the hemolymph, although trehalose is the main circulating carbohydrate (16). This suggests that the fly hemolymph glucose mirrors the physiology of mammalian blood glucose. Once glucose is transported into cells via the transporter, glucokinase (GCK) carries out the first step of glucose breakdown. Similar to GLUT2, GCK also has a low glucose affinity. Therefore, it can function as a glucose sensor when blood glucose levels rise, and it controls systemic glucose levels by stimulating insulin secretion from the pancreas.

Mondo family transcription factors are also a group of important glucose sensors conserved across many species, including humans and the fly. The fly genome also encodes single orthologues of Mondo and Mlx, the interacting partner of Mondo. The Mondo-Mlx complex is required for the maintenance of carbohydrate homeostasis in the fly. Interestingly, emerging evidence shows that Mondo family members not only transit sugar-induced signaling, but they also respond to lipids and amino acids, the other two major nutrient types. The main focus of my PhD project is

studying the physiological role and downstream effectors of Mondo-Mlx complex in the fly.

### 1.1.2 Lipid-sensing pathways

Lipids are generally categorized into eight types: fatty acids, sterol lipids, glycerolipids, glycerophospholipids, polyketides, saccharolipids, sphingolipids, and prenol lipids (17). Lipids serve not only as stored fuel, but also as constituents of cellular membranes due to their hydrophobicity. Many sphingolipid derivatives also act as signaling molecules that bind to its particular receptor to transduce signaling to maintain cellular homeostasis (18, 19).

There are two G protein-coupled receptors, GPR40 and GPR120, responsible for sensing long-chain fatty acids (20) in mammals. GPR40 is predominantly expressed in islet  $\beta$  cells (21) and controls the fatty acids-induced insulin secretion. GPR120 also indirectly promotes fatty acid-induced insulin secretion by stimulating the release of a gastrointestinal hormone named glucagon-like peptide-1 (GLP1; 22), which in turn promotes satiation (23). Deficiency in the GPR120 function has been known to be associated with diet-induced obesity in mice and has been also identified in some obese people. Generally speaking, these receptors mediate insulin sensitivity, insulin secretion, and  $\beta$ -cell function, suggesting that they are anti-diabetic targets. In addition, they have become therapeutic targets for the treatment of type 2 diabetes.

Studies have also suggested that sugar-sensing Mondo family members also sense lipids. However, in contrast to sugar, fatty acids exert an inhibitory effect on the activity of Mondo family members. Evidence indicates that fatty acids significantly induce the AMP level, which directly inhibits the mammalian Mondo protein called the carbohydrate response element binding protein (ChREBP) via an allosteric mechanism (24). In addition, AMP can also indirectly hinder the transactivity of ChREBP through the action of AMP-activated protein kinase (AMPK), by which ChREBP is phosphorylated and therefore inactivated (25).

### 1.1.3 Amino acid-sensing pathways

Amino acids are the building blocks for proteins, the functional units for nearly every cellular process. The absence of any amino acid can lead to failure in peptide-chain

synthesis; therefore, a system controlled by general control nonderepressible 2 (GCN2) kinase has emerged to sense amino acid levels in food, and it is highly conserved from worms to humans (4). GCN2 has a high affinity with all uncharged tRNAs (non-amino acid-coupled tRNAs). Upon a low amino acid level, GCN2 binds to uncharged tRNAs, resulting in the inhibitory phosphorylation of the eukaryotic translation initiator factor 2  $\alpha$  (eIF2 $\alpha$ ) and the global inhibition of translation initiation. Moreover, GCN2 encourages animals to avoid the food-lacking essential amino acids by inhibiting GABA signaling within dopaminergic neurons of the brain (26). This indicates that GCN2 can sense the nutrition levels in food and can encourage nutrition-balanced food sources.

The mechanistic target of the rapamycin complex 1 (mTORC1) signaling pathway and the upstream regulators of mTORC1 activity constitute another system for sensing the intracellular amino acids level. mTORC1 integrates several signals, including hormones, growth factors and nutrients such as amino acids and glucose, to control protein synthesis and cell growth. The amino acid-dependent activation of mTORC1 is regulated by the Rag family of GTPase, which is in turn controlled by several cytosolic amino acids sensors, such as Sestrin2 (SESN2), Leucyl-tRNA synthetase (LRS) and Folliculin (FLCN). These upstream regulators sense specific amino acids inputs, particularly arginine and leucine, to activate and recruit mTORC1 on the surface of the lysosome. In addition, the amino acid transporters, SLC38A9 and SLC36A1 have been identified on the surface of lysosome. The fact that a lack of these amino acid transporters can lead to dysfunctional mTORC1 action in response to amino acids further strengthens the model of amino acid-sensing at lysosomes (27).

Amino acid sensing is also interlinked with sugar sensing through the direct inhibitory action of mTOR on ChREBP. In addition, the inhibition of mTOR drives the expression of a ChREBP target gene, thioredoxin-interacting protein (TXNIP). Recent studies have shown that elevated TXNIP levels can lead to  $\beta$ -cells apoptosis in diabetes (121). In sum, these data indicate that a coordination between sugar- and amino acid-sensing pathways mediated by ChREBP/Mondo and mTOR, respectively, is important for normal  $\beta$ -cell functioning.

### 1.1.4 The metabolic organ system and nutrient sensing in the fly

Nutrient-sensing signaling and metabolic pathways are highly conserved across mammals, insects and worms. *Drosophila* is a particularly powerful model for studying metabolic pathways for several reasons; it has: 1) a short generation time, 2) a wide variety of genetic tools, 3) the possibility of performing high-throughput genetic screening and 4) ~75% similarity to the human genome. Furthermore, many metabolic organs in the fly have functional counterparts in mammals (Table 1.1). For example, the fly and human gut share a similar anatomical structure and physiological function. The fly gut can be divided into three parts: foregut, midgut and hindgut. Food is mixed in the foregut and is then mainly digested and absorbed at midgut. The hindgut is where water reabsorption and waste excretion occur. The Malpighian tubules connect to the gut; they are the site of urine formation in insects and excrete metabolic waste (28). The fly fat body is commonly seen as equivalent to mammalian liver and adipose tissue. Unlike the solid structure of the liver, however, the fat body is a loose organ that is distributed throughout the body.

Meanwhile, the fat body also acts as an endocrine organ similar to mammalian adipose tissue; it regulates larval growth by integrating nutritional and hormonal signals (29). For example, CCHamide-2 (CCHa2), a sugar-responsive hormone, and its receptor, CCHa2-R in insulin-producing cells (IPCs), form a direct link between the fat body and the brain. This crosstalk regulates the release of dILP2 and dILP5 from IPCs, which is essential for the coordination of systemic growth (30). Moreover, it serves as the primary nutrient sensor, and it secretes endocrine molecules in response to the nutritional status, transducing signals to IPCs to coordinate metabolic homeostasis systemically. Fat body-derived Unpaired 2 (Upd2) is the fly equivalent of mammalian Leptin, which serves as a “satiation signal” to mediate the energy balance by reducing hunger (31). Upd2 relieves the inhibitory effect of GABAergic neurons on IPCs; this leads to the secretion of insulin-like peptides (dILPs), which drive nutrient storage (32). In addition to the fat body, specialized cells called oenocytes are required for the mobilization of triglycerides in the fat body during fasting. Its function is similar to that of hepatocytes, so oenocytes are thus considered the functional analog of the mammalian liver (33).

**Table1.1 Conservation of metabolic tissues between flies and mammals**

Fly	Mammal	Metabolic function
Brain	Brain	Feeding behavior Central metabolic coordination
Gut	Gut	Digestion and absorption
Fat body	Liver Adipose tissue	Lipid storage Lipid mobilization Glycogen storage
Oenocytes	Liver	Lipid mobilization
Insulin producing cells	Pancreatic $\beta$ cells	Carbohydrate homeostasis
Corpora cardiaca	Pancreatic $\alpha$ cells	Carbohydrate homeostasis
Malphigian tubes	Kidney	Metabolism and detoxification of xenobiotics
Muscles	Muscles	Glycogen storage Amino acid storage

The basic hormonal regulation of metabolic homeostasis is also conserved in the fly. The fly counterparts of insulin and glucagon are dILPs and the adipokinetic hormone (dAKH; 12-14). The specialized IPCs in the fly brain function as pancreatic  $\beta$  cells, producing four of the eight insulin-like peptides (dILP1, 2, 3, and 5). Other organs secrete dILPs; for instance, dILP4 is expressed in the embryo mesoderm and larval gut (34), and dILP6 is produced in the larval and adult fat body (35, 36). dILP7 is expressed in specialized neurons that innervate the hindgut (37). The selective secretion of different dILPs is regulated by distinct nutritional cues and by nutrient availability (38, 39). Specifically, the release of dILP2 is stimulated by amino acids (40), whereas the secretion of dILP3 from IPCs is promoted by dietary sugars (41). dILP6 expression is enhanced upon low protein diets. Starvation also increases dILP6 expression, while *dilp2* and *dilp5* were decreased or remained the same (36). Corpora cardiaca (CC) secrete dAKH (42); therefore, they are seen as the fly homolog of mammalian pancreatic  $\alpha$ -cells. dAKH binds to its receptors' AKHR in the fat body to induce the breakdown of glycogen (43,44), and carbohydrates are released into circulation. A recent study has indicated that glucose, rather than trehalose, is the main circulating sugar in the fly hemolymph, and it acts as a regulator of appetite through the action of insulin signaling in the fly (45). Collectively, the harmonic

regulation of hormone signaling in response to dietary carbohydrates maintains not only sugar levels in the hemolymph, but also the systemic energy balance in the fly.

Similar to mammals, flies have postingestive mechanisms to detect the calories of food independently of taste. For example, flies can build appetitive memories for odors associated with the tasteless sugar alcohol sorbitol (46). In addition, a recent study indicates that flies can detect the nutritional content of sugars, regardless of taste, through the brain-gut axis, which is connected by neurons that secrete the diuretic hormone 44 neuropeptide (Dh44). Moreover, this Dh44-driven brain-gut axis also mediates the feeding and digestion of sugars through a positive feedback mechanism (47). The other taste-independent system that perceives nutritious food is based on a signal called a calorie-induced secreted factor (CIF), which is secreted by flies after feeding. Flies release CIF signals around the food to inform the presence of nutritive food to other flies. These taste-independent pathways enable flies to choose the food in the most efficient way.

### **1.2 Transcription regulation in response to different nutrients**

#### **1.2.1 Transcriptional regulation of carbohydrate metabolism**

A high glucose level regulates gene transcription either directly or through insulin signaling. The action of insulin stimulates phosphatidylinositol 3-kinase (PI3K) signaling, which further activates the sterol regulatory element-binding transcription factor-1c (SREBP-1c)-induced transcription cascade and the protein kinase B (PKB)/Akt pathway. SREBP-1c regulates the insulin-mediated transcription of glycolytic and lipogenic genes and is particularly important in the lipogenic program in the liver (48). On the other hand, activated PKB/Akt inhibits the activity of the Forkhead box O (FOXO) family transcription factors that integrate insulin signaling to hepatic gluconeogenesis by regulating key gluconeogenic genes, such as phosphoenolpyruvate carboxykinase (*pepck*) and glucose-6-phosphatase (*G6p*; 49). FOXO proteins also control diverse processes, including glucose metabolism (50), cell growth (51), apoptosis (52,53), oxidative stress response and longevity (54). Moreover, FOXO activates the transcription of the insulin receptor (InR) itself, forming a transcriptional feedback loop in the InR pathway. While fasting or lacking

nutrients, FOXO is activated and up-regulates the InR, which allows cells to accumulate higher levels of InR on the membrane. It establishes a sensitized state to signal when it is triggered by changes in insulin levels (55).

The transcription of the key glucose sensor gene *Glut2* is directly regulated by several transcription factors, such as hepatocyte nuclear factor 1 $\alpha$  (HNF1 $\alpha$ ) and pancreatic duodenal homeobox 1 (PDX1). In  $\beta$ -cells, HNF1 $\alpha$  activates *Glut2* and other genes involved in glucose-stimulated insulin secretion and  $\beta$  cell differentiation (56). PDX1 enhances *Glut2* gene expression through binding to the TAAT motif at the *Glut2* promoter (57, 58). The PDX1-GLUT2 pathway is important in maintaining the glucose-sensing ability and insulin secretion in  $\beta$  cells (59). Hepatocyte nuclear factor 4 $\alpha$  (HNF4 $\alpha$ ) increases the expression of another important glucose sensor gene, *GCK*, in the liver when the inhibitory effect of FOXO1 on HNF4 $\alpha$  is eliminated in response to insulin signaling.

Independent of the action of insulin signaling, ChREBP broadly targets lipogenic and glycolytic genes that contain the carbohydrate response element (ChoRE) to regulate their transcription. Animals without ChREBP display severe sugar intolerance and hyperglycemia (60,61), indicating its importance in maintaining glucose homeostasis in organisms. Interestingly, the hepatic *GCK* gene has also been shown to be the direct target of ChREBP, and in turn, GCK is required for the action of ChREBP on the regulation of genes involved in glucose metabolism.

### **1.2.2 Transcriptional regulation of the lipid metabolism**

The two major transcription factor families involved in the metabolism of fatty acids are peroxisome proliferator-activated receptors (PPARs) and SREBPs. The three isoforms of PPARs have been described as PPAR $\alpha$ , PPAR $\delta$ , and PPAR $\gamma$  which display different tissue-specific distribution patterns and functions (62). PPAR $\alpha$  regulates the uptake of fatty acids and  $\beta$ -oxidation by transcriptionally activating the genes involved in lipid catabolism (63,64). Therefore, PPAR $\alpha$  prevents lipotoxicity by reducing the lipid content in the tissues (65). PPAR $\delta$  expresses in a wide range of tissues and cell types (66). In islets, the activation of PPAR $\delta$  enhances insulin secretion, increases fatty acid oxidation and protects  $\beta$ -cells from the adverse effects of prolonged fatty acid exposure (67). In skeletal muscle, PPAR $\delta$  regulates the genes

involved in lipid catabolism, cholesterol efflux and energy uncoupling (68). PPAR $\gamma$  promotes the storage of fatty acids in adipose tissue by enhancing the storage capacity and the uptake of fatty acid into adipocytes. PPAR $\gamma$  also enhances insulin sensitivity by negatively regulating the transcription of genes that impair insulin resistance (69). Moreover, it also has an anti-inflammation effect by inhibiting the transcription of the proinflammatory cytokines genes in adipose tissue (70). There are no orthologs of the PPARs in lower organisms, including flies and worms. In the fly, as fly HNF4 mutants and PPAR $\alpha$  mutant mice share several phenotypes, including increased sensitivity to starvation, enhanced plasma free fatty acids, and a fatty liver with enlarged lipid droplets, Palanker *et al.* have proposed that the ancestral function of HNF4 was replaced by PPAR $\alpha$  during evolution (71). The SREBP family transcription factors are also considered master transcriptional regulators that mediating the expression of genes regulating lipid metabolism, lipid transport and cholesterol synthesis in response to insulin stimulation. Among isoforms, SREBP-1c is highly abundant in the liver, where it promotes lipid synthesis (72), while SREBP2 is the key regulator of cholesterol synthesis (73). The major role of SREBP-1c is to activate the expression of lipogenic and glycolytic genes that contain a sterol regulatory element (SRE) sequence in their promoter. The target genes include fatty acid synthase (FAS), acetyl-CoA carboxylase (ACC), stearoyl-CoA desaturase 1 (SCD1) and glucose-6-phosphate dehydrogenase (G6PD), which are important for fatty acid synthesis (74,75). The enhancement of the SREBP-1c level and the resulting lipogenesis are seen in obesity and may mechanistically explain the onset of fatty liver. The SREBP-1c expression can also be induced by the activation of the liver X receptor  $\alpha$  (LXR  $\alpha$ ), a nuclear hormone receptor that is activated by derivatives of cholesterol such as oxysterols. Mice that lack LXR $\alpha$  display a reduced expression of SREBP-1c, FAS, ACC and SCD1 gene (76). The transcription factors PPARs and SREBP-1c can respond to the changes in lipid levels in tissues, thereby coordinating fat anabolism or catabolism based on the dynamic metabolic states.

### **1.2.3 Transcriptional regulation of amino acid metabolism**

As previously described, the uncharged tRNA activates the GCN2 upon low cellular amino acid levels. GCN2 further phosphorylates eIF2 $\alpha$ , whereby the overall protein

synthesis is repressed, except the expression of activating transcription factor 4 (ATF4), which is an important transcription factor in the regulation of amino acid metabolism (78, 79). ATF4 transcriptionally regulates the expression of genes involved in amino acid synthesis to ease the stress responses derived from the scarcity of amino acids. ATF4 is regulated by histone lysine demethylase KDM4C upon serine deprivation. KDM4C mediates the biosynthesis and transport of amino acids in cancer cell lines, which requires ATF4 to induce relevant genes. KDM4C binds to the promoter of ATF4 and removes the repressive H3K9me3 mark, conferring the active expression of ATF4. These findings link KDM4C-induced H3K9 demethylation and ATF4-induced activation in the reprogramming of amino acid metabolism for cancer cell survival (80).

Glutamine, as the most abundant amino acid in humans, supplies amino groups for the synthesis of amino acids and nucleotides. The formation of glutamine is mainly controlled by the ATP-dependent glutamine synthase (GS), whose expression is transcriptionally regulated by glucocorticoids. The direct binding of the glucocorticoid to the glucocorticoid response element (GRE) within the upstream region of the *GS* gene confers the activation of the GS reporter (81, 82). With regard to the uptake of glutamine, MondoA performs this role in the process by activating the expression of the glutamine transporter SLC1A5.

Although PPAR $\alpha$  is well known as a master regulator in lipid metabolism, it also mediates the expression of genes involved in amino acid metabolism, including deamination, transamination, and the urea cycle (83). Consistently, plasma urea concentration is increased in PPAR $\alpha$ -deficient mice (83). In fact, several transcription factors such as SREBP1-c, PPARs and ChREBP can regulate genes involved in the metabolism of different nutrients. This coordinated regulation in response to various physiological conditions enables the organism to adapt to different nutrition states.

### **1.3 The Mondo protein family as major sugar sensors**

#### **1.3.1 The Mondo protein family belongs to the basic helix-loop-helix leucine zipper (bHLH/LZ) class of transcription factors**

The basic helix-loop-helix (bHLH) proteins constitute a large transcription factor superfamily. A subclass of the bHLH superfamily that features an additional leucine

zipper region is called the basic helix-loop-helix/leucine zipper (bHLH/LZ) regulator. One of the most well-studied networks of bHLH/LZ regulators is the Myc-Max-Mad network. Max sits at the center of the network by interacting with the Myc family of transcriptional activators for gene activation, while dimerizing with the Mad family of transcriptional repressors for gene repression. Consistent with their molecular function, Max-Myc and Max-Mad have opposing physiological roles in growth. Myc-Max heterocomplexes drive cell growth. In contrast, Mad-Max complexes promote cell differentiation. The Mondo protein family belongs to the bHLH/LZ class of transcription factors, as well. Mondo A was identified as the first member of the Mondo protein family (84), followed by the discovery of the second family member, ChREBP (85). Mondo interacts with the bHLH/LZ factor called Max-like protein, Mlx (Fig. 1.1). Like Max, Mlx also interacts with the Mad protein to regulate transcriptional gene repression while Mlx alone with the Mondo family mediate transcriptional gene activation.

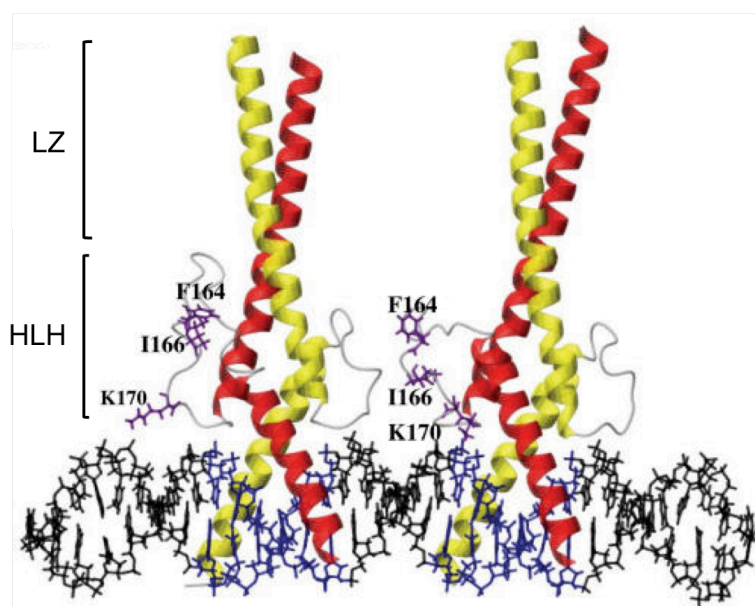


**Figure 1.1. Model of the bHLH/LZ region of two ChREBP/Mlx heterodimers binding to a tandem E box DNA element.** Figure adapted from Ma *et al.*, 2006. LZ: leucine zipper; HLH: helix loop helix.

### 1.3.2 Functional protein domains are conserved in the Mondo protein family

MondoA and ChREBP are paralogous proteins encoded by two distinct genes and are highly conserved in several functional domains. The N-terminal region of MondoA and ChREBP contains a glucose-sensing module (GSM), which includes a low-glucose inhibitory domain (LID) and a glucose-response activation conserved element (GRACE). The GRACE domain confers the sugar-responsiveness of MondoA/ChREBP activity, which is suppressed by the LID domain upon a low glucose condition (87). In addition, there are five identified conserved regions in GSM that are required for the regulation of cellular localization and the activity of MondoA/ChREBP. At the C-terminal region, MondoA/ChREBP has a bHLH/LZ region and a cytoplasmic localization domain (DCD), which allows dimerization with the interacting partner, Mlx, for binding to the target genes (Fig. 1.2).

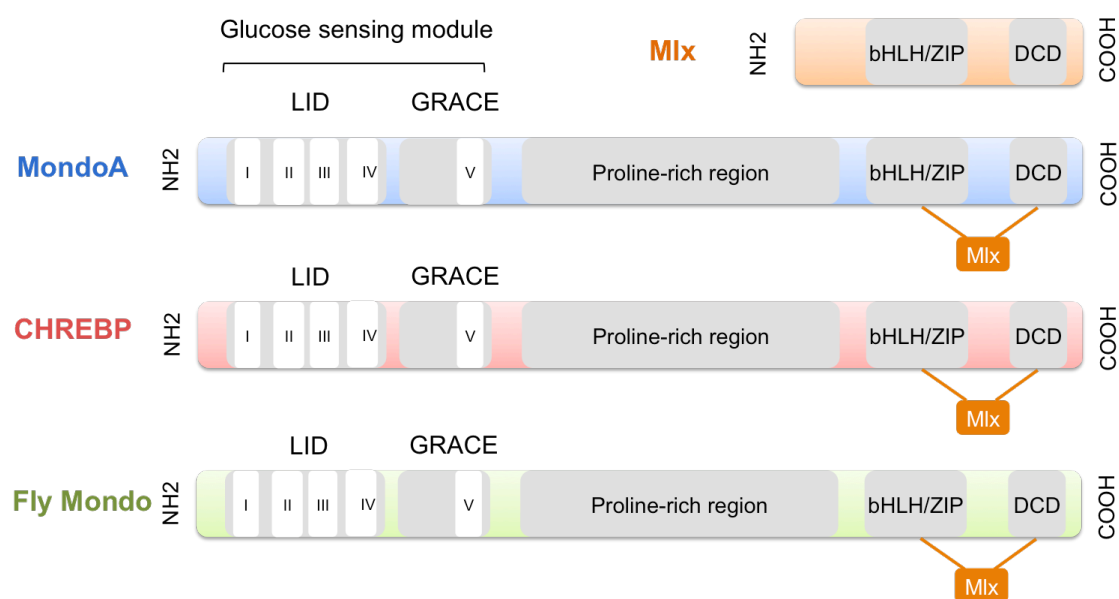


**Figure 1.2. Structural domains of human Mondo and Mlx proteins and fly Mondo.** Figure modified from Ma *et al.*, 2006. The full-length proteins MondoA and ChREBP are highly conserved and share several functional domains: the GSM, which includes the five Mondo conserved regions indicated by the roman numerals; a polyproline region; a basic helix-loop-helix/Zip domain; and a DSD domain for heterodimerization with MLX. The GSM is divided into LID and GRACE domains. The conserved regions are labeled with roman numerals from I to V.

ChREBP and MondoA are products of the genome duplication event in the early vertebrate lineage (88). The conservation in protein domains between ChREBP and MondoA supports common protein function. However, in general, the ChREBP protein sequence shows a greater divergence in most of the domains than MondoA during evolution across most species, suggesting that the MondoA sequence has undergone stronger selection than the ChREBP protein sequence. Hence, MondoA may have a more important role in survival, which causes the evolutionary constraints on these conserved protein sequences, though their biological importance still needs to be better understood.

ChREBP and MondoA both regulate the transcription of glucose-induced genes and share several common target genes, suggesting a redundant function of the paralogs. The major difference between the two is their expression profile. ChREBP is expressed in various tissues, including the liver, gut, adipose tissue, and pancreas (61), but MondoA is mainly expressed in the skeletal muscle (84, 89). To be specific, ChREBP regulates genes involved in carbohydrate metabolism and lipogenesis. Mice lacking ChREBP in the liver display glucose intolerance and insulin resistance (61, 90). Recent studies have shown that ChREBP has diverse roles in different tissues and functions as a central coordinator of metabolism; the tissue-specific function of ChREBP is described in detail in chapter 1.5. MondoA, on the other hand, promotes energy storage in the form of lipid and glycogen through the activation of corresponding enzymes in muscle. Moreover, MondoA inhibits insulin signaling and restricts glucose uptake by upregulating the expression of TXNIP and arrestin domain-containing 4 (ARRDC4), which suppresses insulin signaling (91). As ChREBP and MondoA have some similarities but also have different functions in mammals, it is sometimes difficult to distinguish the impact of these two proteins on downstream effectors. The fly genome contains only a single Mondo gene and thus has no genetic redundancy. Moreover, critical protein functional domains, such as the GSM and bHLHzip domains, are conserved in the fly and humans (Fig. 1.3). These make the fly an optimal animal model for exploring the functions of the Mondo-Mlx complex in metabolic pathways.

# 1. INTRODUCTION

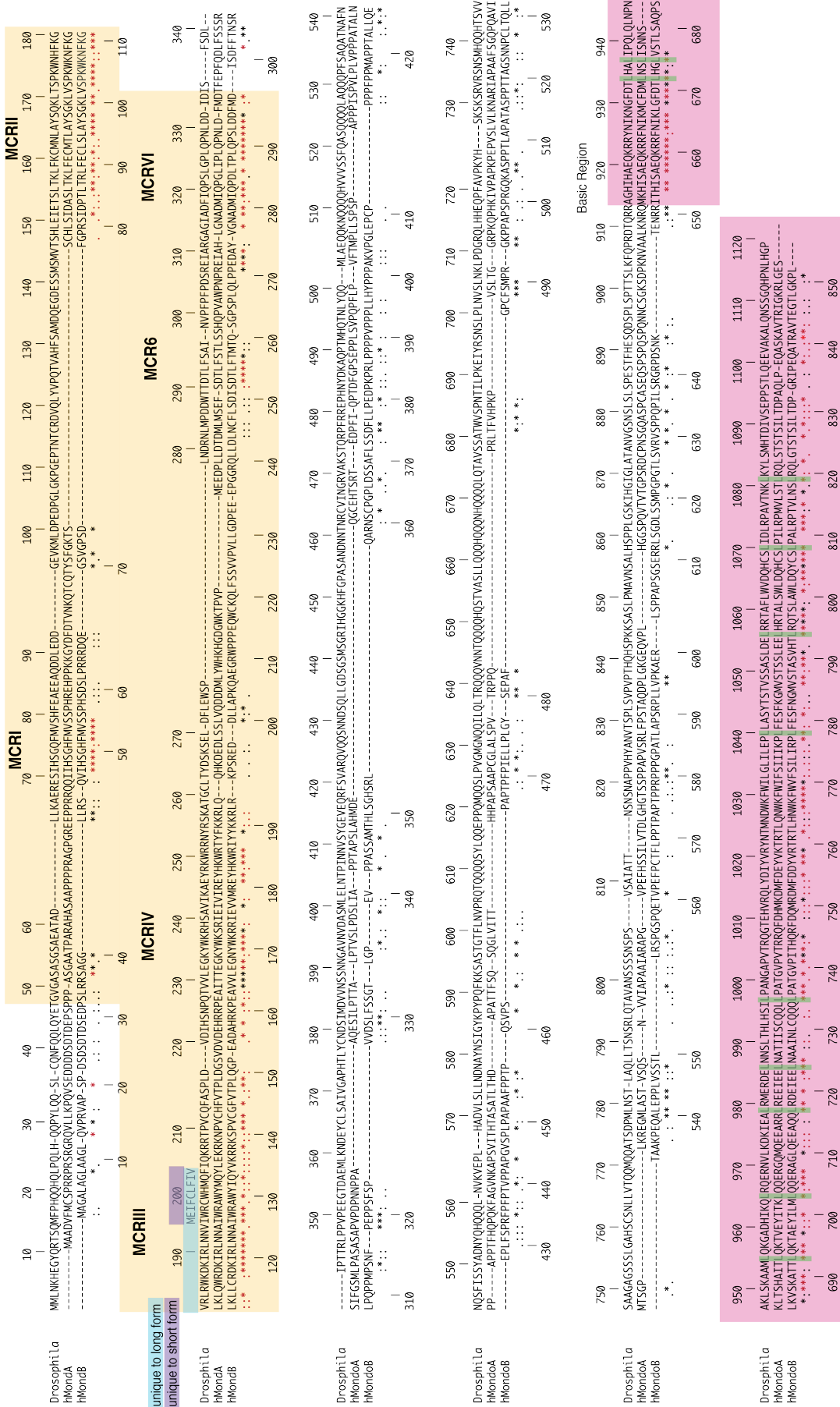


**Figure 1.3. Protein functional domains are conserved in the fly and human.** The protein sequence alignment of the fly Mondo (first line), human MondoA (second line) and human ChREBP (third line) are shown. The domain highlighted in the yellow box is the N-terminal GSM domain, while the one highlighted in the pink box is the C-terminal bHLHzip domain. Those in green within the pink box are the leucine zipper domain, and the conserved residues are labeled with a red asterisk. The figure is adapted from Carla Margulies. This figure uses the same nomenclature as in Figure 1.2, such as using roman numerals for the conserved regions.

### 1.3.3 Regulatory mechanisms of ChREBP activity

Maintaining carbohydrate homeostasis in a coordinated manner is essential to maintaining normal cellular processes and organ functions. Therefore, ChREBP, which has been shown to be a central regulator of carbohydrate homeostasis, needs to be tightly regulated. ChREBP protein activity can be regulated at several levels, such as intra-molecule interaction, binding with interacting proteins, post-translational modification, protein stability and subcellular localization (Fig. 1.4). The coordinated regulation of ChREBP transcriptional activity enables a balanced ChREBP-induced downstream response towards diverse physiological conditions in the organisms.

There are two ChREBP isoforms, ChREBP- $\alpha$  and ChREBP- $\beta$ ; each interacts with Mlx and forms a heterotetramer, which is necessary for DNA targeting and the induction of gene expression. ChREBP- $\alpha$  contains both the LID and GRACE domains in the GSM. Functional analysis of the domain-deleted ChREBP- $\alpha$  reveals that LID and GRACE may interact intra-molecularly and result in a repressive state of ChREBP (93, 94). In other words, under a low glucose condition, the LID domain restrains GRACE function by intra-molecular interaction (93). When glucose levels increase, the repression may be relieved; thus, ChREBP is activated. The newly identified ChREBP- $\beta$  has no LID domain and therefore stays constitutively active, which also supports the repressive LID-GRACE interaction. ChREBP- $\beta$ -promoter-luciferase assays indicate that glucose-induced ChREBP- $\alpha$  is required for the transcription of ChREBP- $\beta$ . In contrast, ChREBP- $\beta$  has been shown to downregulate ChREBP- $\alpha$  signaling in islet cells (95), suggesting a negative feedback loop of glucose-induced gene expression. The current model suggests that the direct binding of metabolites, such as glucose-6-phosphate (G6P) and fructose-2,6-bisphosphate (F-2,6-BP), to the LID domain can lead to a conformational change. Therefore, ChREBP can interact with Mlx and other coactivators (96).

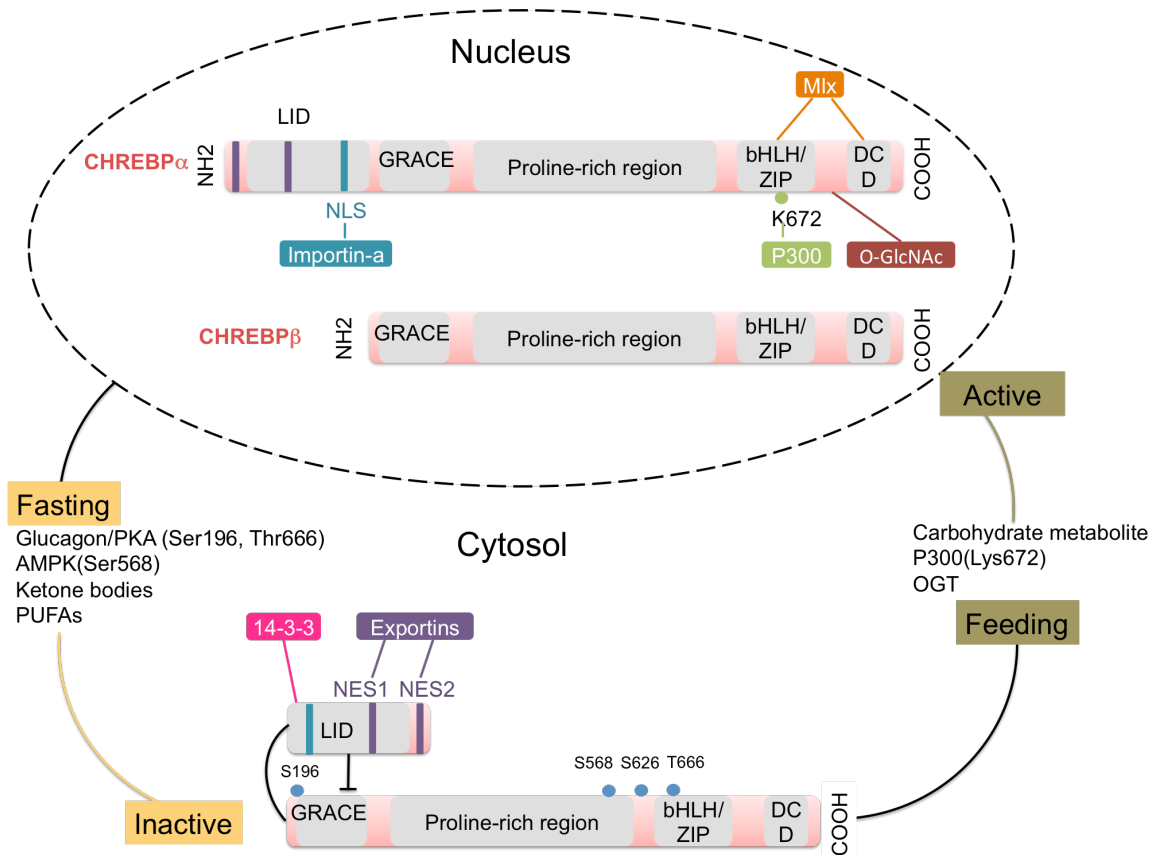


**Figure 1.4. The model of Mondo/ChREBP regulation in response to glucose.**

Figure modified from Abdul-Wahed *et al.*, 2017. The GSM domain of the Mondo/ChREBP protein contains a nuclear import signal (NLS) and two nuclear export signals (NES1 and NES2). The nuclear import factor and nuclear export factors bind to NLS, NES1 and NES2, respectively, to regulate their subcellular trafficking according to the nutritional states. The N-terminal GSM domain contains LID and GRACE domains, by which a dynamic intramolecular inhibition of ChREBP activity is formed. Low glucose levels repress the transactivity of GRACE by LID, whereas this intramolecular inhibition is released with a high glucose level. The shorter ChREBP  $\beta$  isoform lacks the LID domain and thus stays constitutively active (92). ChREBP activity is induced by acetylation on lysine and O-linked GlyNAcylation, while ChREBP is suppressed by phosphorylation on specific serine or threonine residues.

The post-translational modification of ChREBP is a major mechanism whereby ChREBP activity is regulated. Fasting-associated signals, such as AMPK and PKA phosphorylate ChREBP at Ser196, Ser568, Ser626, and Thr666, respectively (25,97), all lead to ChREBP inactivation. Xylulose 5-phosphate (Xu5P) specifically activates the protein phosphatase PP2A, which dephosphorylates ChREBP and therefore activates it. In addition to phosphorylation/dephosphorylation, O-linked GlyNAcylation modification of ChREBP has also been found to be an important mechanism for ChREBP transactivity. O-GlcNAcylation not only increases its transcriptional activity but also stabilizes ChREBP protein (98). The histone acetyltransferase (HAT) p300 interacts and acetylates ChREBP as a transcriptional coactivator, thereby promoting DNA binding of the complex (99). In turn, the activity of p300 activity is hindered by salt-inducible kinase 2 (SIK2), whose activity is regulated by the starvation signal (99, 100). The nuclear localization of ChREBP is regulated by nuclear transport signals and the respective nuclear transport factors.

A nuclear import signal (NLS) and two nuclear export signals (NES1 and NES2) in the N-terminal region of ChREBP appear to be important to the subcellular trafficking of ChREBP (101). The nuclear import factor, importin, binds to NLS within ChREBP to affect its nuclear importing, while nuclear export factor such as exportin and 14-3-3 bind to NES1 and NES2 to regulate nuclear export. Additionally, the binding of 14-3-3  $\beta$  to phosphorylated ChREBP prevents importin  $\alpha$  from binding to the NLS. ChREBP is therefore retained in the cytoplasm under a low glucose condition (102). Several metabolites, such as ketone bodies and adenosine monophosphate (AMP), increase ChREBP's affinity for 14-3-3  $\beta$  in hepatocytes and lead to subsequent nuclear export (24). Therefore, the inactivated ChREBP protein pool is stored in the cytoplasm upon starvation. As the glucose level increases, ChREBP translocates into the nucleus through interaction with importins and regulates the transcription of target genes (103).

The activity of ChREBP may also be affected by a single nucleotide polymorphism (SNP), which is a glutamine 241 to histidine missense mutation in the GSM region. This SNP is associated with a reduction in triglyceride levels, which may be the outcome of reduced ChREBP activity. Kooner *et al.* have hypothesized that the *chrebp* gene is a “thrifty gene” that enables individuals to efficiently convert

food to stored fat during periods of food abundance to provide energy when food is scarce (104). Nakayama *et al.* later supported this hypothesis based on the observing that the frequency of this SNP is much higher among Mongolian, Uyghur and Tibetan populations. Their primary food is dairy products, and their diet lacks sugar content (105). Therefore, the reduction of ChREBP activity may allow them to adapt to a metabolic switch from glucose to amino acids as the main energy source. However, evidence at the molecular level is needed to confirm the reduced activity of the Q241H variant of ChREBP.

In conclusion, the activity of the ChREBP-Mlx complex is coordinated by the regulation of interacting factors and the post-translational modifications that mediate both the cellular localization and transactivity of the protein complex upon different nutritional states. The essence of it is a sugar regulation activation mechanism, which in its molecular detail remains ill-understood.

### **1.3.4 ChREBP is at the center of interlinked transcription networks in response to different nutrition**

ChREBP-Mlx was originally characterized as a transcription factor that specifically mediates the sugar signaling and carbohydrate metabolism (85). Recent studies have suggested that ChREBP/Mondo-Mlx may sit at the center of an interlinked metabolic network by interacting with various transcription factors in response to different nutrient inputs such as sugar, amino acids and lipids (Fig. 1.5). Hence, it confers the ability of ChREBP/Mondo-Mlx to control metabolic adaptation in response to diverse nutrition landscapes.

### **The crosstalk between ChREBP and HNF4 $\alpha$ is responsive to sugar signaling**

Upon glucose induction, many transcription factors have been shown to physically interact with ChREBP. One of them is the HNF4 nuclear receptor, whose expression is stimulated by long-chain fatty acids and sugar (71, 106). Several lines of evidence suggest a direct interaction between HNF4 $\alpha$  and ChREBP. First, HNF4 $\alpha$  and ChREBP share a binding site that contains one E-box sequence within the promoter region of the pyruvate carboxylase gene (107, 108). Second, HNF4 $\alpha$  has been shown to co-immunoprecipitate with ChREBP in primary hepatocytes, indicating that

## 1. INTRODUCTION

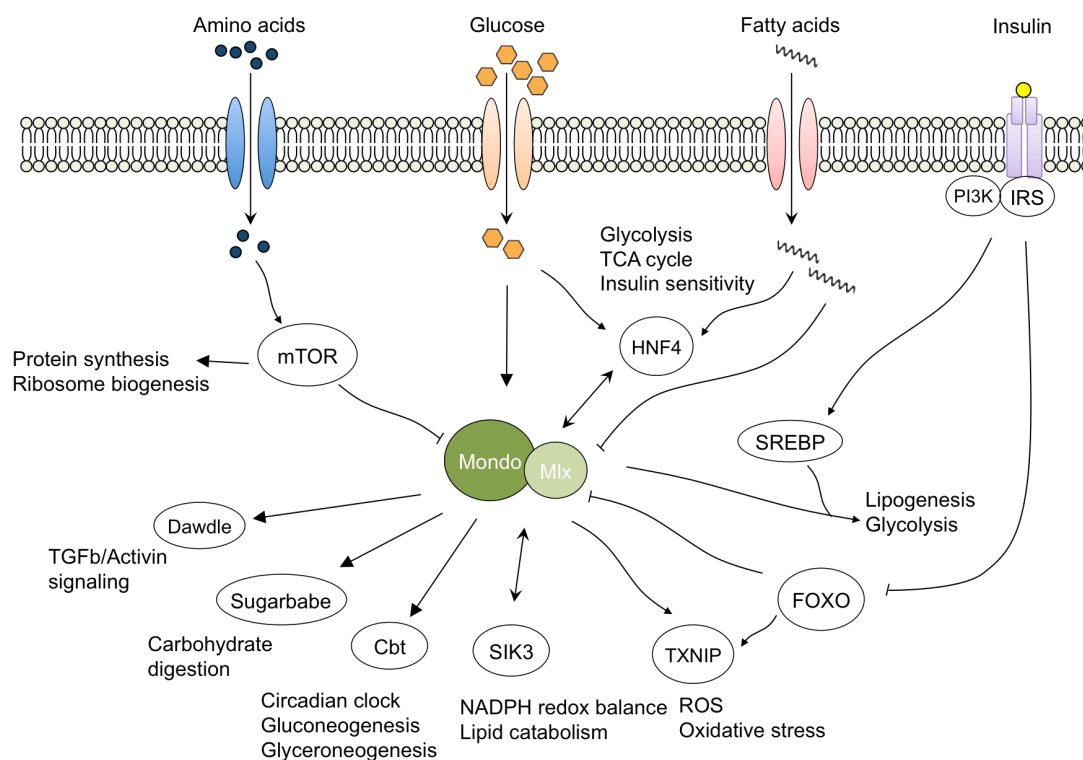


**Figure 1.5. Regulatory network composed of the interplay between ChREBP/Mondo and other nutrient-induced factors and the downstream effector.** ChREBP/Mondo-Mlx activity is directly switched on by sugar and inhibited by signaling factors such as FOXO, mTOR and AMP, which respond to insulin, amino acids and fatty acids, respectively. ChREBP/Mondo-Mlx acts alone with SIK3 on the PPP pathway, with SREBP on lipogenesis and glycolysis, and with HNF4 on the TCA cycle and glycolysis. In addition, Mondo-Mlx regulates the transcription of the second level of transcriptional regulators, including Cabut and Sugarbabe.

HNF4 $\alpha$  may act together with ChREBP to regulate the transcription of metabolic genes containing both ChoRE and direct repeat-1 (DR1) sites at the promoter regions under glucose induction (109). Finally, Burke and colleagues have demonstrated that the binding of the protein complex includes ChREBP and HNF4 $\alpha$ , which are required for the induction of *L-PK* gene in response to glucose (110). Additionally, more than acting jointly with ChREBP on downstream gene transcription, HNF4 $\alpha$  also activates the transcription of both ChREBP isoforms (111). This claim is supported by the observation of the increase in *ChREBP* transcription when HNF4 $\alpha$  is overexpressed and a decline in *ChREBP* mRNA levels when HNF4 $\alpha$  is knocked down. Interestingly,

ChREBP- $\alpha$  works synergistically with HNF4a to directly target to DR1 sites within the promoter of ChREBP- $\beta$ . The cross-talk between ChREBP and HNF4 may be necessary for transducing signals that originate from sugar inputs, as the protein-protein interaction is enhanced while glucose induction is increased (111).

### **ChREBP interacts with Salt-Inducible Kinase 3 (SIK3) to activate the pentose phosphate pathway**

The other example of ChREBP's interacting protein is Salt-Inducible Kinase 3 (SIK3). In the fly, Mlx and SIK3 act synergistically to activate the pentose phosphate pathway (PPP) upon sugar refeeding (112). As Mlx is commonly seen as the interacting partner of Mondo, the activity of the PPP is also considered to be Mondo-dependent (112,113). Evidence indicates that SIK3 enables flies to survive on high-sugar diets by suppressing oxidative stress with the reductive power of NADPH derived from PPP.

### **The interplay between ChREBP and SREBP links glucose and insulin signaling**

ChREBP links glucose signaling to insulin signaling by acting synergistically with the insulin-induced factor SREBP. SREBPs regulate the expression of genes involved in the metabolism of fatty acids, triglyceride and cholesterol in the liver (114,115). The most abundant isoform expressed in the liver is SREBP-1c (116), and it primarily regulates the genes involved in fatty acid biosynthesis (115). ChREBP and SREBP-1c have been shown to synergistically control *de novo* lipogenesis (DNL) and the lipogenic program in the liver. The genetic ablation of either fails to support the expression of lipogenic genes (72). In sum, these data indicate that ChREBP and SREBP-1c are necessary for the activation of glycolytic and lipogenic genes. Only the action of ChREBP on gene regulation is primarily responsive to glucose, but for SREBP-1c, insulin induces signaling.

### **FOXO1 and mTOR exert inhibitory effects on ChREBP activity**

FOXO1 is another transcription factor through which ChREBP links glucose signaling to insulin signaling, though FOXO1 is an inhibitory target of insulin signaling. FOXO1 suppresses ChREBP activity through inhibiting O-glycosylation

(117), an important post-translational modification (PTM), to maintain ChREBP stability in primary mouse hepatocytes (98). In line with this, the deletion of FOXO1 in mice livers leads to enhanced O-glycosylation and ChREBP levels, and the recruitment of ChREBP to the promoter of the L-PK gene (117). In addition, FOXO1 confers the inhibitory effect on TXNIP expression by competing for the binding site with ChREBP without affecting the expression and cellular location of ChREBP in INS-1  $\beta$  cells (118). Significantly, the ChREBP-TXNIP signaling axis has a critical influence on pancreatic  $\beta$  cell death, as it stimulates the generation of reactive oxygen species (ROS) and the resulting oxidative stress, which further leads to apoptosis (119, 120). It is interesting to note that mTOR, a well-known factor responsible for sensing amino acids, exerts signaling against apoptosis as protection in  $\beta$ -cells through direct binding to ChREBP to repress *TXNIP* expression, thereby inhibiting oxidative stress and mitochondrial dysfunction (121). Similarly, the levels of TXNIP and ChREBP are highly increased at both mRNA and protein levels in the diabetic and *mTOR*-deficient background in mouse islets. Conversely, mTOR overexpression decreases the induction of TXNIP and ChREBP and protects the  $\beta$  cell from apoptosis (121).

ChREBP sits at the center of the regulatory network in response to different nutrient inputs by interacting with different factors. Further, ChREBP also targets many second tiers of transcription factors and sits on the top of a transcriptional cascade. For example, in the fly, Mondo directly targets transcription factors such as Cabut and Sugarbabe. Interestingly, Cabut not only controls the expression of metabolic genes, but also those involved in the circadian rhythm in response to sugar feeding. Sugarbabe maintains lipid homeostasis by inducing the expression of lipogenic genes upon sugar feeding. The activation of ChREBP activity predominantly depends on increased sugar signaling. The interplay between ChREBP and other nutrients/insulin-regulated transcription factors not only provides additional levels of regulation on gene transcription by ChREBP, but also integrates the signals from different nutrition inputs, allowing the organism to exert subtle metabolic adaptation to the complex intracellular environment. Meanwhile, the molecular crosstalk between ChREBP and other important metabolic regulators may enable more pharmacological opportunities.

## **1.4 Metabolic adjustment in the fasting-refeeding cycle**

### **1.4.1 Metabolism of the fed state**

The metabolism of the fed state is an anabolic process in which absorbed nutrients are utilized for energy synthesis and storage. In the fed state, insulin is secreted and drives the entry of glucose into the liver, muscle and adipose tissue. Overall, the liver helps maintain blood glucose levels by storing it as glycogen when glucose is abundant and by releasing glucose when food is scarce. When glucose or the glucogenic precursors (such as pyruvate and lactate) exceed the storage capacity of the liver, they can be converted into fatty acids and amino acids. Glucose is also taken up by adipose tissue, where the metabolic-intermediate glycerol-3-phosphate is generated and used for the synthesis of triacylglycerols, which are the storage molecule of fatty acids (122). Moreover, the action of insulin extends to the metabolism of amino acids and protein. Insulin stimulates the uptake of branched-chain amino acids into the muscle in the postprandial period (123). Insulin also stimulates protein synthesis and inhibits protein degradation in muscles (124, 125).

### **1.4.2 Metabolism of the starvation state**

The blood-glucose level needs to be maintained within a narrow range, even upon the starvation condition; therefore, metabolic adaptation to starvation is required to ensure sufficient glucose supply to the brain or RBCs. The metabolism of the starvation state can be divided into early fasting and prolonged starvation states. During early fasting, glucagon is secreted and preferentially stimulates the breakdown of glycogen into glucose in the liver, allowing glucose to be released into the bloodstream again. In addition, glucagon promotes hepatic gluconeogenesis and blocks glycolysis to restore glucose levels. When hepatic glycogen is completely depleted during starvation, the carbon chain of amino acids, particularly alanine and glutamine, become the major source for gluconeogenesis (126, 127). Gluconeogenesis derived from amino acids eventually slows as the supply of amino acids from muscle protein degradation decreases. However, glycerol released from adipose tissue can also contribute to a low level of gluconeogenesis in the liver (128). A low insulin level during starvation also inhibits the uptake of glucose by the liver and muscle, resulting in the switch of fuel usage from glucose to fatty acids in these two tissues. The fatty acids can be

catabolized to acetyl-CoA by the process of  $\beta$ -oxidation; the acetyl-CoA is subsequently oxidized via the TCA cycle for energy production. When starvation is prolonged, the fatty acids are also converted to ketone bodies in the liver (129). These ketone bodies can serve as an energy source for all tissues except those without mitochondria, such as RBCs. The brain, the most energy-consuming organ, also slowly switches to the use of ketone bodies during prolonged starvation.

### 1.4.3 Metabolism of the refed state

During the refed state, fat is metabolized in the same way that it is processed in the fed state. However, the liver does not take up glucose during the transition from fasting to the refed state; rather, other peripheral tissues do. This is because the liver is still in a gluconeogenic mode to restore the liver's glycogen levels (130). After the glycogen stores are replenished in the liver, excessive glucose is processed for fatty acid synthesis, as it is in a normal fed state. Refeeding after a fast also leads to a rapid metabolic switch, including a decrease of serum ketone bodies and free fatty acids (131).

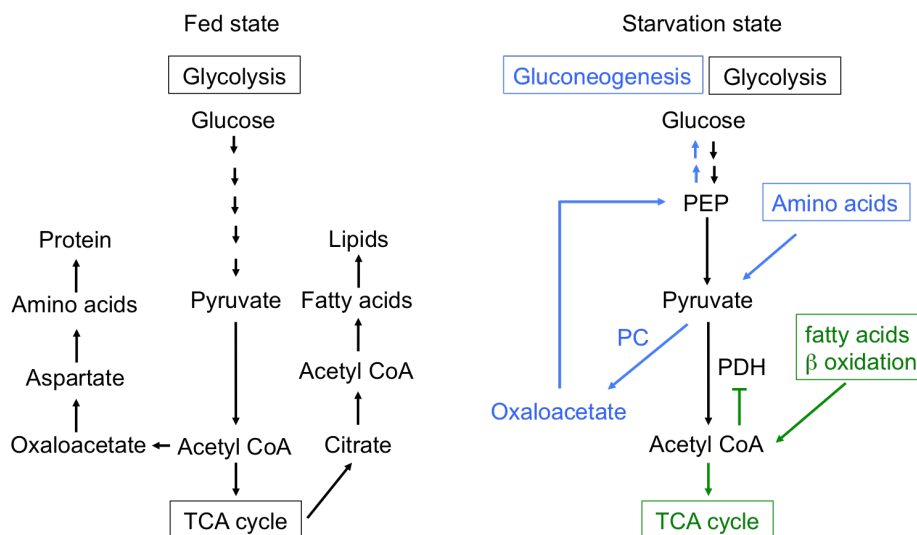


**Figure 1.6. Metabolic adjustment upon fed and starvation states.** In the fed state, carbohydrates are the main source of Acetyl-CoA, which is used in the TCA cycle to generate energy. Upon starvation, glucose is quickly used up for energy generation. Amino acid skeletons are then converted to pyruvate and continue to be made into glucose. Acetyl CoA is then mainly made from the  $\beta$ -oxidation of fatty acids. Green

depicts the  $\beta$  oxidation pathway from fatty acids, and blue depicts the gluconeogenesis pathway from amino acids.

### 1.5 Dynamic functions of ChREBP/Mondo protein in different tissues

ChREBP is predominantly expressed in active sites of *de novo* lipogenesis: the liver and adipose tissues, where it has been shown to be the key regulator of lipid metabolism (61). Additionally, ChREBP is also highly expressed in the pancreatic  $\beta$ -cells and the intestine. To a lesser extent, the expression of ChREBP was also identified in the brain (61,132,133). Owing to the distinct function that ChREBP plays in different tissues, ChREBP is considered the central coordinator of metabolism. ChREBP's role in specific tissues is discussed in this section (Fig.1.7).

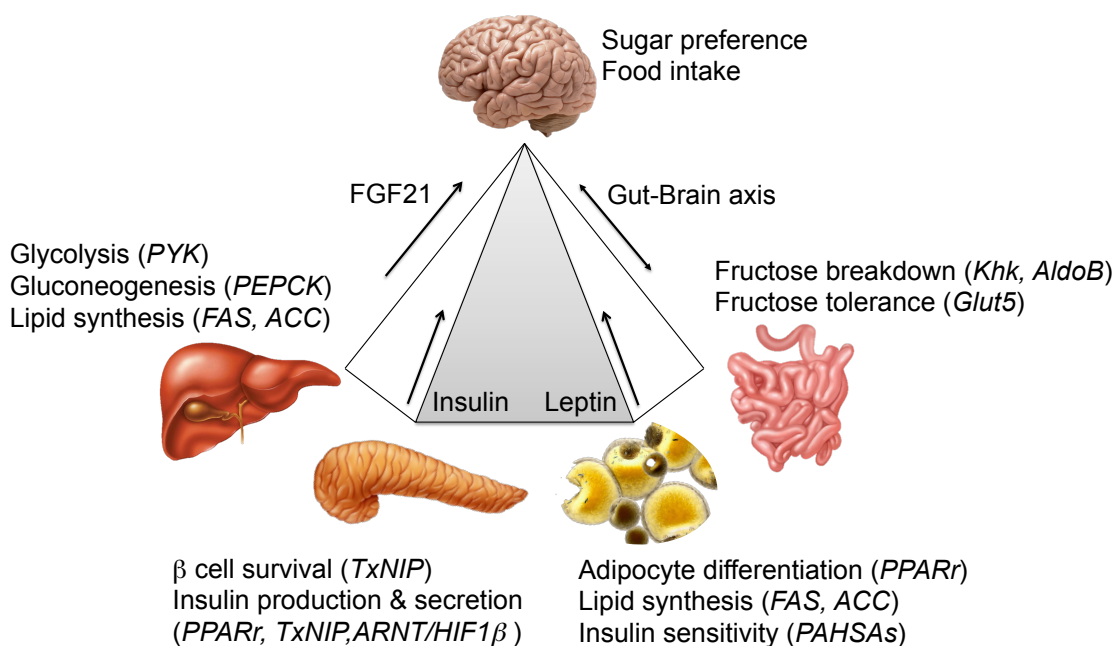


**Figure 1.7. ChREBP functions as a central metabolic coordinator in various cell types.** The functions of ChREBP in each tissue are listed, and the target genes involved are shown in the brackets. ChREBP directly or indirectly regulates the downstream signaling, which is transported to brain and affects the food intake or preference systemically.

### **1.5.1 ChREBP regulates sugar-induced *de novo* lipogenesis in the liver**

The liver is the primary organ where *de novo* lipogenesis (DNL) takes place. Evidence shows that the hepatic ChREBP is essential in regulating lipogenesis in the liver. The downregulation of ChREBP in hepatocytes reduces the expression of genes in glycolysis and lipogenesis, thus decreasing lipid accumulation. This finding is supported in that the inhibition of ChREBP in obese mice leads to the reversal of hepatic steatosis, which exhibits increased hepatocellular triglycerides (TG; 132). However, the global metabolic effects of hepatic ChREBP on insulin sensitivity seem to be controversial in healthy or diseased backgrounds. Mice that are deficient in ChREBP in the liver display intolerance to sugar and insulin resistance (61, 90), whereas the inhibition of hepatic ChREBP in the insulin-resistant obese mice improves insulin sensitivity (132).

In addition, ChREBP and SREBP-1c work synergically to regulate the lipogenic program in the liver. The expression of SREBP-1c at mRNA and protein levels is downregulated in the liver-specific ChREBP knockout mice. The overexpression of nuclear SREBP-1c only restores the expression of lipogenic genes partially, without affecting glycolytic genes. Similarly, ChREBP overexpression is unable to normalize the expression of lipogenic genes in the liver of SREBP-1c deficient mice compared with WT mice (75). Moreover, there is ample evidence that the expression of lipogenic genes through SREBP-1c is stimulated by insulin-mediated signaling (48, 136), while gene regulation by ChREBP mainly depends on increased carbohydrate signals. Taken together, these data demonstrate that ChREBP and SREBP-1c jointly regulate the induction of glycolytic and lipogenic mRNAs. The interplay between ChREBP and SREBP-1c on hepatic DNL ensures that the synthesis of fatty acids in the liver only occurs when insulin and carbohydrates are both present.

### **1.5.2 ChREBP controls adipocyte differentiation and systemic insulin sensitivity**

Two types of adipose tissue can be categorized: white adipose tissue (WAT) and brown adipose tissue (BAT), and they are functionally antagonistic. WAT stores excess energy as lipids, primarily in the form of triglycerides, whereas BAT specializes in burning fatty acids for heat production to maintain body temperature (137). The expression of ChREBP has been reported in both WAT and BAT. In

particular, the ChREBP  $\beta$  isoform has been shown to play an important role in lipogenesis in WAT by regulating the expression of lipogenic genes (94, 138). In addition to lipogenesis, ChREBP in WAT also regulates the genes involved in adipocyte differentiation (139). The increased ChREBP expression during this process has been observed in mouse cell lines and human precursor cells (140, 141), whereas the depletion of endogenous *ChREBP* or the expression of dominant-negative ChREBP in progenitor cells decreases lipid accumulation and hinders adipocyte differentiation (141). WAT ChREBP also contributes to favorable effects on glycemic control, which is supported by the fact that the benefits of the overexpression of GLUT4 in WAT on glycemic control are lost in ChREBP-deficient mice (94). Furthermore, WAT ChREBP is linked to insulin sensitivity. ChREBP directly or indirectly regulates the transport and metabolism of glucose in adipocytes, as well as the secretion of fatty acids, adipokines and cytokines, which are now known to induce systemic insulin resistance.

ChREBP has a significant impact on the regulation of BAT function, as well. Mice that lack ChREBP show a general reduction of adipose tissue, in particular a 43% decrease in BAT. Moreover, these mice become hypothermic when fed a high-sucrose diet (61). It has been shown that the negative feedback loop between ChREBP and PPAR $\alpha$  may maintain the homeostasis of lipid metabolism in BAT (142). A recent study has shown that BAT activity is induced by the active thyroid hormone triiodothyronine (T3), which upregulates the expression of the *ChREBP* gene and the downstream effectors of ChREBP (143). In addition, expanding the activities of BAT reduces metabolic disorders such as obesity in mice (144, 145). These data indicate that ChREBP is a potential target for the therapeutic regulation of BAT activity as a defense against metabolic disorders.

### **1.5.3 ChREBP promotes the proliferation of $\beta$ cells**

ChREBP is expressed during the pancreas development, and its level increases during differentiation (146). In addition, ChREBP expression depends on the regulation of FOXA1/2, the important regulators for the development and maintenance of metabolic-associated tissue (147). Nevertheless, ChREBP does not appear to be necessary for pancreatic differentiation, as homozygous ChREBP knockout

(*ChREBP*<sup>-/-</sup>) mice display an increased insulin response upon high sugar feeding when compared with wild type mice (61). On the other hand, evidence suggests that ChREBP promotes  $\beta$  cell proliferation. In the adult pancreas, ChREBP exerts the glucose-induced proliferative effect on  $\beta$  cells by upregulating the cell-cycle accelerators (148). At the mechanistic level, Schmidt *et al.* have shown that ChREBP mediates the glucose-stimulated expression of the cell-cycle genes by inducing transcription factors, including the RAR-related orphan receptor (ROR)  $\gamma$ , which promotes  $\beta$  cell proliferation (149). In line with the mechanism of glucose-induced  $\beta$  cell proliferation, the calcium influx under a high glucose condition induces ChREBP dissociation from Sorcin, allowing ChREBP to shuttle into nucleus and drive proliferation (150). Besides having a role in mediating  $\beta$  cell proliferation, ChREBP also regulates  $\beta$  cell survival in association with mTOR signaling to decrease the expression of TXNIP, a key inducer of oxidative stress and apoptosis (121).

### **1.5.4 Intestinal ChREBP is required for fructose tolerance**

ChREBP expression has been detected in the intestine (61), but only in recent years has its intestinal function in association with fructose tolerance been uncovered. The intestine is the first place for the absorption and breakdown of fructose. The fructose absorption capacity of the GLUT5 in the small intestine is limited under a high fructose condition (151); thus, the overconsumption of fructose can lead to fructose malabsorption, which is known to be a potential cause of irritable bowel syndrome (152). ChREBP regulates the expression of the fructose transporter (Glut5), fructolytic enzymes and gluconeogenic genes in the small intestine. ChREBP deficiency in the intestine can result in fructose intolerance. It is supported by the observation that high-fructose-fed ChREBP knockout mice display a distended cecum and serious diarrhea, indicating the incomplete absorption of fructose (153). In sum, intestinal ChREBP is indispensable for fructose tolerance, which is potentially important in the prevention of inflammatory bowel disease.

### **1.5.5 ChREBP in the brain may mediate feeding behavior**

ChREBP/Mondo has been detected in the brains of mice, rats and flies (61, 132, 133, 154, 155), and its role in the brain has begun to be explored. Docherty *et al.* have

shown that the pan-neuronal knockdown of Mondo leads to enhanced triglyceride and glycogen levels, while the knockdown of Mondo specifically in insulin-producing neurons leads to increased food intake associated with an upregulation of dILP3. These data indicate that Mondo in the brain may control systemic carbohydrate homeostasis through mediating feeding behaviors. Interestingly, the crosstalk between peripheral ChREBP and PPAR $\alpha$  contributes to the expression of fibroblast growth factor 21 (FGF21) in the liver, which later acts on specific brain regions to mediate sugar preference (156).

# Chapter 2

## Investigating sugar- and starvation-induced phenotypes of the Mondo-Mlx-deficient fly

### 2.1 Summary

In this chapter, Mondo is shown to play different roles at different developmental stages and in different nutritional states in flies. A severe lethality during development has been observed in Mondo<sup>K05106</sup> mutants, CRISPR-induced Mondo mutants and Mondo knockdown flies that have been raised on a high-sugar diet in comparison to their corresponding genetic controls and low-sugar-diet controls. The death of Mondo-deficient flies before entering the adult stage has also been observed during high-glucose and fructose diets, indicating that Mondo is required for survival on a high-sugar diet, regardless of the sugar type. Overall, these data confirm that Mondo is essential in maintaining carbohydrate homeostasis during development.

Nevertheless, adult flies show a different phenotype compared to developing flies. Adult Mondo<sup>K05106</sup> mutants only display sugar intolerance when they are fed sugar-based food. They are able to tolerate the high sugar level provided that the food is nutritionally balanced (sucrose and yeast). Although WT adult flies can survive better than mutants that have been fed sugar-based food, these WT flies still behave worse than those on a nutritionally balanced diet. Collectively, these data suggest that Mondo has different roles in the larvae and the adult flies.

In addition, a potential role of Mondo in response to starvation has recently been discovered. Surprisingly, Mondo<sup>K05106</sup> mutant flies are more sensitive to starvation compared to WT flies that have been fed protein-based food instead of sugar-based food. Hence, the underlying mechanism of this Mondo-dependent phenotype in terms of starvation warrants further investigation.

Mondo's expression profile in different tissues was determined with the GFP-tagged Mondo fly line, which harbors functional fused GFP-Mondo protein. A

prominent GFP signal was mainly observed in the fat body of the flies. In addition, the contribution of tissue-specific Mondo to sugar tolerance was examined. However, sugar-induced lethality was not observed among the flies lacking Mondo in the fat body, neuron and glia. In addition, there was no observable alteration to the food intake in the tissue-specific Mondo knockdown flies.

## 2.2 Introduction

In the past two decades, Mondo/ChREBP has been shown to be the key regulator in sugar and lipid metabolism. This role has been supported by the intolerance to sugar and the change in metabolic gene expression profile displayed in Mondo/ChREBP-deficient animals (113, 157, 158). In addition, ChREBP<sup>-/-</sup> mice have been characterized as suffering from hypothermia and hyperglycemia. The lethality rate of these mice has also been shown to be greater than 50% upon a high-sugar diet (61), reflecting the adverse effects of sugar toxicity on Mondo/ChREBP-deficient animals.

The *Drosophila* Mondo has been identified from a screen for genes that increase the hemolymph glucose levels in larvae (16). Mondo-dependent lipogenesis confers protection against hyperglycemia in high sugar-fed larvae (60). Interestingly, the ablation of Mondo in the fly fat body leads to feeding aversion, suggesting its potential role in the coordination of feeding behavior with nutrient availability (159). The role of Mlx, the interacting partner of Mondo, in sugar metabolism has also been assessed in flies. Havula *et al.* have previously shown that sugar metabolism is mis-regulated in Mlx mutant larvae. In addition, evidence from chromatin pull-down assays (157, 160) and the modeling of the protein-DNA binding structure (161) support the finding that Mondo requires Mlx for DNA binding. The formation of a heterodimeric complex of Mondo-bound-Mlx has been shown to regulate sugar metabolism.

Mondo/ChREBP has been demonstrated to be an important factor involved in metabolically distorted conditions. On the other hand, Mondo may be involved in adaptation upon starvation, as it interacts with several “starvation factors” such as FOXO and FGF21 (162, 163). It is intriguing to study whether Mondo is required for energy mobilization upon starvation. In addition, several studies have demonstrated

the function of Mondo/ChREBP at the systemic level; however, the tissue-specific function of Mondo/ChREBP is still unclear. Mondo/ChREBP is expressed in the liver, intestine, adipose tissue, muscle, kidney and brain (61, 133). In mice, hepatic ChREBP has been shown to regulate FGF21 to mediate the preference for sugar (134, 135, 164). Havula *et al.* have also reported a fat body-specific Mlx expression can rescue the development and the adult emergence of the Mlx mutants. In addition, the neuronal-specific expression of Mondo rescues pupation of the Mlx mutants up to 20%, as well. The expression of fat body-specific Mlx has also rescued the overly high circulating glucose in Mlx mutants. These findings indicate the functional importance of Mondo-Mlx in the fat body, and potentially in the central nervous system. In addition to the essential role in sugar sensing and metabolism in the fat body, several lines of evidence suggest that Mondo also plays a role in the brain in the control of nutrient storage and feeding behavior (155). Thus, this project investigates the tissue-specific functions of Mondo, particularly in the fat body and CNS.

In this project, I have focused on understanding the role of Mondo by addressing its function upon different nutritional statuses (feeding/starvation), at different life stages (larva/adult), on different sugar diets (glucose/fructose) and in different cell types (fat body/CNS). I report that the sugar intolerance phenotype has been observed in Mondo knockdown flies and two different Mondo mutants (Mondo<sup>K05106</sup> and CRISPR-Mondo). Mondo has been shown to have different roles in sugar tolerance between the adult and larval stages. In addition, I show that Mondo is involved in starvation adaptation in a nutrient-dependent manner. Surprisingly, Mondo mutants that have been on a protein-based diet instead of a sugar-based diet did not survive after 21 hours of starvation. This suggests that Mondo may regulate the storage or mobilization of protein as an energy source. Lastly, we studied the effect of knocking down Mondo in the fat body, neurons and glia on the survival of flies on high-sugar diets. However, these cell-type-specific Mondo knockdowns did not result in lethality during development.

### 2.3 Methods

**CRISPR/Cas9 Mondo knockout fly was done in collaboration with the lab technician Teresa Burrell. Hui-Lan designed the CRISPR strategy and cloned the constructs. Embryo injection and fly characterization were done by Teresa Burrell. CAFÉ experiments were also performed by Teresa Burrell.**

#### 2.3.1 Fly husbandry

Flies were kept on standard media at 25°C for maintenance. The following strains were used: 2202U2 (wild-type; 165) Mondo<sup>K05106</sup> mutant (Kyoto center stock no.102338), tubulin-GAL4 (Bloomington stock center no.5138), takeout-GAL4 (166), ppl-GAL4 (Bloomington stock center no.58768), nsyb-GAL4 (Bloomington stock center no. 458), repo-GAL4 (167), Act5C-Cas9,lig4 p[169] (168), PBac{Mondo-GFP.FPTB}VK00033 (Bloomington stock center no.42279), w[1118];PBac{768.FSVS-0}Mio[CPTI003395] (Kyoto center stock no.115402).

#### 2.3.2 Fly food

For standard fly maintenance, food containing agar 0.84% (w/v), dry yeast 6% (w/v), cornmeal 7.6% (w/v), sucrose 3.14% (w/v), glucose 6.27% (w/v), sodium potassium tartrate 0.87% (w/v), calcium chloride 0.07% (w/v) and Nipagin (methylparaben) 0.26% (w/v) was used. Additional dried yeast was added on top of the food before use. For studies on defined nutrients, larvae were grown on food containing 10% (w/v) dry yeast, 1% (w/v) agar and 2.5% (v/v) Nipagin in PBS supplemented with varying concentrations of sucrose, glucose or fructose.

#### 2.3.3 Viability assay

The Mondo<sup>K05106</sup> mutant and Tubulin-Gal4 driver were balanced with *CyO* and TM3 marked with both stubble bristles (*Sb*) and serrated wings (*Ser*), respectively, due to homozygous lethality on the standard laboratory fly food. For the Mondo<sup>K05106</sup>/*CyO* mutant, crosses were set up with 10 females and males on no sucrose (10% yeast) and high sucrose food (10% yeast+20% sucrose). Viability was calculated based on the emergence of Mondo-deficient (adult flies with straight wings) and Mondo-

heterozygous adult flies (adult flies with *CyO* wings). Homozygous *CyO* flies die. If 100% of the homozygous mondo mutant flies survive to adults, the expected ratio of the heterozygous *CyO* with wild-type mondo and the mondo mutant is 2:1. Therefore, the expected viability was calculated as  $100 \times \{(2 \times \text{No. flies with straight wings})/\text{No. flies with } CyO\}$  for Mondo mutant. A similar scheme was used for the ubiquitous knockdown experiments. The Tubulin-Gal4 driver was kept over the TM3, *Ser*, *Sb* balancer and crossed with a homozygous UAS-RNAi line. The expected outcome if 100% of the flies survived was half would have the genotype TM3, *Ser*, *Sb*; UAS-RNAi where the RNAi is not expressed, and half of the flies would have Tublin-Gal4; UAS-RNAi where the RNAi is expressed. The expected viability for ubiquitous knockdown flies was calculated as  $100 \times (\text{No. flies with straight wings}/\text{No. flies with } Ser, Sb)$ .

#### 2.3.4 RNA extraction and RT-qPCR

The total RNA of the whole fly was extracted using Trizol (Life Technologies, 15596018). RNA was treated with TURBO DNase I (ThermoFisher, AM1907) to digest double-stranded DNA. Reverse transcription was conducted to synthesize complementary DNA by using SuperScript III Reverse Transcriptase (Life Technologies, 18080085) and a random hexamer primer (Life Technologies, 48190011). RT-qPCR was carried out by using power up POWERUP SYBR Master Mix (Life Technologies, A25778) and a Chromo4 Real-Time PCR Detector (BioRad). Fly genomic DNA was used to make standard curves for the quantification of target genes. Quantification was normalized to the mRNA coding for the endogenous ribosomal protein rp49. The Mondo primers (Forward: GCGGCGTTACAACATAAAGA, Reverse: CTCCATGCGCAAAGCTTCAA) and rp49 primers (Forward: GGTTACGGATCGAACAAGCG, Reverse: TAAACGCGGTTCTGCATGAG).

#### 2.3.5 CRISPR Mondo mutant design

The general CRISPR mondo mutant approach used the scheme to insert a cassette that included an alternative splice site upstream of a stop codon. To aid screening for transgenic animals, the DsRed gene and an alternative splice site upstream of a stop

2. INVESTIGATING SUGAR- AND STARVATION- INDUCED PHENOTYPES OF  
THE MONDO-MLX-DEFICIENT FLY

---

codon were also included in the cassette (168). To target this cassette, single-strand guide RNA (sgRNA) target sites were designed by the web tool (<http://CRISPR.mit.edu>) from the Zhang laboratory for sequences of the fourth intronic region in the Mondo gene. The sgRNA template was produced using overlap PCR with a common scaffold primer, a shorter antisense amplification primer and a gene-specific primer containing a T7 promoter and sgRNA sequence. The sequences of all sgRNA primers are summarized in table 2.1.

Table 2.1 Primers used in generation of CRISPR-based Mondo mutant fly

Primer name	Primer sequence
<b>gRNA synthesis</b>	
Scaffold oligo	AAAAGCACCGACTCGGTGCCACTTTTTCAAGTTGATAACGGACTAGCCTTATTTTAAC TTGCTATTCTAGCTCTAAAAC
Antisense primer	AAAAGCACCGACTCGGTGCC
gene-specific primer-sgRNA1	TAATACGACTCACTATAGGGCAGTGTGGTCGGTTAGGTTTTAGAGCTAGAAATAGC
gene-specific primer-sgRNA2	TAATACGACTCACTATAGGGCGTGGGTATATTATTTAGTTTTAGAGCTAGAAATAGC
<b>T7 endonuclease I assay</b>	
Control primer-forward	ACACAAATAAGACTTTGGGACCT
Control primer-reverse	GCTCCACTTTTGCATAATTTT
gRNA1-500bp-forward	CGATCTGGCTATGTTTGCAT
gRNA1-500bp-reverse	GTGGGACTTTTTGCAGTGTT
gRNA2-500bp-forward	GAACAACAGTCTGCGTGGTT
gRNA2-500bp-reverse	TTTTGCACGGCATAACATACAT
<b>Homology arms</b>	
Left-Homology arm-forward	CGTCTCAGGACTTCTTGATGATACTTTTGTG
Left-Homology arm-reverse	CGTCTCACTGGACCGACCAACACTGCCATTCTTTA
Right-Homology arm-forward	CGTCTCATGTTTTAAGGATGTACAATAAGGTTTT
Right-Homology arm-reverse	CGTCTCAGCATATCCGAGTCGATTCCACATAGCCAT

The PCR product was checked by agarose gel electrophoresis with the expectation of seeing a single band. The PCR product with the correct pattern was then purified with the Qiagen MinElute kit (Qiagen, 28006). The *in vitro* transcription of the sgRNAs was performed using the T7-MEGAscript<sup>TM</sup> Kit (AM1354, Life Technologies). The purification of sgRNA was performed with the MEGAclear Transcription Clean-Up Kit (Life Technologies, AM1354). The activity of sgRNAs for each specific target site was evaluated in *Drosophila* Schneider 2 (S2) cells expressing myc-Cas9 (169). Cells were cultured in Schneider's *Drosophila* medium supplemented with 10% fetal calf serum (Life Technologies, 10270106) to 5-10 x 10<sup>6</sup> cells/ml at 25 °C. The cells were then diluted to 0.7 x 10<sup>6</sup>/ml and plated 1ml per well in a 24-well plate. 1 ug of sgRNA was diluted in a 50 ul serum-free medium in one tube. 4 ul FuGENE<sup>®</sup> HD transfection reagent mix (Promega, E2311) was added in a 46 ul serum-free medium in another tube. Then, the sgRNAs and FuGENE reagent

were mixed and incubated for 45 min at room temperature before being added to the well and mixed gently. After 72 hours, genomic DNA was extracted with the QIAamp DNA mini kit (Qiagen, 51304) followed by a T7-endonuclease I assay.

### **2.3.6 Plasmid construction**

Left and right homology arms with lengths of approximately 1.5 kb were amplified from the fly strain that was used for homology-directed repair. These two fragments were subsequently cloned into the pJET-1.2 vector by following the manual of the CloneJET PCR Cloning kit (Fisher Scientific, K1231). The golden gate cloning reaction was assembled from plasmids contain each homology arms and CRISPR donor cassette. The ligation reaction was performed using the following cycles: 10-15 cycles of 37°C, 5 mins and 16°C and 10 mins in a PCR machine. The plasmid-safe nuclease reaction was assembled and incubated at 37°C for 60 mins. 5–10 ul of the reaction were transformed in bacteria. The primers used to clone homology arms are listed in table A2.1.

### **2.3.7 Embryo injection**

Approximately 1,000 Act5C-Cas9,lig4p embryos (168) were injected with pBS-donor (500ng/μl) and two sgRNAs (100 to 500 ng/μl each) using an inverted compound microscope and microinjector (Narishige IM-300). Survivor G0 flies were mated with 2202u white-flies, a Cantonized W1118 (165). The F1 progeny were screened for fluorescent red eyes. To avoid complications of carrying the Act5C-Cas, lig4 on the X chromosome, males were used to isolate any CRISPR insertions from continued Cas expression. The three positive insertions were mapped to the second chromosome, and the insertions verified the targeting event by genomic DNA PCR and sequencing.

### **2.3.8 Starvation resistance assay**

WT and Mondo<sup>K05106</sup> mutants were raised on yeast-only food with additional live yeast to obtain homozygous mutant flies. One- to two-day old flies were collected and maintained on yeast-only food for flies to mate. Mated females were separated from males on CO<sub>2</sub>; the flies were exposed to CO<sub>2</sub> for no longer than five minutes. The flies were transferred on yeast-only food to recover for one day. Flies were fed on

yeast-only, yeast + 20% sucrose food and sucrose-only food for another day, and they were then starved on agarose medium for 21 hours. Fly survival was calculated after.

### **2.3.9 Feeding assay**

Flies starved for 21 hours were transferred to fresh food containing 0.5% Brilliant Blue FCF and fed for 1 hour. After feeding, flies were homogenized in 200  $\mu$ l of PBS + 1% Tween 20 (PBST). Samples were centrifuged, and 100  $\mu$ l supernatant was added into a 96-well plate. The absorbance of samples was measured in a plate reader (TECAN infinite M1000) at 630 nm. Flies exposed to non-dyed food were used as the baseline during spectrophotometry. The amount of labeled food in the fly was calculated from a standard curve made by serial dilution in PBST of blue dye.

### **2.3.10 Immunohistochemistry**

Adult flies were fixed with 4% paraformaldehyde (PFA) for 1 hour at 4°C and then embedded in cryo gel (Structure Probe, Inc.). The sample was frozen in liquid nitrogen before sectioning at 40  $\mu$ m horizontally on a cryostat. Frozen samples can also be stored at -80°C. The slides were washed with 1x phosphate-buffered saline (PBS) buffer for 30 min and subsequently incubated in the blocking solution (PBS, 2% Bovine serum albumin, 0.2% Triton X-100) for another 30 min. Rabbit anti-GFP antibody (Life Technologies A-11122, 1 : 200) was used to probe GFP protein. The immunohistochemical signals were detected with goat anti-rabbit IgG, Alexa Fluor® 488 conjugate (ThermoFisher, 1:200) for GFP. Nuclei were counterstained with Hoechst reagent (Fisher Sci. 1:1000). The coverslips were then slowly placed on the slides to avoid bubbles and sealed with transparent nail polish. The images of the samples were obtained with a confocal laser-scanning microscope (LSM-710, Zeiss), and were processed using Fiji (ImageJ 1.48r, <http://imajej.nih.gov.ij>)

### **2.3.11 Statistical analysis**

The statistically significant difference between the controls and experimental group was determined by an unpaired Student's t-test with assumed unequal standard deviation in each group. Data are shown as mean  $\pm$  SEM.

## 2.4 Results

### 2.4.1 *Drosophila* requires Mondo-Mlx to develop on high-sugar food

Mondo and its interacting partner Mlx have an essential role in the regulation of carbohydrate metabolism in the developing fly (113, 157, 159). Mondo-deficient animals, both in mice and fly models, have elevated blood/hemolymph sugar levels and die on a high-sugar diet (61,157). To confirm this developmental sugar intolerance phenotype caused by Mondo deficiency in the fly, survival to the adult stage was examined with the Mondo<sup>K05106</sup> mutants containing a P-element insertion in the intronic region of the *mondo* and *Gr39a* gene (170) and several RNAi-induced Mondo and Mlx knockdown flies while raising them on high- or low-sugar food ( Fig. 2.1A).

The Mondo<sup>K05106</sup> mutants and wild type flies were raised on yeast-only and yeast +20% sucrose food, and the number of adult flies that emerged was counted. On food lacking additional sucrose, mutant flies develop normally into adult flies that are comparable to WT flies. In contrast, on food containing 20% sucrose, the Mondo<sup>K05106</sup> mutants are not viable (Fig. 2.1B). ) This Mondo-dependent phenotype was supported by the observation from RT-qPCR showing that the *mondo* mRNA expression level is significantly lower in the Mondo<sup>K05106</sup> mutant compared to the levels in WT, regardless of gender (Fig. 2.1C). However, because the P-element insertion in the Mondo<sup>K05106</sup> mutant line may affect the expression of *Gr39a* gene (171), we generated a CRISPR-induced Mondo mutant in which only the *mondo* expression was affected. The strategy was to use CRISPR/Cas9 to generate DNA double-strand breaks in the intronic region of *mondo* gene, then integrate the donor cassette containing a splice acceptor and a SV40 polyA terminator together with a 3xP3-dsRed eye reporter into the chromosome using the homology-directed repair (HDR) pathway (172; Fig.2.2A). The splice acceptor and SV40 polyA terminator enable the creation of a strong loss of function allele while a 3xP3-dsRed eye reporter was used to screen for mutant flies quickly under a fluorescent dissecting microscope. Three candidate mutants were isolated and mapped to the second chromosome, where the *mondo* gene is located. To help avoid the off-target effect, CRISPR mutation in the second chromosome was isolated genetically from the other founder chromosomes. In addition, the mutant was outcrossed to a wild-type genetic

background to avoid other potential CRISPR off-target mutations. The rate of three positive insertions to the approximately 1,000 injected embryos is similar to the rate reported by Zhang *et al.*, 2014. The screening identifies that only one of the positive DsRed flies had a significantly lower expression of *mondo* measured by RT-qPCR (Fig. 2.2B). This CRISPR *mondo* mutant is also not viable on high sugar (Fig. 2.2C), similar to the *Mondo*<sup>K05106</sup> mutant.

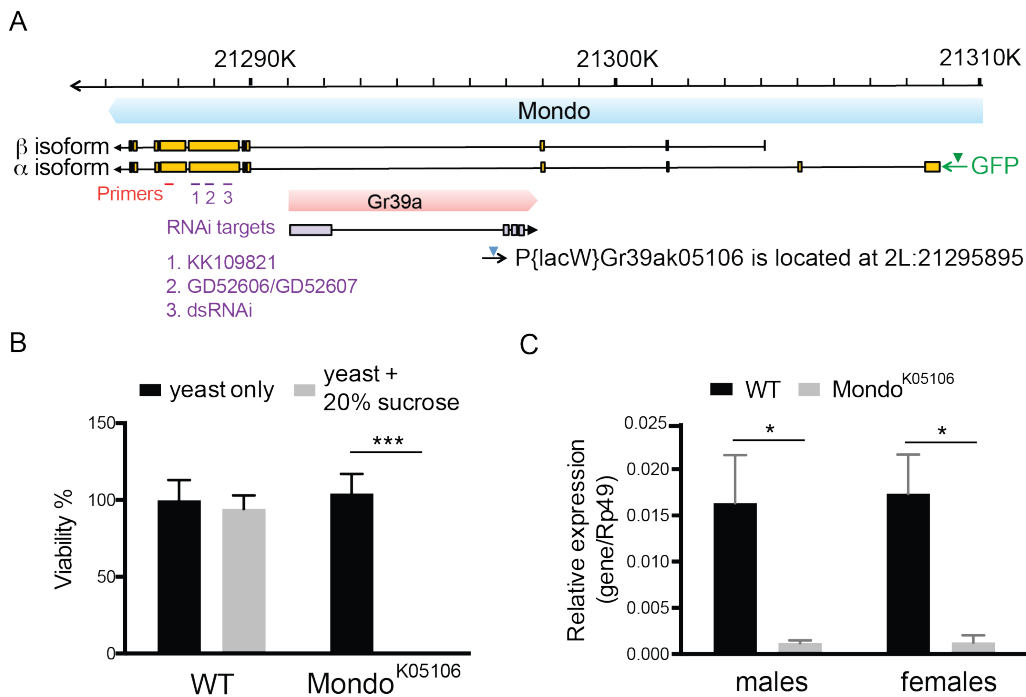


**Figure 2.1. *Mondo*<sup>K05106</sup> mutant fly is not viable on high sugar food.** (A) Schematic presentation of the P-element insertion site in the *Mondo*<sup>K05106</sup> mutant. The *mondo* gene is indicated in blue, with the 5' end of the gene orientated to the right and the 3' end at the left side of the diagram. The two transcripts originating from two different promoters are indicated in yellow. In pink, the gustatory receptor gene *Gr39a* is oriented in the opposite direction from *mondo*. One of the *Gr39a* transcripts is indicated in gray. The upside-down blue triangle indicates the insertion site of the P-element K05106. The RNAi targets for *mondo* appear in purple. A red line indicates the location of the *Mondo* primers used in RT-qPCR. The green text indicates the location of the GFP protein fusion in line Mio[CPTI003395]. (B) The *Mondo*<sup>K05106</sup> mutant can develop on yeast-only food but not on high-sugar content food. (C)

2. INVESTIGATING SUGAR- AND STARVATION- INDUCED PHENOTYPES OF THE MONDO-MLX-DEFICIENT FLY

Mondo expression is low in both male and female *Mondo*<sup>K05106</sup> mutants. The error bars represent  $\pm$  SEM (\*  $p < 0.05$ ; \*\*  $p < 0.01$ ; \*\*\*  $p < 0.001$ )

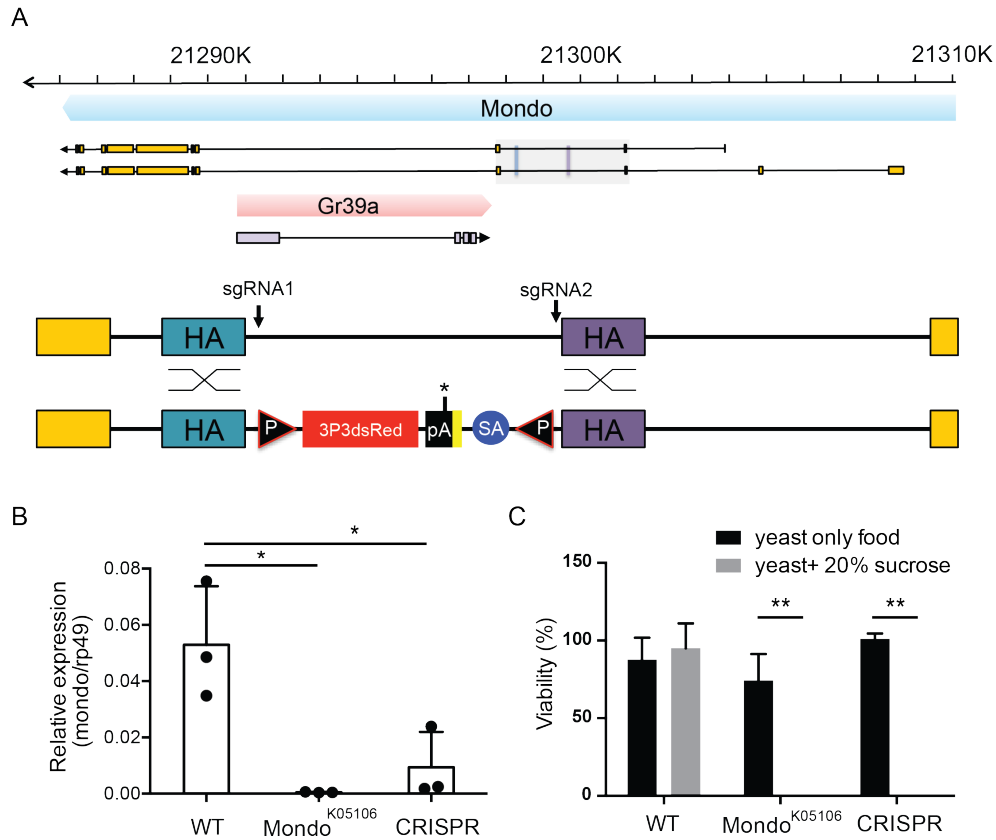
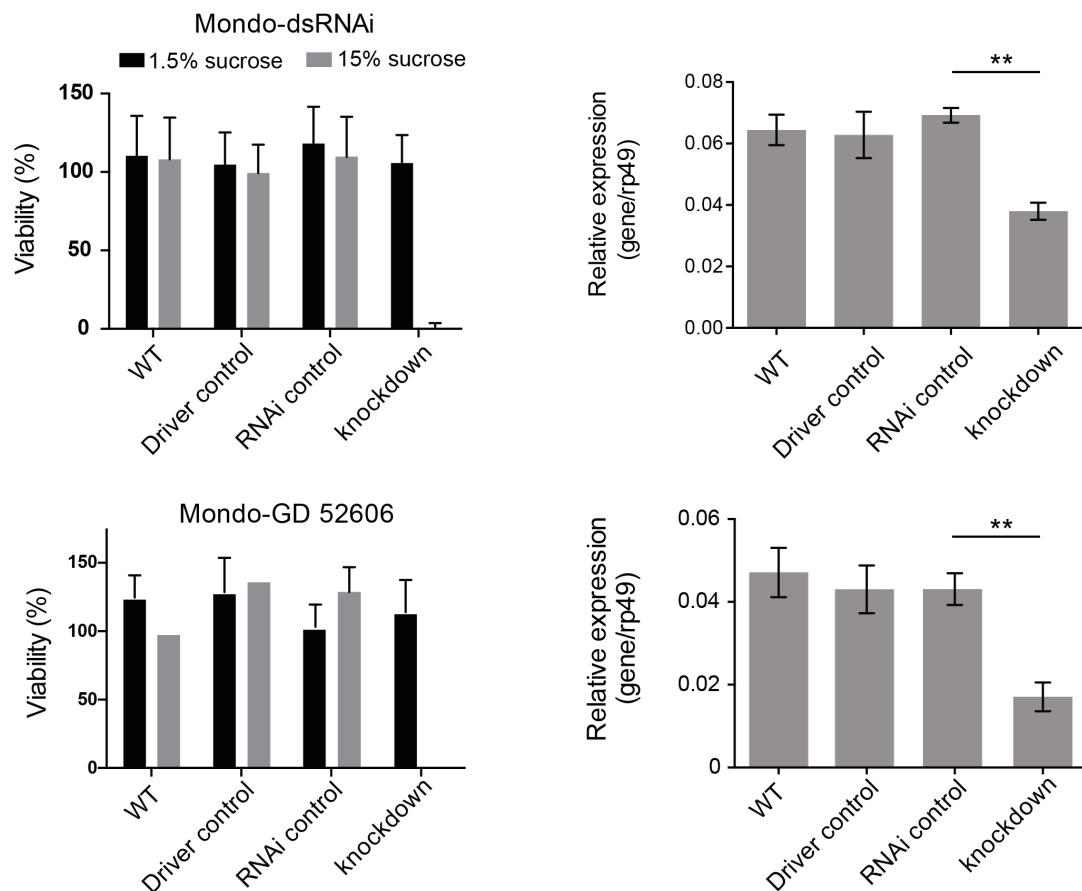


**Figure 2.2 Generating CRISPR/Cas9 *mondo* knockout fly.** (A) The strategy used to generate the *mondo* mutant. The top part of the diagram shows a map of the *mondo* gene, which is indicated in blue, and its two transcripts are indicated in yellow. The internal *Gr39a* gene is indicated in pink, and one of its transcripts indicated in gray. The gray box indicates the third intron of the *mondo* gene, the target of our CRISPR/Cas strategy. Within this box, the two homology arms are indicated, the left in blue and the right in purple. The bottom of the diagram contains the CRISPR donor cassette. HA: homology arms (blue and purple rectangle), a splice acceptor (blue circle), and a 3xP3 promoter with DsRed gene (red rectangle), P: attP sites (black triangles). pA: S40 poly A terminator (black rectangle), Stop codon (\*). (B) *mondo* expression in CRISPR *Mondo* mutant fly. (C) WT flies can survive on both yeast only and yeast+20% sucrose. *Mondo*<sup>K05106</sup> and CRISPR *Mondo* mutant flies died on high sugar. The error bars represent  $\pm$  SEM (\*  $p < 0.05$ ; \*\*  $p < 0.01$ ; \*\*\*  $p < 0.001$ )

## 2. INVESTIGATING SUGAR- AND STARVATION- INDUCED PHENOTYPES OF THE MONDO-MLX-DEFICIENT FLY

In addition, RNAi lines specific to *mondo* and *Mlx* mRNA were used and replicated the published results from the Hietakangas laboratory (157). The ubiquitous knockdown of Mondo and Mlx with Mondo or Mlx RNAi, respectively results in poor viability of flies. On no-sucrose food, there is no significant difference in viability between control groups and the Mondo and Mlx knockdown groups, except for knockdown flies by KK109821 Mondo RNAi flies (Fig. 2.3, left panel), which may be due to the off-target effect. The knockdown efficiencies from four separate Mondo RNAi lines and one Mlx RNAi line are between 25–60% (Figure 2.3, right panel). This data recapitulated the sugar phenotype shown in the Mondo<sup>K05106</sup> mutant and the CRISPR mutant. Taken together, these data indicate that the Mondo-Mlx complex has an important role in maintaining carbohydrate homeostasis in the fly.



2. INVESTIGATING SUGAR- AND STARVATION- INDUCED PHENOTYPES OF THE MONDO-MLX-DEFICIENT FLY

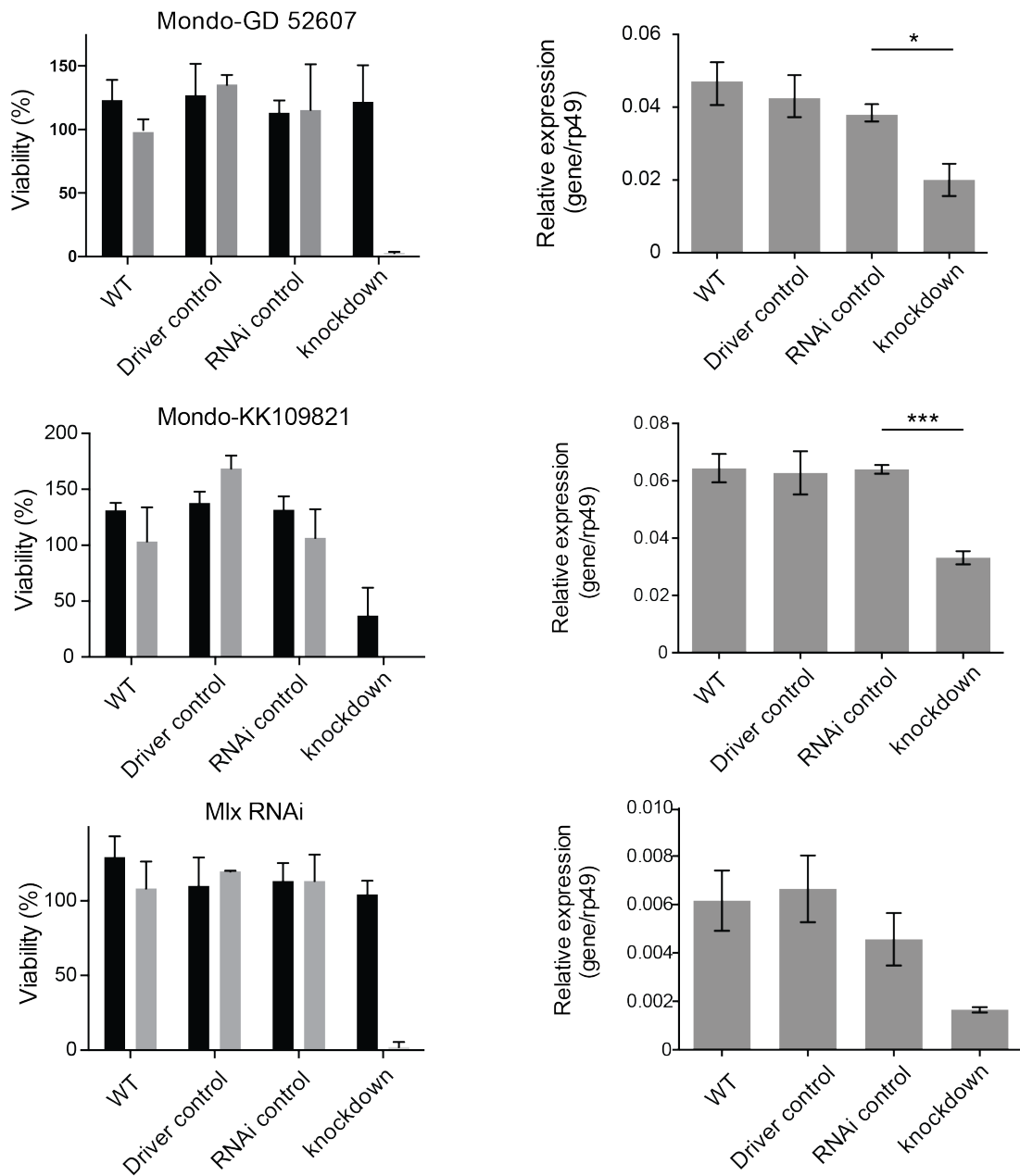


**Figure 2.3. Flies require Mondo and Mlx to survive on high-sugar food.** Mondo was ubiquitously knocked down in the fly with four different Mondo RNAi lines. Mlx was ubiquitously knocked down with an Mlx RNAi line. Monod/Mlx knockdown flies and control group flies were raised on low- (1.5% sucrose) and high-sugar (15% sucrose) food. Viability was calculated. The results of RT-qPCR on Mondo-Mlx are shown on the right. Error bars represent  $\pm$  SEM (\*  $p < 0.05$ ; \*\*  $p < 0.01$ ; \*\*\*  $p < 0.001$ ).

#### **2.4.2 Mondo is required for the fly to develop on both high-glucose and high-fructose diets**

Evidence from the human population study supports the correlation between the consumption of high-fructose corn syrup (HFCS) and the development of type 2 diabetes (173). However, it is still highly debated whether added sugar is the causative agent for the increased prevalence of metabolic diseases (174, 175). With regard to the metabolism of fructose and glucose, they are in fact not metabolized equivalently, though they share the same chemical formula. In a human study, an isotope tracer demonstrated that postprandial fructose but not glucose is incorporated *de novo* into triglycerides (176). In mice, fructose consumption increases hepatic *de novo* lipogenesis and serum triglycerides to a greater extent than isocaloric glucose loads and impaired inulin signaling over a 12-week period (177). Nevertheless, the effects of fructose on body weight are inconsistent across different studies.

Several studies have also investigated the regulation of ChREBP levels in response to fructose and glucose. Increased nuclear ChREBP protein is observed in the livers of mice with high-fructose diets compared with high-glucose diets or control diets (no supplementary fructose; 177, 178). As glucose and fructose undergo different metabolic pathways, and ChREBP is regulated by carbohydrates, ChREBP may have different roles in metabolizing different sugars. Because Mondo is clearly required for flies to develop on a high-sucrose diet (Fig. 2.2 C), and considering that sucrose is composed of glucose and fructose, the viability of Mondo-deficient flies was tested on high-glucose and high-fructose food. The same viability assay on ubiquitous Mondo knockdown flies was performed on 15% of glucose and fructose diets. Poor viability of Mondo knockdown animals on both high-glucose and high-fructose diets was observed, indicating that flies require Mondo to survive under either condition (Fig. 2.4). In addition, genetic controls and the wild type developed equally well on both monosaccharides. Surprisingly, Rovenko *et al.* have observed a small decrease of survival to pupa on 10% glucose compared with fructose (179). Although food content is largely the same between my experiment and the Rovenko experiment, the difference is that I left out propionic acid and used Nipagin as a fungus retardant. Another interesting point is that life spans of adult flies were shorter

when fed on sucrose (180). It is worth further study to see whether fructose and glucose cause the lethality in Mondo mutant larvae with the same mechanisms.

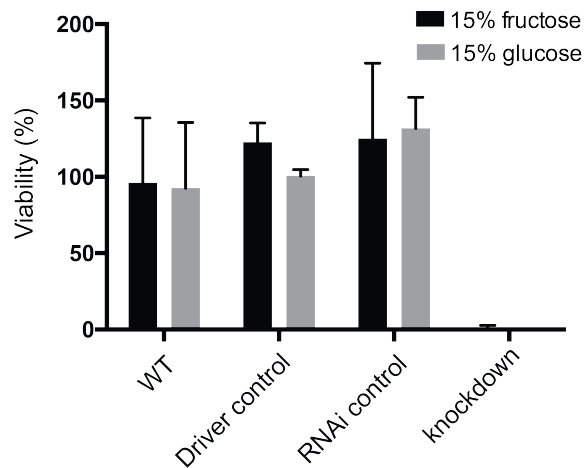


**Figure 2.4. Mondo knockdown flies are not viable on high-glucose and high-fructose food.** Mondo knockdown flies could not survive on either on high-glucose or high-fructose food compared to other control groups.

### 2.4.3 Does Mondo have a different role in the adult than in the developing organism?

Above, we and other laboratories have observed that Mondo is required for larval development on high-sugar food (Fig. 2.1-2.4). However, it remains unclear how a high-sugar diet affects Mondo-deficient flies at the adult stage. Therefore, I tested whether Mondo is required for adult survival on diets with different nutrition contents. To be specific, WT and Mondo<sup>K05106</sup> mutant larvae were raised on 10% yeast food until eclosion, and then the adult flies were transferred to 10% yeast only, 20% sucrose only and 10% yeast + 20 % sucrose diets. To our surprise, adult Mondo mutants survived just as well as WT flies on the 10% yeast + 20 % sucrose diet (Fig. 2.5). This is in contrast to Mondo mutant larvae, which failed to develop on this same diet (Fig. 2.1). In addition, on the 10% yeast diet without extra sucrose, the Mondo mutant flies had a similar life span to WT flies. However, flies on a 10% yeast diet displayed an overall shorter life span compared to flies on a 10% yeast + 20 % sucrose diet. This indicates that a diet balanced in carbohydrates and proteins is required for the survival of adult flies. Interestingly, when yeast is removed from the high-sugar diet, Mondo mutants have a shorter life span than WT. Fifty percent of the Mondo mutant flies died 14 days earlier than when 50% of WT flies died. Accordingly, I interpret this to mean that yeast extract provides specific nutrients to mitigate the high-sugar diet for the adult flies. This is in contrast to the developing

animal lacking Mondo, where the yeast extract does not mitigate the high sugar toxicity for the animal. Further experiments can be conducted on a chemically defined diet in which the components can be controlled to identify the essential nutrients from yeast extract for adult flies (181).

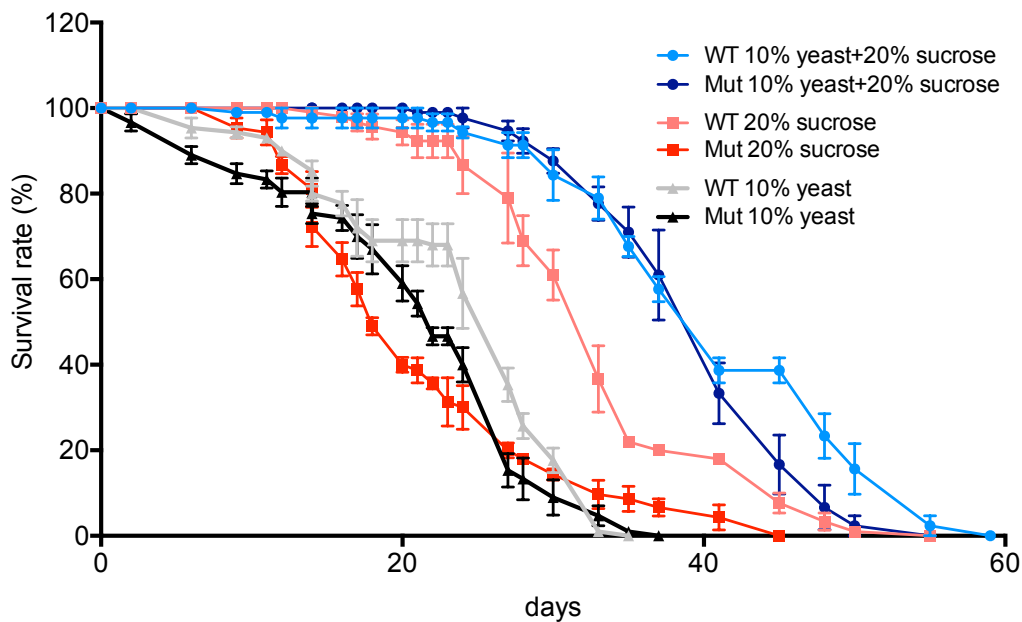


**Fig 2.5. Adult Mondo mutant has a reduced life span when fed a high-sucrose only diet.** Both WT and Mondo<sup>K05106</sup> mutant flies have similar life spans on 10% yeast + 20 % sucrose diet, however, mutants have reduced survival on a sucrose-only diet compared to WT flies over 60 days. Lacking carbohydrate in the diet shortens the life span of flies, regardless having Mondo or not.

#### 2.4.4 Flies deprived of sugar are more sensitive to starvation

To continue to probe the role of Mondo in sugar metabolism, particularly during starvation state in which stored carbohydrate can be quickly used up, I tested how Mondo mutants respond to starvation when they are fed in advance on either sugar-based or protein-based food. The hypothesis is that Mondo mutants would have difficulties using sugar-derived energy during starvation, as they lack the major regulator in sugar metabolism, which can lead to death. The experiment was conducted by raising the WT and Mondo mutant flies on 20% sucrose, 20% sucrose + 10% yeast, and 10% yeast food overnight, and subsequently fasting them on an

agarose-based medium for 21 hours. Unexpectedly, both mutant and WT flies that were pre-fed on diets containing sucrose survived 21 hours of starvation (Fig. 2.6A). However, mutant flies that had a diet of yeast-only food showed increased morbidity compared with WT during starvation for 21 hours (Fig. 2.6A).

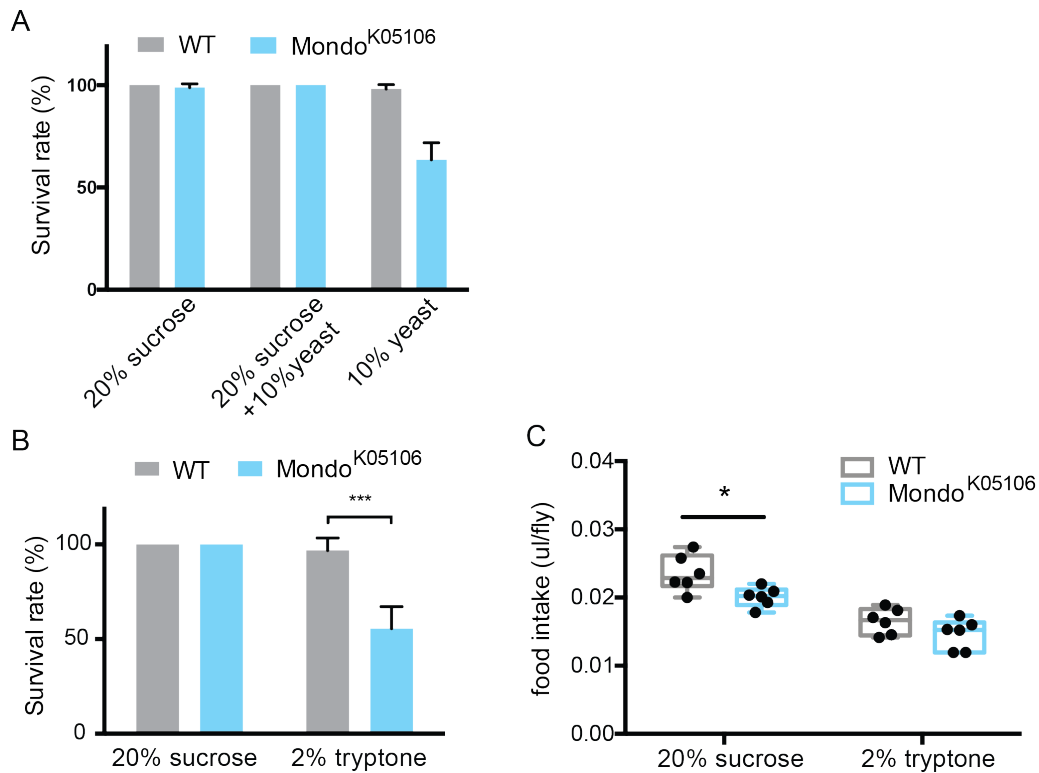


**Figure 2.6. Flies deprived of sugar require Mondo to survive upon starvation.** (A) Starvation resistance of WT and Mondo<sup>K05106</sup> mutants was tested on flies that were previously fed on sugar only, yeast+20% sucrose or yeast-only food and then starved for 21 hours. Survival was recorded after starvation. (B) The same starvation resistance experiment was performed on WT and Mondo<sup>K05106</sup> mutants that were previously fed on 20% sucrose or 2% tryptone. (C) Food intake of 20% sucrose and 2% tryptone was measured by color spectrophotometry assay after starvation for 21 hours. WT and Mondo<sup>K05106</sup> mutant flies consumed a similar amount of sucrose and the same for tryptone food. Error bars represent  $\pm$  SEM (\*  $p < 0.05$ ; \*\*  $p < 0.01$ ; \*\*\*  $p < 0.001$ )

Because WT flies displayed similar survival rate across three diet groups, the increased morbidity of mutant flies observed in the group pre-fed on 10% yeast is less likely due to toxicity from yeast extract. To confirm this nutrient-dependent phenotype, the same experiment was performed on a diet containing pure source of protein: tryptone. Similarly, the mutants pre-fed on 20% sucrose survived 21-hour starvation, as WT flies did, whereas the Mondo mutants pre-fed on 2% tryptone had 50% morbidity after starvation (Fig. 2.6B). However, this phenotype may also result from the decreased consumption of protein-based food among mutant flies, which could explain their vulnerability to starvation. To eliminate this possibility, food intake was measured by spectrophotometric assay after flies were fed on sucrose or tryptone diets. WT and Mondo mutants displayed a difference in food intake while fed on the sucrose diet, but not on the tryptone diet (Fig. 2.6C). One possible explanation for this nutrient-dependent phenotype during starvation is that Mondo mutants have defects either in converting protein into stored energy or in mobilizing the protein-derived fuel upon starvation. In sum, this is the first evidence suggesting that Mondo could have a regulatory role upon starvation, likely by mediating the usage of amino acids.

#### **2.4.5 Mondo is most highly expressed in the fat body**

Determining where Mondo is expressed will allow us to better understand its physiological role in the fly from the perspective of organ function. Two GFP-tagged Mondo flies are available for this purpose. One contains a GFP tag at the N-terminal end of the endogenous *mondo* locus (GFP-Mondo fly; 182), and the other contains a BAC construct that includes a GFP tag at the C-terminal end of *mondo* at the exogenous locus (Mondo-GFP fly) {Spokony:2012em}. I determined whether these GFP-fused Mondo proteins are functional by examining fly viability on high-sugar food. N-terminal-tagged GFP-Mondo flies were viable on high sugar food (Fig. 2.7A). The fused GFP-Mondo protein was also detected in GFP-Mondo flies by western blot (Fig 2.7C), suggesting that GFP-Mondo is functional in the fly. In contrast, the C-terminal-tagged Mondo-GFP did not rescue the viability of the Mondo<sup>K05106</sup> mutant on a high-sugar diet (Fig. 2.7B). Using anti-GFP antibodies, GFP expression was identified in the GFP-Mondo fly with a distribution similar to the

2. INVESTIGATING SUGAR- AND STARVATION- INDUCED PHENOTYPES OF THE MONDO-MLX-DEFICIENT FLY

expression of the fat body pattern (Fig. 2.8), suggesting that Mondo is most highly expressed in the fat body.

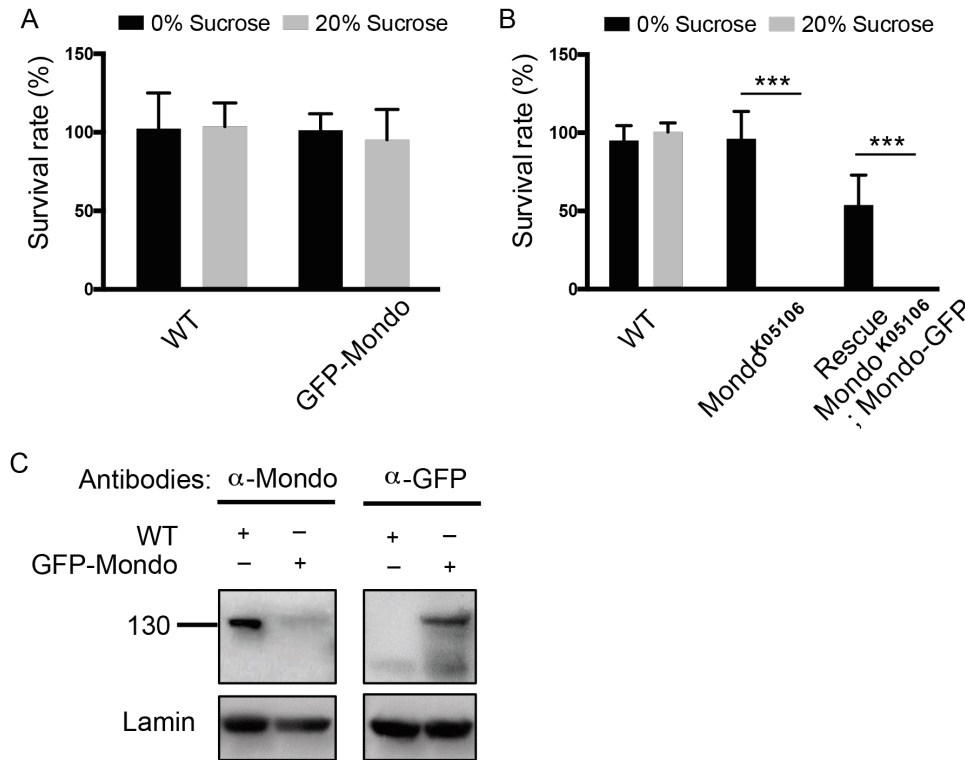


**Figure 2.7. Functional characterization of N-terminal and C-terminal GFP-tagged Mondo protein in the fly.** (A) Endogenous N-terminal GFP-tagged Mondo flies survive on high-sugar food. (B) The fly with C-terminal GFP-tagged Mondo is not functional and fails to rescue the sugar intolerance displayed in the Mondo<sup>K05106</sup> mutant. (C) The Mondo antibody was able to probe Mondo protein in both WT and GFP-Mondo flies (left panel). GFP-tagged Mondo protein was detected in the protein extract from GFP-Mondo flies (right panel). Lamin was used as a loading control. Error bars represent  $\pm$  SEM (\*  $p < 0.05$ ; \*\*  $p < 0.01$ ; \*\*\*  $p < 0.001$ ).

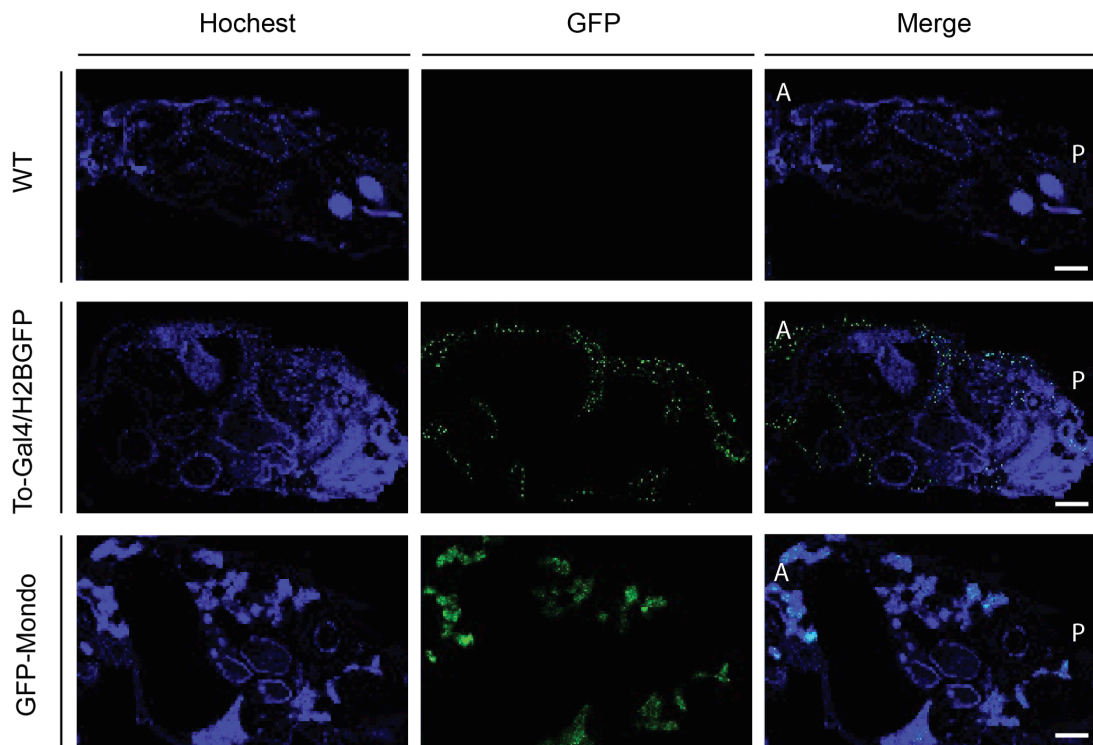


**Figure 2.8.** GFP expression in the fat body-GAL4 driven H2B-GFP fly and the N-terminal tagged GFP-Mondo fly. Scale bar=300 um. A: anterior. P: posterior.

#### 2.4.6 Investigating the cell-type-specific role of Mondo in sugar tolerance

Docherty *et al.* have demonstrated that Mondo has a role in the CNS (155); thus, we aim to functionally dissect the contribution of Mondo in neurons and the glia for high-sugar viability. We took advantage of the Mondo RNAi lines to knockdown Mondo in the fat body, neurons and glia by using fat body- (ppl-GAL4), neuronal- (nsyb-GAL4) or glia- (repo-GAL4) specific driver lines. The cell-type-specific knockdown animals were raised on high-sugar and low-sugar food. Ubiquitous Mondo knockdown flies were used as a positive control and showed severe sugar intolerance on high-sugar food. Both RNAi lines expressed using the Tublin-Gal4 behave in a highly reproducible compared with previous experiments (Fig 2.3 and 2.9). Unexpectedly, none of the cell-type-specific knockdown animals displayed sugar intolerance on high-sugar food (Fig. 2.9). This result was particularly surprising with the fat body driver ppl-GAL4, as it has been shown to rescue the viability of the Mlx mutant to

about 80% of wild type (157). This may be due to poor knockdown efficiency in each tissue, even though UAS-dicer was incorporated to increase RNAi interference. Other laboratories that use RNAi lines in the fly have found that RNAi knockdown is more efficient when flies are kept at 27°C; we think that Mondo likely is required in the fat body to survive on high-sugar food, and thus it is worth repeating these experiments. The tissue-specific rescue in the CRISPR-induced Mondo mutant that we generated can be an alternative to investigate the tissue-specific contribution of Mondo to the sugar-induced phenotypes.

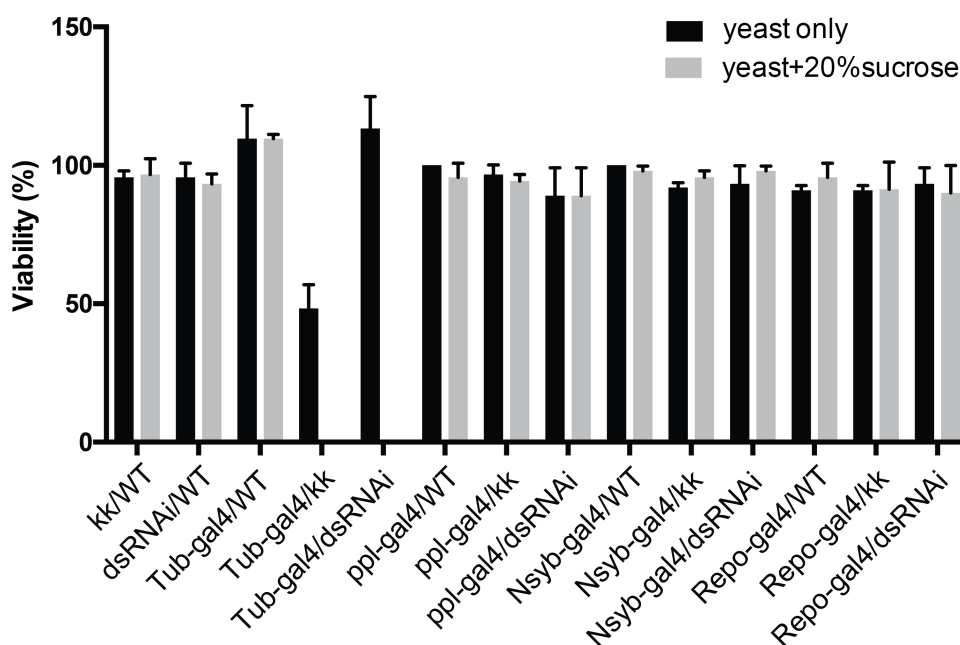


**Figure 2.9. Investigating the sugar-dependent viability of flies by knocking down Mondo in the fat body, neuron and glia.** KK109821 Mondo RNAi and Mondo dsRNAi lines were previously combined with UAS-dicer2 flies for the purpose of increasing knockdown efficiency. Mondo was knocked down tissue-specifically in the fat body, neuron and glia by crossing the RNAi lines with the fat body- (ppl-GAL4)-, neuronal- (nsyb-GAL4)- and glia (repo-GAL4)-specific GAL4 drivers. The same experiment was conducted with ubiquitous Mondo knockdown flies (tub-GAL4) as an active control. Lethality was only observed with ubiquitous Mondo knockdown flies, but not with tissue-specific Mondo knockdown flies on high-sugar food.

## 2.5 Discussion and future directions

Our data suggest that Mondo may regulate sugar metabolism differently at different developing stages. The results show that Mondo-deficient larvae fail to develop on a 10% yeast + 20% sucrose diet, whereas the adult Mondo mutant flies lived as long as WT flies on the same diet. One of the explanations of the higher sugar tolerance of adult Mondo mutants on high-sugar food is that sugars may have distinct impacts on organisms at different stages. It has been shown that hyperglycemic exposure for longer than 24 hours is toxic to early embryo development in mice (183); nevertheless, hyperglycemia more often causes chronic effects, such as diabetes and fatty liver in adult mice. Therefore, the difference in viability between larvae and adult mutants on a high-sugar diet may result from the detrimental effect of hyperglycemia on early embryo development. Moreover, the underlying Mondo-regulated network in adult flies may be different from that in larvae, which may allow adult flies to be more tolerant of high sugar levels. However, interestingly, when adult Mondo mutant flies were fed on a sugar-only diet (20% sucrose), they showed a reduced life span compared with WT flies. This implies that the extent of sugar toxicity derived from nutrient-balanced food is smaller than that from pure sugar food, even though the sugar proportion is the same in both diets.

The role of Mondo in response to starvation was also investigated. I hypothesized that Mondo mutants fed on sugar-based food would be more vulnerable to starvation, as sugar may not be used efficiently as fuel due to the misregulation of carbohydrate metabolism in Mondo mutants. However, in contrast to what we expected, almost half of the Mondo mutants died after a 21-hour starvation if they were previously fed on protein-based food, but only fewer deaths were seen in those fed on sugar-based food. The lethality was not due to an alteration in food intake in mutants, since no significant difference in consuming protein-based food was observed between WT and mutant flies. This nutrient-dependent phenotype suggests that sugar could still be metabolized and utilized in adult Mondo mutants, possibly by other signaling pathways, such as HNF4 and FOXO1 pathways. On the other hand, Mondo mutants may have defects in utilizing protein as an energy source or in converting protein into stored energy. However, a defect in using protein as fuel is excluded because amino acids have been reported to be utilized in the absence of

Mondo-Mlx in the fly (157). Moreover, it has been shown that amino acids are materials for gluconeogenesis to maintain glucose supplies to the body upon starvation. Therefore, a deficiency in gluconeogenesis supplied by amino acids may be another explanation of this phenotype in Mondo mutants. To further study the mechanism underlying this phenotype, one can measure the level of glycogen and triglyceride, the two major forms of stored energy, in WT and mutant flies fed on sugar- or yeast-only food before and after starvation. Meanwhile, we can examine the metabolic profile in each group by conducting mass spectrometry-based metabolomics. It should be noted that the Mondo<sup>K05106</sup> mutant was used for most of the experiments. However, for the long term, it is useful to use the CRISPR-Mondo fly without interrupting the *gr39a* gene, as the adult phenotypes discussed here may also be the result of the disruption of the gustatory receptor gene. Repeating the experiment with the CRISPR-Mondo fly will help validate the starvation phenotype.

The CRISPR-Mondo fly can be transformed into different genetic tools, as the donor cassette used to generate the knockout allele contains attP sites that can be further replaced with any interested DNA fragment by recombinase-mediated cassette exchange (RMCE). For example, a GAL4 construct can be introduced to make the fly into a GAL4 driver line under the endogenous mondo promoter, while the same knockout allele is kept. By crossing the Mondo-GAL4 driver with the UAS-reporter fly, one can potentially determine the expression profile of Mondo in the fly. Moreover, to functionally characterize the protein domains of Mondo *in vivo*, we can cross the GAL4 Mondo mutant with the UAS-Mondo mutant fly to see whether Mondo mutant proteins rescue the sugar phenotype.

To gain insight into the physiological roles of Mondo in different cell types, Mondo was knocked down specifically in the fat body, different types of neurons and glia in the fly, followed by the examination of its sugar tolerance and feeding behavior. However, neither a reduction in viability on high-sugar food nor an alteration in food consumption compared with the control groups was observed. As an alternative method, a cell-type-specific rescue experiment with the Mondo mutants can be considered. Regarding the feeding assay, I adopted the methods from Docherty *et al.* The age of fly, food type, temperature and humidity were all controlled in the same way; however, I used wet kimwipes instead of agar to keep the flies from

## 2. INVESTIGATING SUGAR- AND STARVATION- INDUCED PHENOTYPES OF THE MONDO-MLX-DEFICIENT FLY

---

dehydrating in the feeding assay. The genetic backgrounds between each experimental group, a factor that often leads to inconsistency in behavior assays, were also controlled by outcrossing them with WT flies. One should first establish a positive control of the feeding assay with the Mondo mutant before revisiting the influence of Mondo in specific cell types in feeding behavior.

# Chapter 3

## Genome-wide identification of target genes for the Mondo-Mlx complex in the fly

### 3.1 Summary

In this chapter, I demonstrate the kinetic profile of sugar-regulated transcriptome. The sugar-regulated genes are first categorized into four clusters based on the temporal expression profile. Next, to globally determine the direct target of the Mondo-Mlx complex, the Mondo-Mlx ChIP-seq was performed with the respective generated antibodies. The specificity and sensitivity of these antibodies were first examined by western blot on recombinant proteins and fly protein extract, as well as by ChIP-qPCR on putative Mondo-Mlx target sites. With the Mondo and Mlx antibodies against the N-terminal GSM domain and the full-length Mlx protein, respectively, Mondo-Mlx ChIP-seq was performed on WT and Mondo<sup>K05106</sup> mutants to identify the direct target genes of Mondo-Mlx. Downstream analyses, such as genomic distribution, motif searching and GO term analysis, were executed to functionally characterize the target genes of Mondo-Mlx in the fly. To understand how Mondo regulates the transcription of target genes via RNA polymerase II (Pol II), I also performed RPB3 (Pol II subunit) ChIP-seq on WT and Mondo mutants. Mondo has been shown to regulate the gene transcription via Pol II at two levels: 1) the recruitment of Pol II to the transcription start site (TSS) and 2) the elongation of Pol II at the gene body. In addition, these results suggest that Mondo may act either as an activator or a repressor of targeted genes, which the published Mondo-Mlx RNA-seq data further supports.

### 3.2 Introduction

Organisms consume sugar as an energy source to live, but they also need to maintain the blood sugar level within a narrow range to avoid glucose toxicity. Thus, a sophisticated regulatory network has evolved to maintain carbohydrate homeostasis in organisms. Studying the kinetics of sugar-induced signaling will help us understand how this happens.

In addition to insulin/glucagon signaling, the two major hormonal regulators that systemically regulate blood glucose levels, the Mondo protein family has also been characterized as key sugar-responsive regulator of glucose metabolism in recent decades. Uyeda *et al.* have identified ChREBP as one of the Mondo family members that recognizes the ChoRE within the promoter of L-type pyruvate kinase (L-PK; 85). It has been shown that ChREBP target genes are involved in glycolysis, lipogenesis, hormone regulation, cell survival and the circadian rhythm (108).

Genome-wide analyses of ChREBP targets have been done in HepG2, a human hepatocellular carcinoma cell line (184), and in mouse livers and white adipose (108) to globally unbiased identified ChREBP targets. Consistent with the phenotypic importance of ChREBP, the pathway analysis of ChREBP targets genes from these two studies and shows a significant role of ChREBP in regulating a wide range of metabolic pathways. The *Drosophila* genome contains only a single mondo gene and thus has no genetic redundancy, making the fly an optimal model to investigate the function of Mondo-Mlx in nutrient metabolism. Havula *et al.* have performed Mlx ChIP-qPCR to confirm several Mondo-Mlx target sites in the fly larvae. In order to focus on the role of Mondo in the adult fly by addressing the genes to which Mondo directly binds, several Mondo antibodies were developed, and ChIP experiments were performed for this project. The target sites of Mondo-Mlx were identified by comparative Mondo-Mlx ChIP-seq on WT and Mondo<sup>K05106</sup> mutants.

The binding of transcription factors to target genes is commonly coupled with the levels of steady-state mRNA as a readout to study how transcription factors (TFs) regulate gene expression. However, the mRNA levels are not only affected by the activity of TFs and transcription mediated by Pol II, but they also depend on the RNA turnover rate. The integrated analysis of genome-wide TF binding and Pol II occupancy provides important insights into the regulatory mechanisms of gene

expression. Specifically, gene expression depends on the recruitment of Pol II to TSS and the levels of Pol II occupancy in the gene body. Another key mechanism for rapid induction of gene expression in response to extracellular cues is Pol II pausing. It has been suggested that ChREBP acts as either an activator or repressor based on the fact that some ChREBP target genes are up-regulated under a high sugar condition, whereas the others are down-regulated (184). ChREBP has been shown to bind directly to the ARNT/HIF-1 $\beta$  proximal promoter and negatively regulates ARNT/HIF-1 $\beta$  gene expression in living clonal  $\beta$ -cells (185). However, the concern with a secondary effect on the gene expression by other TFs or quick mRNA turnover is also present in both studies. I performed RPB3 ChIP-seq on WT and Mondo mutants to directly elucidate how Mondo regulates gene transcription via Pol II. The results showed that, in a majority, Mondo regulates the Pol II elongation at the gene body, but it also regulated Pol II recruitment at the TSS of some genes. Moreover, both increased and decreased Pol II occupancy at different TSS and gene bodies were observed, indicating that Mondo could act as either a transcriptional activator or a repressor.

### 3.3 Methods

**The antibodies against the N-terminal activation domains of Mondo and Mlx were previously generated by Teresa Burrell. The antibody against the C-terminal DNA binding domain of Mondo was generated by Hui-Lan Huang.**

#### 3.3.1 Plasmid construction and recombinant protein expression of pETMCN

##### MondoDBD plasmid

The Mondo DNA binding domain sequence was amplified by polymerase chain reaction (PCR) from genomic DNA of wild-type flies and then sub-cloned into a pETMCN vector. The primers used for PCR amplification contains Age I and XbaI restriction sites. The PCR product and pETMCN vector were double digested with Age I and XbaI. The map of the expression construct is shown in appendix figure A3.1. The pETMCN MondoDBD His plasmid was transformed into BL21 E. coli. A single colony was selected and grown in a 20 mL culture within LB medium+ chloramphenicol overnight at 37°C. This overnight culture was used to inoculate 1 L LB + chloramphenicol, and it was grown at 37°C to an optical density close to 0.6. For the un-induced control, 20 mL of the culture was placed into a new flask and grown side-by-side with the rest of the 1L culture, to which isopropyl  $\beta$ -D-1-thiogalactopyranoside (IPTG) was added to a final concentration 0.4 mM. Both the induced and un-induced cultures were grown for two to three hours at 37°C. To assess the protein expression, 200 ul of un-induced and induced culture samples were taken into labeled eppendorf tubes and spun down at the speed of 14,000 rpm, 4°C for 1 minute. Supernatants were carefully removed from the eppendorf tubes, and pellets were re-suspended in a 100 ul buffer (500 mM NaCl, 50 mM Tris 7.5, 2 mM DTT, 2mM PMSF, 1x protease inhibitor). Next, protein samples were denatured in SDS loading buffer at 95°C for 5 minutes. Protein samples were then run on the SDS page, followed by coomassie staining to examine the result of protein expression. The rest of the culture was spun down at 4,000 rpm at 4°C for 10 minutes. The supernatant was discarded, and the pellet was frozen in liquid nitrogen and stored at -80°C until protein purification continued. Because the expressed His-tagged Mondo DBD protein was not soluble, the purification protocol for insoluble protein was used and is described below.

### 3.3.2 Purification of insoluble His-tagged proteins

Ni-NTA Agarose beads (ThermoFischer R90110) were used to purify the His-tagged Mondo DBD protein. Beads need to be handled gently and pipetted exclusively with end-cutting tips. 4mL of bead slurry and 50 ml of distilled water were added to a 50mL falcon tube followed by gentle mixing. The beads were then spun down at 1,000 rpm at 4°C for 3 minutes, and the supernatant was discarded. To continue the wash and equilibration of beads, 50mL of buffer 4 (500mM NaCL, 50mM Tris 7.5, 10mM Imidazol, 2mM PMSF, 6M Urea) was added. The beads were gently mixed with the buffer 4 and were spun down again. The wash of beads with buffer 4 was repeated two more times.

The pellet from the culture (see 3.3.1) was re-suspended and thawed in buffer 4. The sample was sonicated for 2 minutes a total of three times, until the sample was not goeey. Then, the sonicated sample was spun down at 18,000 rpm at 4°C for 20 minutes. Supernatant was added to the beads via gentle rotation for 1 hour at 4°C. The beads were spun down at 1,000 rpm at 4°C for 3 minutes. The supernatant was placed in a tube labeled “unbound.” The beads were washed with the buffer 4 five times (50mL per wash), and each time, the sample was spun down at 1,000 rpm, and the supernatant was removed. 100µL of supernatant from each wash was taken. Finally, protein was eluted out from the beads with buffer 5 (500mM NaCL, 50mM Tris 7.5, 500mM Imidazol, 2mM PMSF, 6M Urea; 10-15 mL if the protein expressed well, otherwise, less was used). The original culture, unbound fraction, washes and eluent were run on SDS page gel followed by coomassie staining to examine the efficiency of protein purification.

### 3.3.3 Generation of the antibody

Because the expressed Mondo DBD protein was not soluble, protein had to be run on an SDS page and transferred onto nitrocellulose membrane. The membrane was stained with Ponceau (Sigma Aldrich, P7170) for 1 minute and washed with distilled water. The stained band at the expected size was cut out and dried under red light in an eppendorf tube and kept at -20°C before injection. Before an experiment begins, one must test whether the animal is suitable for the required antigen. The rabbit serum was tested for cross reactivity to *Drosophila* denatured extract by western blot. If a

clean blot is obtained, injection can be initiated. The injection of antigen for immunization and bleeding were scheduled and performed by the animal facility in the physiological biochemistry department, LMU. Serum was prepared from the clotted blood by following the standard lab protocol. Then serum was snap frozen in liquid nitrogen and stored at -20°C.

### **3.3.4 Western blot assay**

#### **3.3.4.1 Preparing, running and transferring the protein samples**

Recombinant protein was diluted in a 4 X SDS sample loading buffer at a 1:1 ratio, boiling for 5 minutes at 95°C and was then stored at -80°C. Fly samples were ground using a micro pestle 50 times in a 2X SDS sample loading buffer. Samples were then boiled at 95°C for 5 minutes and centrifuged at full speed for 5 minutes. The supernatant was transferred into a new eppendorf and stored at -80°C until it was required. In general, several freeze and thaw cycles should be avoided. 10% acrylamide gel was cast using 4.5 mL acrylamide (30 %), 2.25 ml 4x Tris-Cl/SDS buffer (pH 8.8), 2.25 mL H<sub>2</sub>O, 40 µL APS (10 %) and 18 µL TEMED. Normally, one fly or 10 heads are loaded. Samples were loaded on SDS-PAGE and were run at 200 V and 30 mA for 45 minutes. A transfer cassette containing the gel and nitrocellulose membrane (Protran BA 83 Whatman, GE Healthcare Life Sciences) arranged between layers of paper and sponges was assembled. Proteins were transferred from gel to a transfer buffer at 100 V and 400 mA for 1 hour on ice.

#### **3.3.4.2 Antibody staining and membrane development**

The Mondo long antibody was first diluted at a ratio of 1:4,000 in blocking buffer, and it was pre-absorbed on a blot with transferred protein extract from Mondo<sup>K05106</sup> mutants overnight at 4°C. The pre-absorbed Mondo long antibody was ready to use or could be stored at -20°C.

The membrane with transferred protein samples was blocked at RT for 1 hour in blocking buffer (1X TBS, 0.1% Tween 20, 5 % milk), and then incubated with the primary antibody in the blocking buffer with rotation overnight at 4°C. Mondo short (No. serum 521.9, 1:5000), Mondo DBD (No. serum 536.10, 1:10000), and pre-absorbed Mondo long (No. serum 522.14, 1:10000) antibodies were used to detect

either recombinant or endogenous Mondo proteins. It was expected that lamin protein would not change under different conditions, and it was thus seen as loading control for fly protein extracts. Lamin antibody (DSHB, ADL67.10, 1:5000) was used to probe endogenous lamin protein. After the incubation of primary antibody, the membrane was washed three times with TBST with rotation, and each wash was 10 minutes. Then membrane was subsequently incubated with secondary antibody goat anti-rabbit HRP (BioRed, 1706515, 1:10000) or goat anti-mouse HRP with rotation at RT for 1 hour. The membrane was subsequently washed three times with TBST with rotation, and each wash was 10 minutes. The membrane was then incubated with Immobilon Western HRP Substrate (Millipore, WBKLS0500) and exposed to photographic film in the dark for signal detection (Kodak).

### **3.3.4 Generation of the UAS-Mondo transgenic fly**

#### **3.3.4.1 Plasmid construction**

The Mondo full-length coding sequence was amplified using PCR from pETMCN-Mondo RJ plasmid and then sub-cloned into a pUAST vector. The primers used for PCR amplification contained Bgl II and XbaI restriction sites. The PCR product and pUAST vector were double digested with Bgl II and XbaI and purified by gel purification (Metabion, mi-GE100). PCR amplification was performed using the following components and conditions: the ligation of the Mondo RJ (FlybaseID: FBtr0301461) insertion and the pUAST vector was performed in the reaction containing 100 ng of vector, 15 ng of insert, 1  $\mu$ L T4 ligase (NEB), 1 x T4 DNA ligase buffer, and H<sub>2</sub>O to 20  $\mu$ L. Ligation reactions were incubated at RT for 20 minutes, followed by bacterial transformation. Positive clones were screened by colony PCR and sequencing. The construct map is shown in appendix figure A3.2.

#### **3.3.4.2 Generation of transgenic lines**

The company BestGene generated the transgenic fly. The UAS-Mondo RJ transgenic fly was generated using random P-element insertion to incorporate the transgene into the genome. *Mini white* ( $w^{+mC}$ ) was used as a selective marker for positive transgene carriers. The transgene insertion site was mapped to a particular chromosome, and the transgenic flies were then outcrossed for six generations.

### **3.3.5 Chromatin immunoprecipitation (ChIP) assay**

#### **3.3.5.1 Preparation of Chromatin**

The fly heads with the desired genotype was firstly measured 0.5 mL in eppendorf tube and then were ground into powder with a precool mortar and pestle on dry ice. The ground sample was transferred to a dounce and 25 mL NE buffer was added for 5 minutes of incubation on ice. The sample was homogenised by using a 100 mL homogeniser at 2,000 rpm for 20 times at 4°C. The sample was then cross-linked with 1% formaldehyde with rotation at room temperature for exactly 10 minutes. The formaldehyde was quenched by adding 1.25 mL 2.5 M glycine into the sample. The sample was rotated at room temperature for another 5 minutes. The sample was filtered through a 60 µm filter (Millipore) and then centrifuged at 2,000 rpm for 5 minutes at 4°C to pellet the nuclei. The supernatant was carefully removed and the pellet was gently resuspended in 1 mL RIPA buffer with a cutted 1ml tip. The sample was transferred to a 1.5 mL low-binding eppendorf (Sigma CLS3207). Next, the pellet was washed with 1 mL RIPA buffer after centrifugation at 2,000 rpm for 1 minute at 4°C; This wash was repeated twice. After the second wash, the pellet was resuspended in 300 µL RIPA buffer and sonicated by using a Branson Sonicator with the settings: intensity 3; pulse 40; 20 seconds of pulsing followed by a 45-second break. This process was repeated six times with breaks on ice for 1 minute. The sample was then transferred into covaris tube and sonicated by using the covaris sonicator with following settings: power 150, duty cycle 20, burst 200, 7 min. After sonication, the samples were centrifuged at full speed at 4°C for 10 minutes. The supernatant was transferred into a new low-binding eppendorf with sample name labeled, and 50 ul of the supernatant was kept in another tube for a size check. The rest of sample was stored at -80°C until use.

#### **3.3.5.2 Preparation of beads**

Bead preparation was consistently performed at 4°C in a cold room or on ice. ProteinA Sepharose Cl-4B (GE healthcare, 17096302) beads were prepared by washing them three times in 1 mL of nuclease-free water for 15 min while they rotated on a tube rotator. To reduce none-specific binding, the beads were blocked for 1 hour in RIPA buffer with sperm DNA (1 mg/ml) and BSA (1 mg/ml) added (RIPA:

150 mM NaCl, 25 mM HEPES [pH 7.5], 1 mM EDTA, 1% Triton-X 100, 0.1 % SDS, 0.1% DOC). Complete EDTA free protease inhibitor (Sigma, 05056489001) and 1mM PMSF were freshly added. The beads were then washed three times with RIPA buffer for 5 minutes with rotation. After the last wash, the beads were resuspended in the same volume of RIPA buffer.

### **3.3.5.3 Chromatin immunoprecipitation**

These assays were always performed at 4°C in a cold room or on ice. To reduce non-specific binding to the beads, 10 ug of chromatin diluted in 650 ul RIPA buffer were incubated with 20 ul blocked and equilibrated beads in 1.5 ml low-binding eppendorf tubes for 1 hour with mixing on a tube rotator. To remove the beads, each reaction was centrifuged at full speed (15,000 rpm). The preabsorbed chromatin (supernatant) was transferred into a new, low-binding eppendorf. The optimal amount of antibody was added to the preabsorbed chromatin and incubated overnight on a tube rotator. A 50 µL sample of the antibody-chromatin reaction was collected as a 10% input sample. For the ChIP, 500 µL of the antibody-chromatin reaction was incubated with 20 ul of blocked and equilibrated beads and rotated for 3 hours at 4°C. The ChIP sample was centrifuged at 500 rpm for 1 minute to spin down the antibody-chromatin coupled beads, and the supernatant was discarded. To reduce non-specific binding, the beads were washed with 1 mL of RIPA buffer and rotated for 5 minutes. The samples were centrifuged at 500 rpm, and the supernatant was carefully removed. The beads were then washed three more times. For a last wash, the beads were incubated with LiCl buffer (250 mM LiCl, 1 mM EDTA, 10 mM Tris-Hcl [pH 8], 0.5% DOC, 0.5% NP-40; protease inhibitor complex and PMSF were freshly added) for 10 minutes. The beads were centrifuged at 500 rpm, and then the supernatant was discarded. The beads were rapidly rinsed with 1 mL of TE buffer twice. The beads were again centrifuged at 500 rpm. The supernatant was discarded with little buffer remained inside the tube, and then the beads were resuspended in TE buffer to 100 µL. 50 µL of TE buffer was added to each 50 uL 10% input sample. The eppendorf tubes containing input and ChIP samples were tightly sealed with parafilm and incubated overnight at 65°C with shaking at 1,000 rpm. The samples were incubated with 1 µL RNase A (ThermoFisher, EN0531) at 37°C for 30 minutes with shaking at

1,000 rpm. 5  $\mu$ L SDS and 1  $\mu$ L proteinase K (10 mg/ml, Roche) were added into the sample and the reaction was incubated at 55°C with shaking at 1,000 rpm for 1.5 hours to reverse cross-link and degrade the proteins in each sample. The DNA was then purified using Ampure-XP beads (Agencourt, A63882) by following the manual with some modified steps: 500  $\mu$ L 80% freshly prepared ethanol were used at step 6, the samples were dried for 5-10 minutes, and 20  $\mu$ L of water was used for elution. Samples were stored at -20°C until use.

### **3.3.6 RPB3 ChIP on WT and Mondo mutants**

ChIP was performed as described in the methods section in chapter 3. The Rpb3 antibody was used for immune-pull down.

### **3.3.7 ChIP-qPCR**

A qPCR reaction is composed of DNA 6ul, PowerUp SYBR Green Master Mix (Applied Biosystems, A25742) 7.5 ul, and primer pairs 1.5 ul. Primers targeted the putative Mondo target sites of *ACC*, and *Cbt* genes were designed as previously described (113, 186) and used to evaluate Mondo-Mlx ChIP efficiency in this project. Primers targeting 28bp upstream of the *fas2* gene were used to assay the binding of Pol II to this region in Pol II ChIP. The respective negative control primers were also included in each ChIP experiment. Sequences of primers and product sizes are shown in appendix table A3.1. Quantitative PCR amplification was performed using a 7500 FAST Real-Time PCR system (Applied Biosystems) with a PowerUp amplification program with a melting curve. The percentage of input was calculated based on the CT values obtained from 1% and 10% input and the ChIP sample.

### **3.3.8 Statistic analysis**

Statistical significance was determined with an unpaired Student's t-test with an assumed unequal standard deviation in each group. Data are shown as mean  $\pm$  SEM for a minimum of three independent biological replicates.

### 3.3.9 DNA library preparation and ChIP-sequencing

Technical replicates of the ChIP samples that were previously tested by ChIP qPCR were pooled together. The concentration of DNA was measured using the Qubit dsDNA high-sensitivity assay (Thermo Fisher, Q32854). The quantity of the starting material for library preparation is 0.5 ng, and the library was prepared with the NEBNext® Ultra™ II DNA Library Prep Kit (NEB, E7645L) by following the manual with modifications regarding the purification of libraries; this is described in what follows. 50 ul of Ampure-XP beads (Agencourt, A63882) were added to 50 ul of PCR reaction and gently mixed. The sample was left to stand on the magnetic rack for 2 minutes, until magnetic beads were separated from the supernatant, 50 ul of which was then transferred to a new, low-binding tube. 30 ul of Ampure-XP beads were added to the supernatant with gentle mix. The sample was left to stand on the magnetic rack for 2 minutes, and 80 ul of supernatant was transferred to a new, low-binding tube. 20 ul of Ampure-XP beads were again added into the supernatant via gentle mixing. Beads were separated from the supernatant on the magnetic rack, and this time, the supernatant was discarded, and beads were washed twice with freshly prepared 80% ethanol. The beads were dried for 2 minutes, and then the DNA library was eluted with 15 ul of 0.1xTE buffer. The concentration and size profile of DNA libraries were checked on a DNA 1000 chip on Bioanalyzer (Agilent 2100). Single-end sequencing was performed on an Illumine Hiseq2000 to an average depth of 20 M reads and a sequencing length 50 bp by Lafuga, the sequencing facility in Gene Center, Martinsried, Germany.

### 3.3.10 Bioinformatics analysis of ChIP-seq data

#### 3.3.10.1 Mapping and data transformation

The mapping of raw sequencing reads to the *Drosophila* genome release 6 (dm6) was performed using the mapping tool bowtie 1.1.2 (187) with the command line: bowtie -S -m 1 drosophila\_index <input file> <output path/filename>. The sorting of the mapped bam files was carried out using the samtools sort function. The average mapping rate of the samples is around 80%. The mapping and sorting were performed on the high-performance computing cluster of the Bioinformatics Core facility at the Biomedical Center (BMC).

### 3.3.10.2 Peak calling and differential binding analysis of Mondo-Mlx ChIP-seq data

MACS2 (model-based analysis of ChIP-seq) was used for peak calling using the input data as the control sample. A MACS2-derived output excel file was imported in R, and peak filtration was performed by setting the threshold at 2 to filter out small peaks. The DiffBind package (188) was used to identify the differential Mondo and Mlx target sites between WT and the Mondo mutant, while the fold change was set at 2.

### 3.3.10.3 Genomic distribution

The Cis-regulatory Element Annotation System (CEAS) tool (189) was used to characterize ChIP binding sites at important genome features, such as upstream open reading frames, promoters, gene bodies, introns, and exons. CEAS needs two input files: the gene annotation table file (sqlite3) and the BED file with ChIP regions (.txt). The gene annotation table was created based on the *Drosophila* genome sequence Release 6 with the following command line: `build_genomeBG -d dm6 -g refGene -w <wig file> -o dm6.sqlite3`. The bed file containing the Mondo-Mlx targeted regions was used as input for the analysis, and the command `ceas -g dm6.sqlite3 -b <bed file> --name <output name>` was then run to obtain the result.

### 3.3.10.4

A fastq file was first generated from a bed file containing the regional information of putative Mondo-Mlx target sites by using the following command line: `fastaFromBed -fi drosophila genome file -bed peak.bed -fo output.fa`. Next, the fastq file was uploaded in MEME ChIP webtool (190) for motif finding. The analysis was done by MEME ChIP with the default setting (MEME options: motif width: 6-30 bp and count of motif, 3. DREME options: E-value<0.05. CentriMo options: minimum acceptable match score  $\geq 5$  and E-value threshold for reporting centrally enriched regions  $\leq 10$ ). The logos of different motifs were generated from MEME-ChIP analysis. The output graph displays the distribution of the best matches to the motif in the sequences as found by a CentriMo analysis (190).

### 3.3.10.5 Gene ontology (GO) term enrichment

Gene Ontology (GO) terms classification was performed by DAVID bioinformatics software v 6.7. The pre-built default background, including all annotated *Drosophila* genes, was used in the analysis. P-values were obtained with the overrepresentation Fisher Exact Test, which was calculated by the EASE method in DAVID.

### 3.3.10.6 Peak calling and differential binding analysis of Rpb3 ChIP-seq data

MACS2 was used for peak calling, while input data was used as control. A MACS2-derived output Excel file was imported in R, and peak filtration was done by setting the threshold at 1 to filter out small peaks.

The regional information of transcripts in the whole fly genome was obtained by using the TxDb.Dmelanogaster.UCSC.dm6.ensGene package, which is an annotation database generated from UCSC. Then, 500 bp downstream of TSS was removed, and only the genebody region was kept. To be specific, the following code was used in R to define 500 bp around the TSS of all annotated genes:

```
> library(TxDb.Dmelanogaster.UCSC.dm6.ensGene)
> t<-transcripts(TxDb.Dmelanogaster.UCSC.dm6.ensGene::TxDb.Dmelanogaster.UCS
C.dm6.ensGene)
> t <- data.frame(chr=seqnames(t), start=start(t),end=end(t),strand=strand(t))
> positive_gene <- data.frame(t[which(t$strand=="+"),])
> negative_gene <- data.frame(t[which(t$strand=="-"),])
```

To remove 500 bp around tss:

```
> positive_gene_500 <- data.frame(chr=gsub("chr", "", paste(positive_gene$chr)),
start=positive_gene$start+500,
end=positive_gene$end,
strand=positive_gene$strand)
> negative_gene_500 <- data.frame(chr=gsub("chr", "", paste(negative_gene$chr)),
start=negative_gene$start,
end=negative_gene$end-500,
strand=negative_gene$strand)
```

To combine positive and negative:

```
> t_genebody <- rbind(positive_gene_500,negative_gene_500)
```

To remove genes where the length of the gene is less than 500 bp:

```
>t_genebody_remove_bed> t_genebody[t_genebody$start<t_genebody$end,]
```

```
>t_genebody_remove_bed <- t_genebody_remove_bed[,1:3]
```

```
>t_genebody_remove_bed <- unique(t_genebody_remove_bed)
```

The DiffBind package was used to identify the differential Rpb3 targeted regions at peaks identified by MAS2 and genebody separately between WT and Mondo mutants.

### **3.3.10.7 Average profile of Pol II occupancy at Mondo-Mlx target genes**

The average profile plots of Pol II occupancy were generated using NGS-plot tool (158). They were generated by applying the following commands: `ngs.plot.r -G dm6 -R tss -C <config.file> -O <output path/output file name>` `ngs.plot.r -G dm6 -R genebody -C <config.file> -O <output path/output file name>`.

### **3.3.11 RNA-seq on whole heads of flies**

Wild-type flies (2202U2; 165) were kept on standard media at 25°C. One- to two-day-old flies were starved for 21 hours and refed on 20% sucrose-only agarose food for 0.5, 1, 2, 3 and 6 hours. In each case, the flies were collected and frozen in liquid nitrogen at the same time of the day. 10 heads from female flies then underwent RNA extraction and subsequent ribosomal RNA depletion by using the NEBNext® rRNA Depletion Kit (Human/Mouse/Rat). cDNA libraries were prepared by using the NEBNext® Ultra™ II Directional RNA Library Prep Kit for Illumina®. Pair-end sequencing was performed with illumina Hiseq2000 to an average depth of a 20 M read sample and a sequencing length of 100 bp at the Lafuga sequencing facility at Gene Center, Martinsried, Germany.

### **3.3.12 Bioinformatics analysis of RNA-seq data**

#### **3.3.12.1 Mapping**

The mapping of raw sequencing reads to the *Drosophila* genome was performed by using the mapping tool STAR, which must be run on a high-performance cluster computer. The detailed command lines are as follows:

```
STAR --runThreadN 8 \  
--readFilesCommand gunzip -c \  
--quantMode GeneCounts \  
    --genomeDir /path/to/reference genome\  
--readFilesIn paired sequencing fastq file 1 paired sequencing fastq file 2\  
    --sjdbGTFfile /path/to/annotations.gtf\  
    --outSAMtype BAM SortedByCoordinate \  
    --outFileNamePrefix /path/to/output directory/output file name\  

```

The output STAR-derived samples.ReadsPerGene.out.tab files were imported into R, and differential expression analysis was done with the Deseq2 package.

### **3.3.12.2 Clustering analysis**

Hierarchical clustering was performed using Cluster 3.0 (191). Gene expression levels were adjusted with Log transformation, and genes that did not have at least one observation and at least an absolute value of 1.5 were removed. Genes whose maximum minus minimum values were less than 0.7 were also filtered out. Subsequently, genes were centered on the median. Clustering was performed using average linkage and centered correlation as the metric. Heat maps were generated using Java TreeView (192), and MaSigPro was used to find genes with a significant change in temporal expression by applying a two-step regression strategy. The cut-off value for the R-squared of the regression value was 0.6.

### **3.4 Results**

#### **3.4.1 The time-course of sugar-induced transcriptome reveals the dynamics of sugar response**

Determining the dynamics at the levels of the individual gene and the whole transcriptome in response to sugar consumption can provide valuable insights about the sugar-induced pathways at specific time points and the mechanism by which carbohydrate homeostasis is maintained. To this end, I determined the kinetics of the sugar-induced transcriptome in the fly by performing a time-course RNA-seq experiment in which flies were refed on sucrose-only food for a different period of time after overnight starvation. To control for the effect of the circadian clock, flies kept on the starvation medium were used as a control for the sugar refeeding group at indicated time points. In this setting, we were able to specifically focus on sugar signaling.

The reproducibility of each biological replicate in the RNA-seq data, as well as the correlative relationships between each condition, were examined in PCA analysis (Fig. 3.1). The biological replicates of each condition were in proximity to each other in PCA plot and were generally closer in principle component 1, indicating a satisfactory reproducibility. Moreover, all of the data can be grouped into four major clusters, which may reflect the similarity in terms of transcriptome level in groups from the same cluster. In particular, the first cluster only includes the groups before the start of refeeding, while the second cluster mainly contains the starvation control groups at 0.5, 1, 2, 3 and 6 hours, as well as the groups refed for 0.5 hours. In fact, only 14 differentially expressed genes (DEGs) were identified at the 0.5 hour refeeding time point, supporting the grouping of data from this refeeding condition with those from starved conditions, as shown in the PCA plot. Groups refed on sucrose for 1 and 2 hours were in the third cluster, while groups refed on sucrose for 3 and 6 hours were in the fourth one. In sum, each cluster represents a profile of the fly transcriptome in response to dietary sugars or starvation. In addition, the analysis also shows how nutrition states (refed vs. starved) or feeding paradigms (feeding length: 0.5, 1, 2, 3, 6 hours) are associated with the sugar-induced transcriptome.

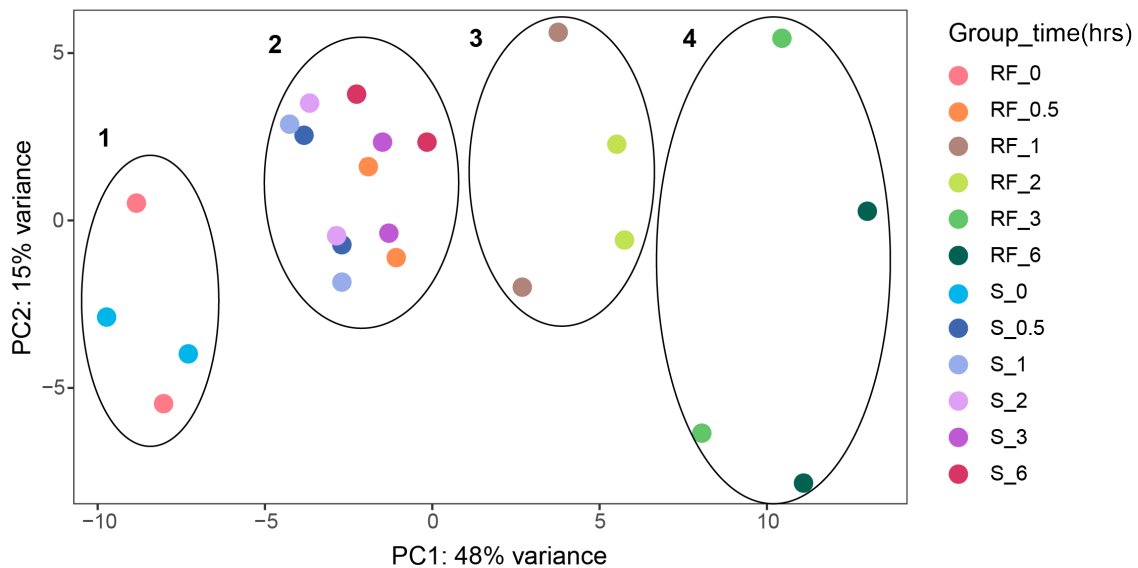


**Figure 3.1. PCA analysis shows the reproducibility of biological replicates and the correlative relationships between each condition in the RNA-seq experiment.** The satisfactory reproducibility of biological replicates is shown in the PCA plot. The data can be basically grouped into four major clusters, which reveals the correlative relationships between each condition. Each experiment condition is color-coded in the same color, and each point represents an experimental group: RF: refed group. S: starved group.

The heatmap of the hierarchical clustering of DEGs pooled from the data of every refeeding time point demonstrates the grouping of DEGs in terms of the expression level, along with the feeding length (Fig. 3.2). In essence, four major clusters with distinct expression patterns are observed in the heatmap. The genes upregulated by sugar refeeding are functionally clustered in “membrane protein” and “oxidoreductase”, while those presenting a late upregulated expression pattern are related to “ribosome biogenesis” and “aminoacyl-tRNA biosynthesis”. Interestingly, the sugar-downregulated genes are involved in several metabolic pathways, such as “fatty acid degradation,” “beta-oxidation of fatty acid,” and “valine, leucine and isoleucine degradation.” In consistent with this finding, the downregulation of these metabolic pathways was also observed after feeding for 6 hours in our unpublished,

starved-refed RNA-seq, in which flies were refed on the regular yeast/sugar fly medium (data not shown). Moreover, because catabolism of fatty acids mostly happens in the starved state, the downregulation of the genes involved in the breakdown of fatty acid in our sugar-induced transcription indicates a metabolic switch from the starved to the refed state.

To find genes for which there are significant gene expression profile differences from starvation controls in the time course, a regression-based approach was applied in the analysis based on the temporal expression profile of identified DEGs. They could be simply categorized as cluster 1, “early-expressed genes”; cluster 2, “late up-regulated genes”; cluster 3 “down-regulated genes”; cluster 4, “down-regulated genes”; and cluster 5, “circadian-dependent genes” (Fig. 3.3). Several known target genes of Mondo, such as *cabut*, *dawdle* and *sugarbabe*, were identified in cluster1, suggesting that Mondo may be rapidly activated by sugar and subsequently regulate its downstream effector genes. Bartok *et al.* (2015) have demonstrated that many key metabolic genes were rapidly repressed by Cabut upon sugar feeding in the sugar-induced transcriptome, in which flies were refed for 6, 12, and 18 hours on 5% sucrose food after 16 hours of starvation (186). Based on the fact that Cabut is the direct downstream effector of the Mondo-Mlx complex in the fly, Mondo may function as the upstream factor in response to dietary sugars. Schmidt *et al.* (2016) integrated the time course sugar-induced transcriptome and the time course ChREBP binding events in INS-1E  $\beta$  cells. The results reveal that ChREBP contributes to a biphasic glucose response: metabolic genes are activated during the first wave of gene transcription, and the genes involved in proliferation are indirectly activated by ChREBP during the second wave. Collectively, Mondo/ChREBP may have a more direct role in the early sugar refeeding time points. Hence, to understand how Mondo is involved in the early response to sugar signaling, I aim to determine the direct target genes of Mondo genome-wide in the fly and later compare these with the time course sugar-induced transcriptome to study how Mondo contributes to the dynamics of sugar responses.

### 3. GENOME-WIDE IDENTIFICATION OF TARGET GENES FOR MONDO-MLX COMPLEX IN THE FLY

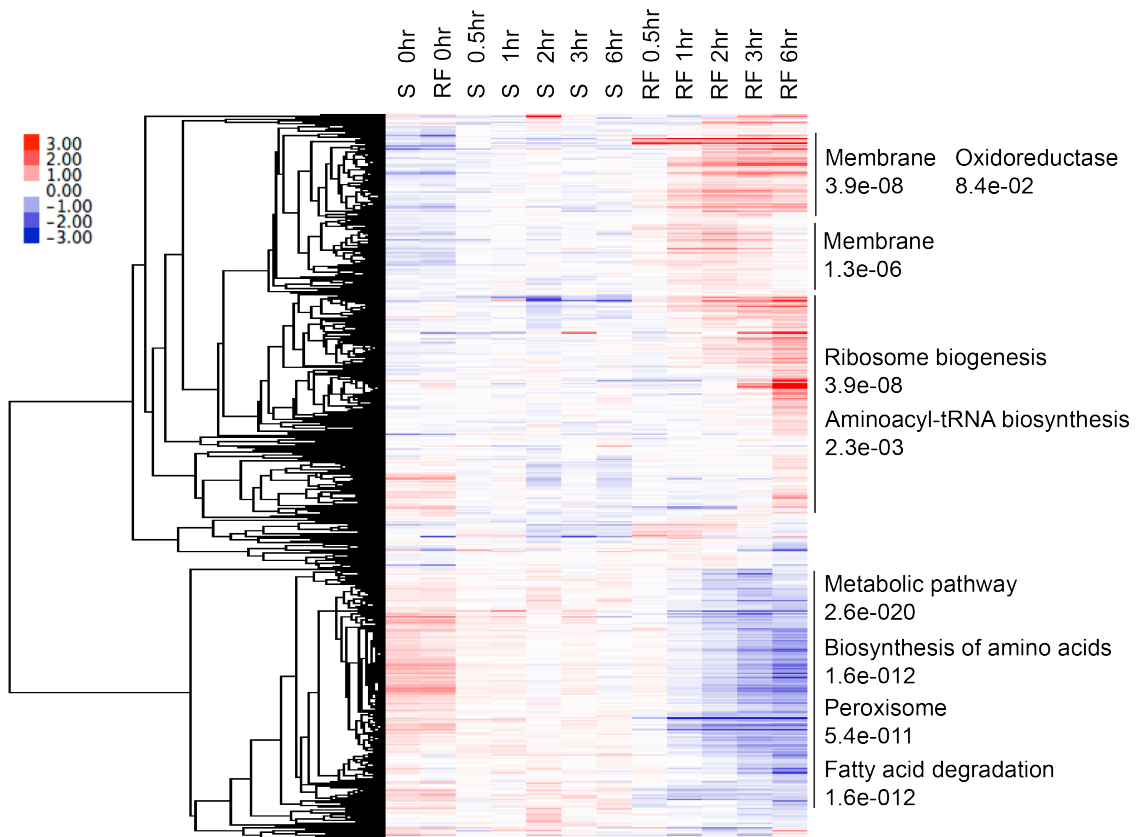


**Figure 3.2. Hierarchical clustering of the time-course sugar-induced transcriptome.** The heatmap of the hierarchical clustering of DEGs identified from the time-course sugar-induced transcriptome demonstrates four clusterings based on expression levels. GO terms and the associated p values were depicted next to each cluster. Red indicates the higher expression values, and blue indicates the lower expression ones (Log Expression Count).

### 3. GENOME-WIDE IDENTIFICATION OF TARGET GENES FOR MONDO-MLX COMPLEX IN THE FLY

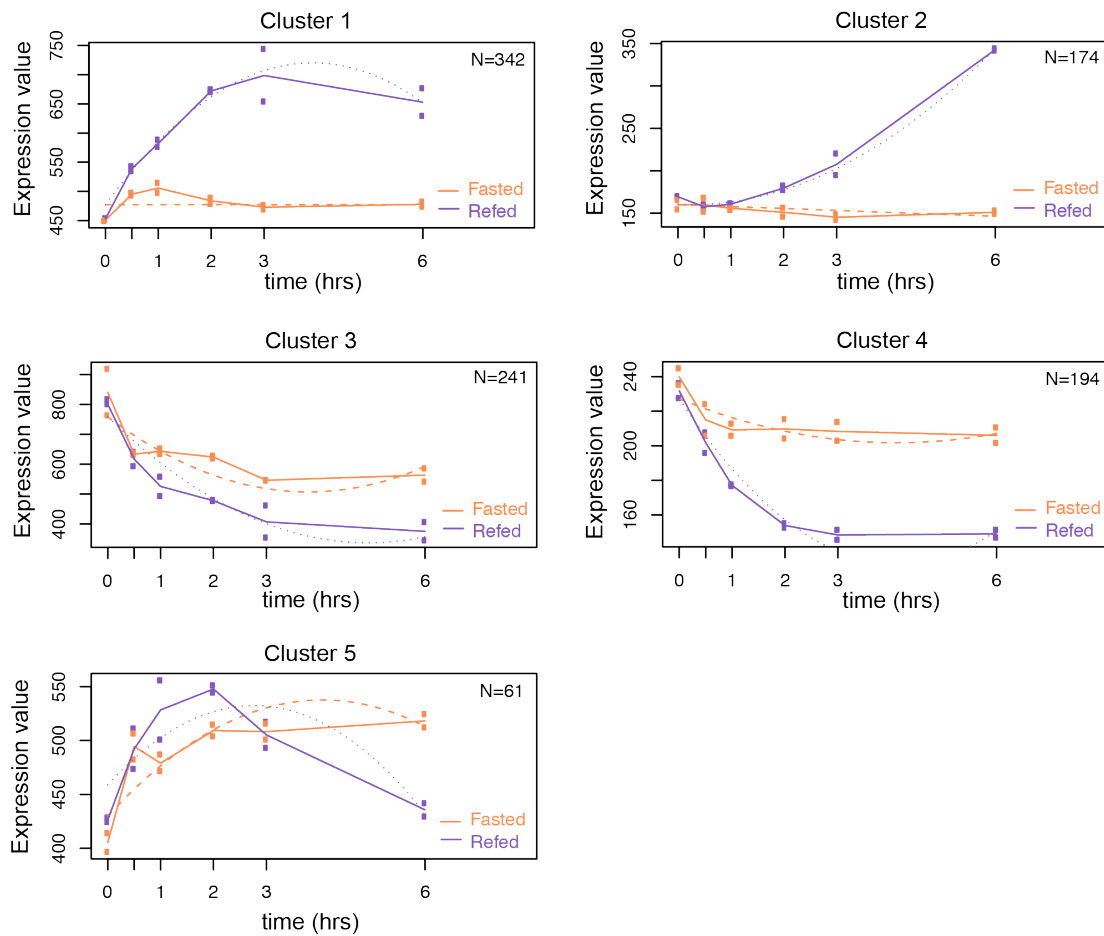


**Figure 3.3 Clustering of the time-course *Drosophila* transcriptome profiling based on the gene expression differences between sugar-refeeding and starvation groups.** DEGs upon sucrose refeeding were clustered into five groups with characteristic expression patterns in the time course. The gene expression profile of the refeed group is depicted in purple, and the fasted group in orange. The number of genes grouped in each cluster is shown in the upper right corner.

#### 3.4.2 *Drosophila* Mondo antibodies show specificity to recombinant and endogenous Mondo protein

In order to identify the direct target genes of Mondo genome-wide by ChIP-seq approach, a ChIP-grade antibody is required for the assay. We used different antigens against several functional Mondo domains to obtain a ChIP-grade antibody. Two antibodies were raised against different lengths of the GSM at the N-terminus and thus called Mondo-short and Mondo-long, respectively. The third antibody was raised



### 3. GENOME-WIDE IDENTIFICATION OF TARGET GENES FOR MONDO-MLX COMPLEX IN THE FLY

Subsequently, protein purification was done, and its efficacy was checked on SDS page (Appendix Fig. A3.3); these proteins were used as antigens for antibody generation. The sensitivity and specificity of each antibody were tested by western blot analysis. The Mondo-long and Mondo-short antibodies can detect the sub-nanogram of a purified Mondo protein (Fig. 3.5A, 3.5B). The Mondo DBD antibody is less sensitive and can detect Mondo when 6 ng of Mondo is loaded for SDS-PAGE (Fig. 3.5C).

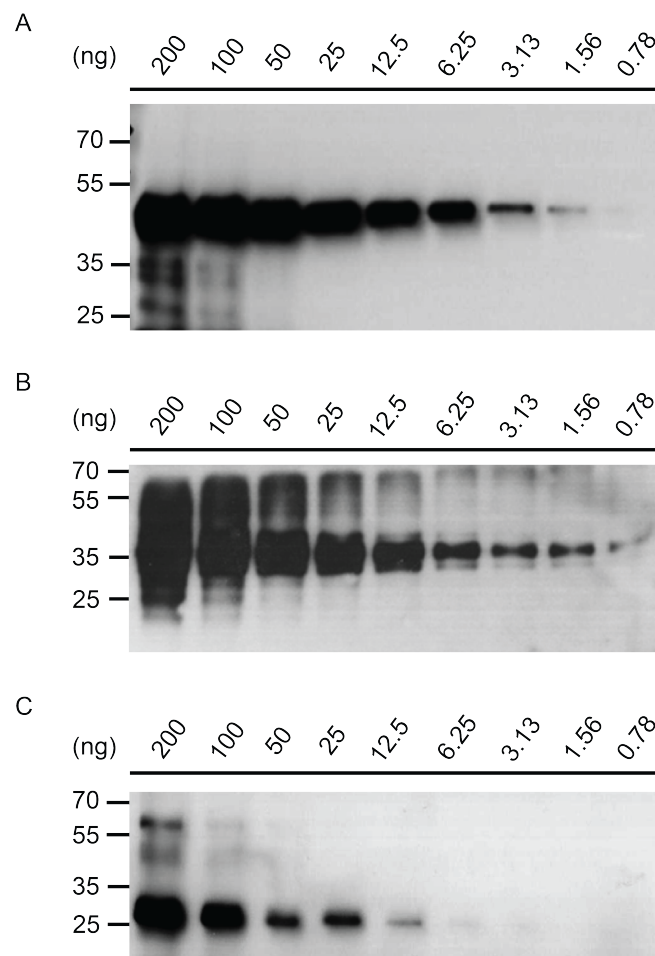


**Figure 3.5. Assessing the sensitivity of Mondo antibodies on the serial titration of recombinant proteins.** Antibodies developed from specific antigenic peptides can detect the recombinant proteins, Mondo long (A), Mondo short (B) to sub-nanogram levels, and Mondo DBD to at least 6.25 ng (C). The molecular weights of Mondo long, Mondo short and Mondo DBD are 50KD, 35KD and 28KD.

Next, Mondo long and Mondo DBD antibodies were tested for specificity on endogenous Mondo in the fly protein extracts. Western blot analysis was performed on extracts made from WT flies, as well as from negative control flies, Mondo<sup>K05106</sup> mutants and CRISPR Mondo mutants, and as a positive control, from flies overexpressing Mondo (heat-shocked and non-heat-shocked hsp70 promoter-driven Gal4, UAS-Mondo). As expected, the antibodies identified a 130 KD protein, which is seen in most WT samples and is increased in the overexpression flies, but it is not seen in the Mondo mutant flies (Fig. 3.6A, 3.6B). A peptide in the CRISPR Mondo flies with the molecular weight at 40 KD was detected by the Mondo long antibody (Fig. 3.6A) but not by Mondo DBD antibody, suggesting that a truncated N terminal part of Mondo was still translated and terminated by the stop codon in the CRISPR cassette. To summarize, we were able to produce antibodies that recognize Mondo in WT fly extracts.

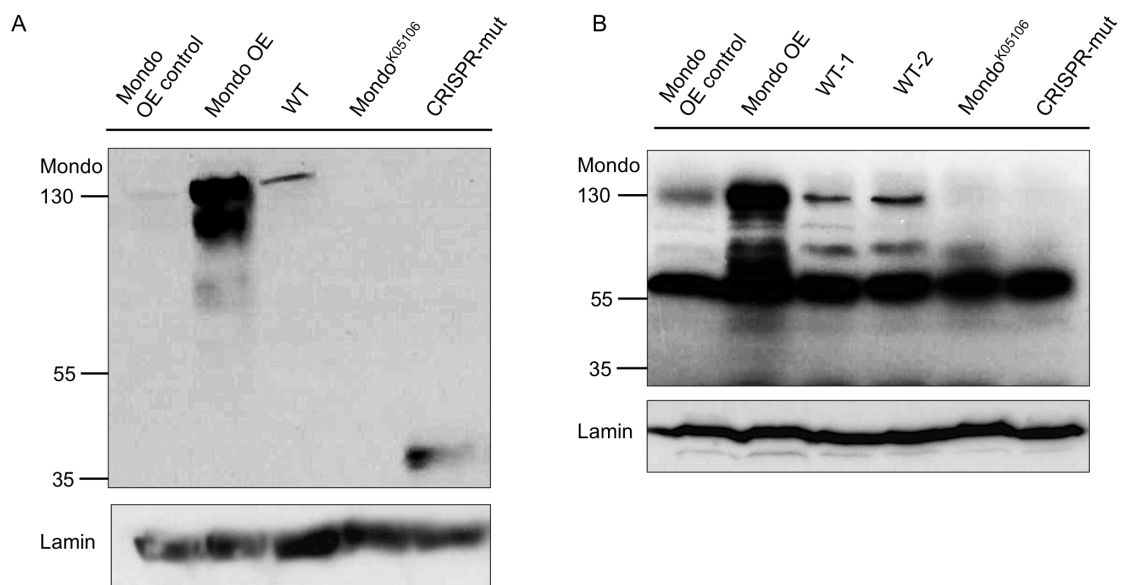


**Figure 3.6. Western blot analysis on fly protein extracts with Mondo antibodies.** (A) Overexpressed and endogenous Mondo were detected by Mondo long antibody probed in the fly, but not in Mondo mutants. (B) The Mondo DBD antibody probed Mondo protein in Mondo overexpressed flies and WT flies, but not in Mondo mutants. Lamin was used as a loading control.

Lastly, these antibodies were tested to determine whether they were able to immunoprecipitate Mondo in ChIP assay. Mondo ChIP was performed on the flies, which were continuously fed on 20% sucrose + yeast food. ChIP assay was then followed by qPCR, which was performed against the Mondo target site. The acetyl-CoA carboxylase (*acc*) gene was used as a putative target for Mondo to test these antibodies. Several lines of evidence suggest that the *acc* gene is a direct target of Mondo in mammals and flies. The mammalian ChREBP can bind directly to the mammalian *acc* gene and regulates *acc* expression (193). The *acc* mRNA expression is down-regulated in Mondo<sup>k05106</sup> (159) as well as in the *Drosophila* Mlx mutant Mlx<sup>1</sup> (157). In addition, the ChoRE site within the *acc* gene was identified in Mlx mutant Mlx<sup>1</sup> (113), and the same ChoRE site was used as a putative target of Mondo in the ChIP-qPCR.

For negative controls, 700 bp upstream of the *acc* ChoRE site and a polycomb binding site upstream of the *ubx* gene (194) were used in qPCR. The results show that the Mondo long antibody was enriched for the *acc* ChoRE site compared to both negative controls, and it performed better than the other two antibodies (Figure 3.7A). The Mondo long antibody also displayed a better enrichment in comparison to the preimmuneserum. In contrast, the other two antibodies had little enrichment when compared with their respective preimmuneserums (Figure 3.7B). Taken together, the Mondo long antibody will be useful to immunoprecipitate Mondo and was therefore used for the ChIP-seq experiments to identify the direct target genes of Mondo in the fly.

3. GENOME-WIDE IDENTIFICATION OF TARGET GENES FOR MONDO-MLX COMPLEX  
IN THE FLY

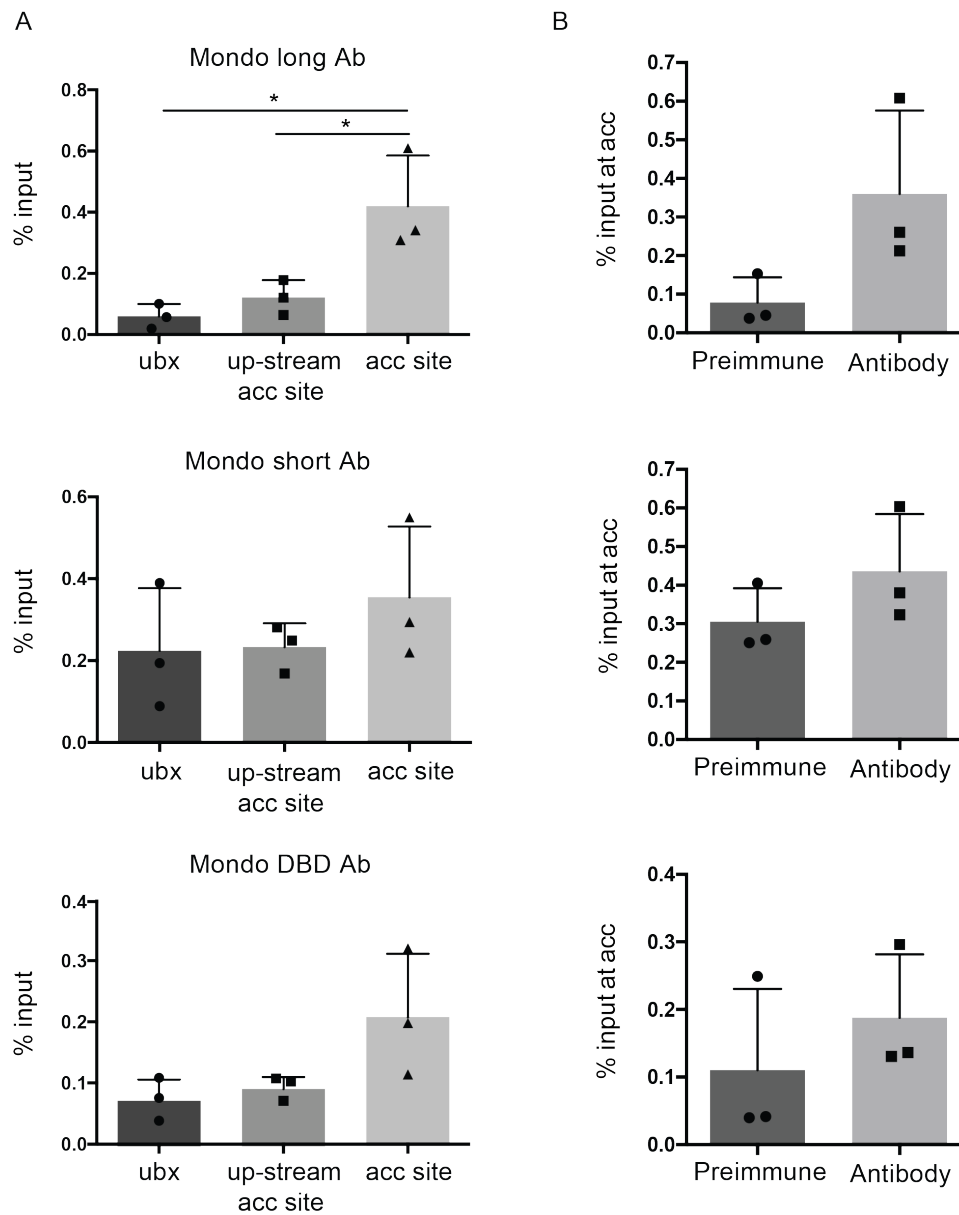


**Figure 3.7. The efficiency of the Mondo-ChIP experiment with three Mondo antibodies is evaluated with qPCR.** (A) ChIP-qPCR against the Mondo binding site at the *acc* promoter and non-binding sites indicates a better ChIP result with a Mondo-long antibody. (B) qPCR following ChIP with Mondo antibodies and the corresponding pre-immune serums shows a better ChIP result with Mondo-long antibody. Error bars represent  $\pm$  SEM (\*  $p < 0.05$ ; \*\*  $p < 0.01$ ; \*\*\*  $p < 0.001$ ).

### 3.4.3 Mondo is most active at the early sugar-refeeding time point

In order to know when Mondo is activated, I performed RT-qPCR on flies that were refeed on 20% sucrose-only food for 0.5, 1, 2, 3 and 6 hours after 21 hours starvation (Fig. 3.8A). We observed that the expression of *cbt*, a known Mondo target, was already increased after refeeding for 0.5 hr (Fig. 3.8B). This indicates that Mondo rapidly responds to sugar and regulates the transcription of its direct target genes. In support of this observation, a time course Mondo ChIP-qPCR showed that Mondo is more enriched at the putative ChoRE site of the *cbt* gene after 1 hour of sugar refeeding compared with the later refeeding time points. Thus, I applied the feeding paradigm with which flies were first starved and refeed for 1 hour on 20% sucrose food for the ChIP-seq experiment to achieve better ChIP results.

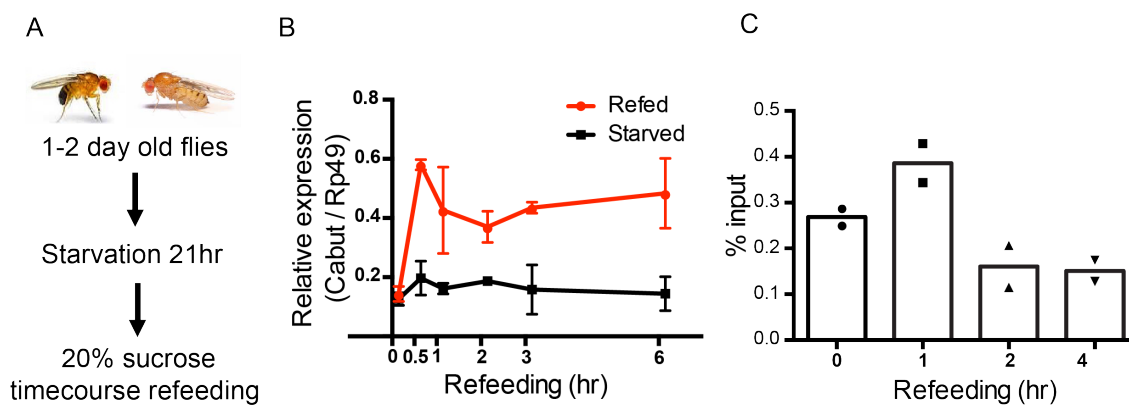


**Figure 3.8. Mondo is most active at the 1 hour sugar-refeeding time point.** (A) Schematic presentation of the starved and sugar-refeeding paradigm used in the time-course feeding experiment. (B) RT-qPCR showed the *cbt* mRNA expression pattern from the flies that were refeed on 20% sucrose for different periods of time. (C) qPCR against the *cbt* gene following the timecourse Mondo ChIP shows that Mondo is more enriched at the 1 hour sugar-refeeding time point.

### 3.4.4 Identification of Mondo direct targets in the adult fly head

Performing ChIP-seq to identify the genome-wide target sites of Mondo allows the globally unbiased determination of the target genes of Mondo, and it also helps identify the overall enriched biological and molecular pathways by functional

clustering analysis. Mondo ChIP was performed on adult WT flies and Mondo<sup>K05106</sup> mutants. Because the Mondo mutant is adult viable and appears to be a protein-null mutant (Figure 3.6), it is an exemplary control for Mondo ChIP. Ideally, it is expected that the Mondo-specific antibody would only enrich for specific DNA sequences from WT chromatin, but not from Mondo mutant chromatin. In addition, Mlx ChIP was also performed on WT and Mondo<sup>K05106</sup> mutant chromatin. Mlx is commonly seen as the only bHLHZip partner of Mondo (160, 195); thus, we expect that Mlx should bind to many and maybe to all of the Mondo binding sites. However, this bHLHZip transcription factor family often has several different interacting partners and forms a protein heterodimer to bind to a DNA target. By comparing Mondo and Mlx binding sites, we could test the current model of Mondo interacting with Mlx as a binding partner to recognize cis-regulatory elements.

RNA polymerase II (Pol II) ChIP was also performed using a Rpb3 antibody on chromatin isolated from WT flies and Mondo mutants. The rationale for including the Pol II ChIP in this experiment was to investigate the mechanisms by which Mondo activates transcription. In the past, transcription factors were thought to only activate transcription by recruiting RNA polymerase to promoters (196, 197). Since then, the genome wide-profiling of Pol II has indicated that Pol II is already recruited at many promoters well before any signal of transcription is given (198-200), thus modifying the model of how transcription factors activate transcription. Some transcription factors, such as pioneering factors and the GAGA factor, recruit Pol II to promoters in accordance with the classic model of the transcription function (201, 202). In contrast, other transcription factors, such as the bHLHZip transcription factor c-Myc (203), have been shown to induce elongation or promoter escape. In addition to adding the mechanistic understanding of Mondo transcriptional activity, the Pol II ChIP serves as a control for the quality of the chromatin, particularly for the Mondo mutant chromatin. In contrast to Mondo and Mlx, which should not ChIP this mutant chromatin, Pol II should still bind to chromatin in the mutant, thus verifying the quality of the mutant chromatin. As when testing the antibodies, chromatin was prepared from flies that were refeed sucrose for 1 hour after fasting for 21 hours. To test for the quality of the Mondo and Mlx ChIP, qPCR was used to assess the enrichment of protein at a putative binding site. Here, the binding site for Mondo-Mlx

in the Krüppel-like transcriptional repressor, the *cbt* gene was used. This gene, like the *acc* gene, was also previously identified as a putative target for Mondo, as it also has two ChoRE sites, and the Mondo binding partner Mlx binds to the *cbt* ChoRE site in a glucose-dependent manner in *Drosophila* cell culture (186). The ChIP-qPCR showed that both Mondo and Mlx were enriched at the *cbt* ChoRE site in WT flies, and were much less enriched at 28 bp downstream of the *fas2* gene that can be bound by Pol II but be targeted by Mondo-Mlx (Fig. 3.9A and 3.9B). On the other hand, Pol II was enriched at 28 bp downstream of the *fas2* gene but not at ChoRE site in both WT and Mondo mutants (Fig. 3.9C). Taken together, the ChIP-qPCR results reveal the satisfactory quality of ChIP experiments, therefore sequencing libraries were made of these ChIPs and input DNA via Illumina sequencing.

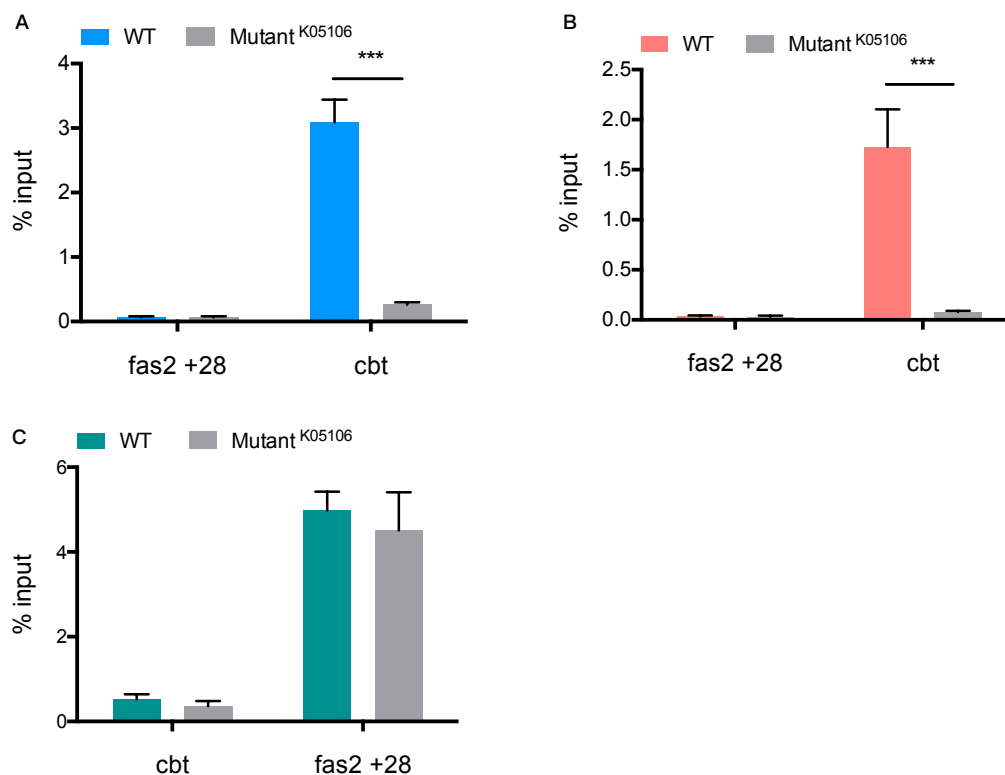


**Figure 3.9. Mondo-Mlx ChIP-qPCR on WT and Mondo mutant flies.** ChIP-qPCR shows that Mondo (A) and Mlx (B) were enriched at the target site of the *cbt* gene but not at 28 bp downstream of the *fas2* gene that is considered as a negative Mondo-Mlx target site. (C) ChIP-qPCR shows that Pol II was enriched at 28 bp downstream of the *fas2* gene. Error bars represent  $\pm$  SEM (\*  $p < 0.05$ ; \*\*  $p < 0.01$ ; \*\*\*  $p < 0.001$ ).

Principle component analysis (PCA) based on total read counts was first conducted to examine the quality of sequencing samples in terms of the reproducibility of the biological replicates (Fig. 3.10A). An acceptable reproducibility is shown if the biological replicates are clustered in proximity. As expected, the input chromatin clustered closely, indicating a similar background in the replicates. Both WT and mutant Rpb3 ChIP-seq data cluster away from inputs, while Mondo and Mlx ChIP-seq data are clustered particularly for the first principle component. Rpb3 ChIP-seq data for the mutant and WT cluster together suggest that there are no large changes in Pol II binding to chromatin in the presence or absence of Mondo. In contrast, both the Mondo and Mlx ChIP-seq data cluster away from the input samples and the Rpb3 ChIP-seq data. The WT Mondo ChIP-seq data cluster separately from the mutant Mondo ChIP-seq data along the second component axis. Similarly, Mlx ChIP-seq on Mondo mutant chromatin clusters separately from the Mlx ChIP-seq on WT. This suggests that there are differences in Mondo and Mlx binding in the WT and mutant. In addition, Mondo and Mlx were shown bind to the known Mondo-Mlx target genes in WT but not in Mondo mutants (Fig. 3.10B), indicating that our data are reliable in terms of continuing the analyses.

To identify the direct targets for Mondo and Mlx, I compared the peak sets in the ChIP-seq data from WT (2,849 peaks) and mutants (2,593 peaks). To our surprise, 1,875 of the peaks called in the WT Mondo-ChIP-seq were also seen in the Mondo mutant. Although the Mondo ChIP-seq appears to have a high background, using the data from the Mondo mutant to perform differential analysis, I have excluded the non-specific background to obtain 1,252 putative Mondo binding sites (Fig. 3.11A). Because of the non-specific binding of chromatin in the Mondo ChIP-seq, it is highly possible that the same non-specific binding occurs in the Mlx-ChIP-seq. Therefore, instead of using the Mlx and the Mondo ChIP-seq to identify the genes that Mondo regulates independently of Mlx and the genes that Mlx regulates independently of Mondo, Mlx-ChIP-seq was used to validate the Mondo binding sites, as Mlx is known to be interacting partner of Mondo. For this purpose, I identified the 2,248 differential peak regions in the WT Mlx ChIP-seq compared to the data from the Mondo mutant (Fig. 3.11B). To create a list of Mondo target sites with high stringency, I overlapped the differential Mondo binding sites with differential Mlx binding sites that requires

3. GENOME-WIDE IDENTIFICATION OF TARGET GENES FOR MONDO-MLX COMPLEX  
IN THE FLY

Mondo for DNA binding, resulting in 1,104 identified binding sites for Mondo-Mlx complex (Fig. 3.11C). In total, 88% (1,104 out of 1,251) of the Mondo binding sites were also targeted by Mlx, suggesting that Mondo interacts with Mlx for most of the putative target genes. In addition, the list of Mondo-Mlx binding sites was used for subsequent analyses.

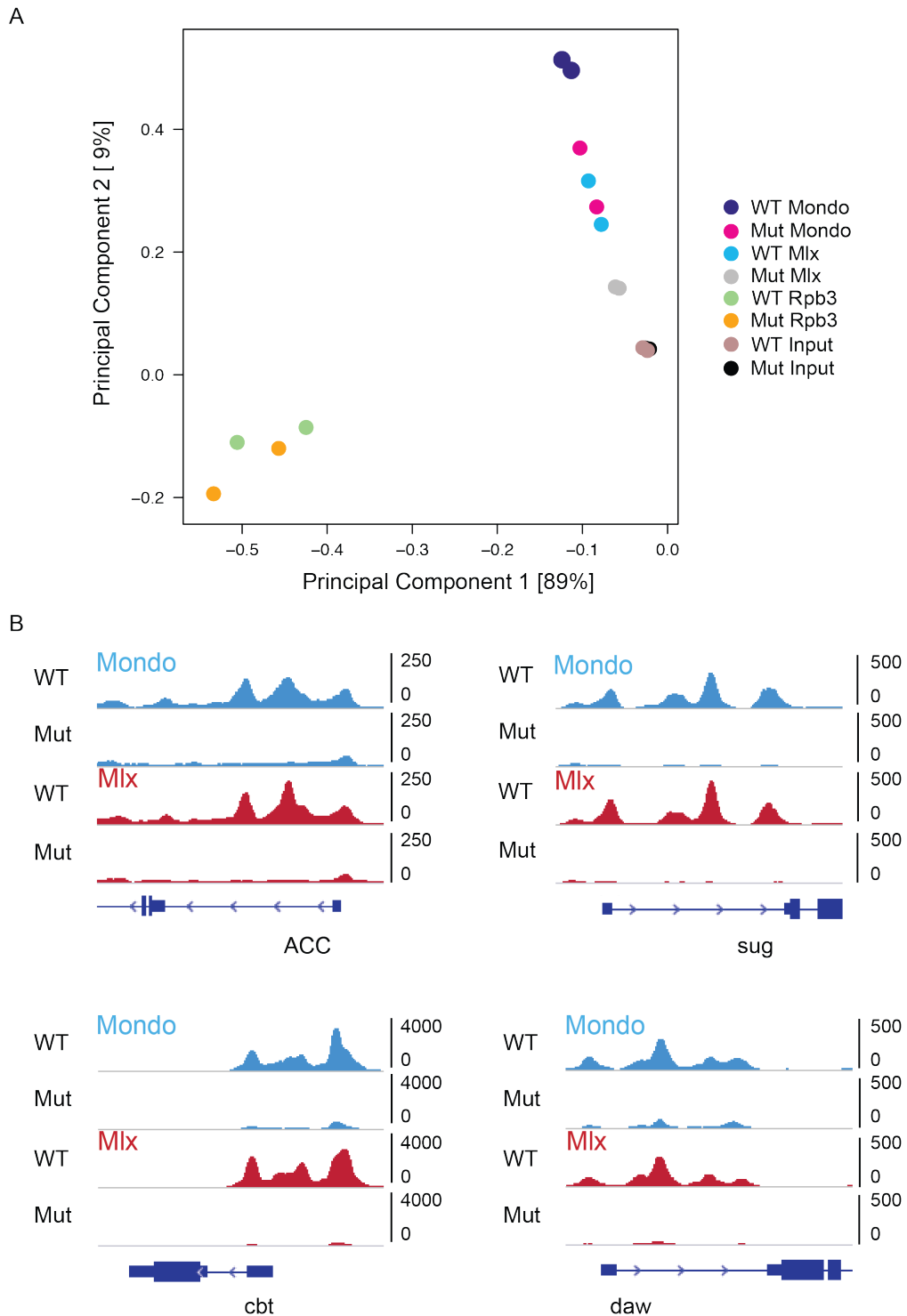


**Figure 3.10. PCA analysis and the Mondo-Mlx peak profile at known target sites.**

(A) PCA analysis on the read counts of each data is presented as dots in the plot. Biological replicates of the same group are color-coded in the same color. (B) The peak profile of Mondo and Mlx at known target genes in WT and the Mondo mutant indicate convincing ChIP-seq results.

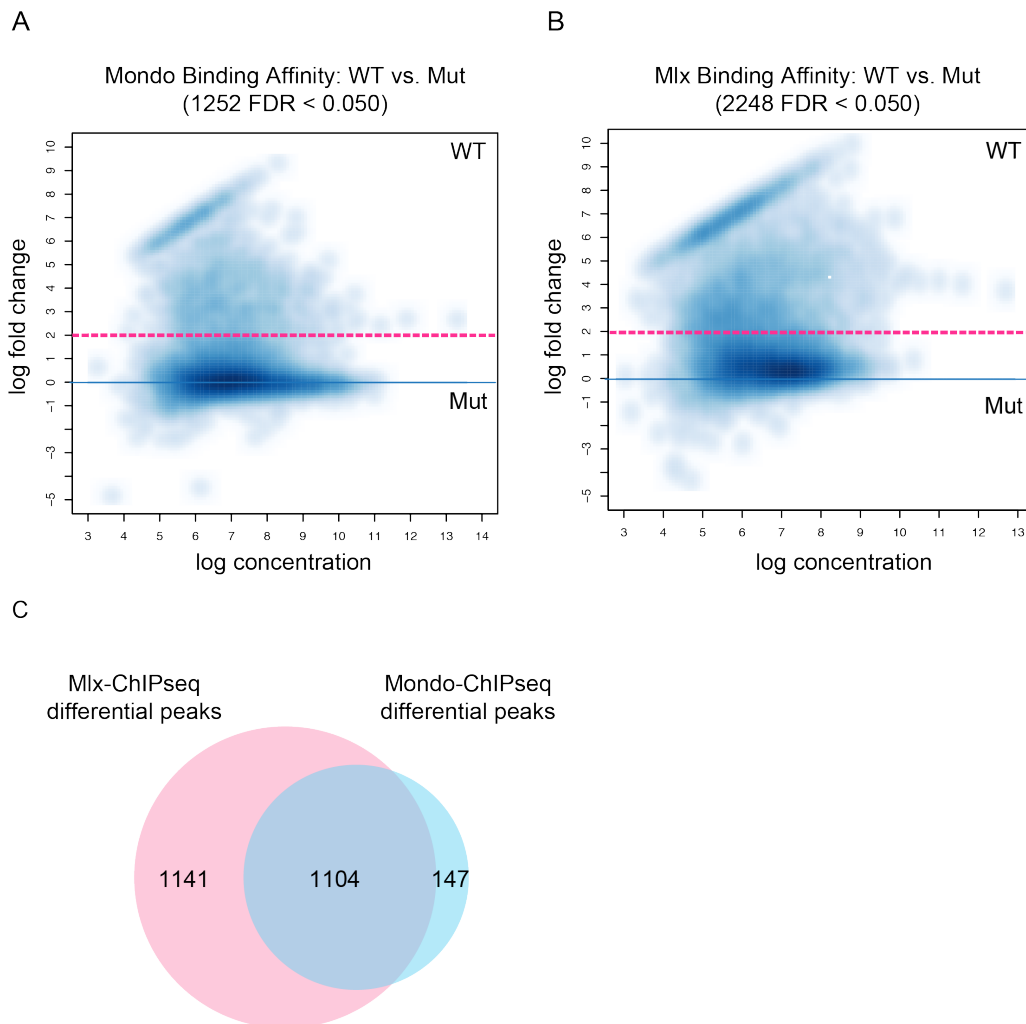


**Figure 3.11. Differential binding analysis of Mondo and Mlx targeted sites.**

Mondo (A) and Mlx (B) binding analysis between WT and Mondo mutants. The line in blue is the baseline for differential peaks in WT or mutants. The dashed line in pink indicates the threshold (fold change > 2) set for the differential peaks identified in WT. (C) The Venn diagram shows the overlapping between putative Mondo and Mlx target sites.

### 3.4.5 Mondo-Mlx binds primarily to promoters and intronic regions

Transcription factors are commonly thought to bind to regulatory regions, such as promoter and transcription start sites, to regulate gene transcription. In order to understand the regions Mondo most likely binds to, the Mondo-Mlx binding sites are characterized based on their relative positions to the closest genes using the *Drosophila* genome sequence release 6 (dm6). The distribution of the genetic features in the genome background was characterized (Fig. 3.12 A). Among Mondo-Mlx-binding regions, approximately 30.7% are in the promoter ( $\leq 1,000$  bp) of the genes. An additional 39% are located in introns that may represent enhancers or silencers, or TSS for the shorter isoforms of the gene. The remaining site distributions are within 5' UTRs (3.9%), 3' UTRs (1.7%) and exons (4.8%; Fig. 3.12 B).

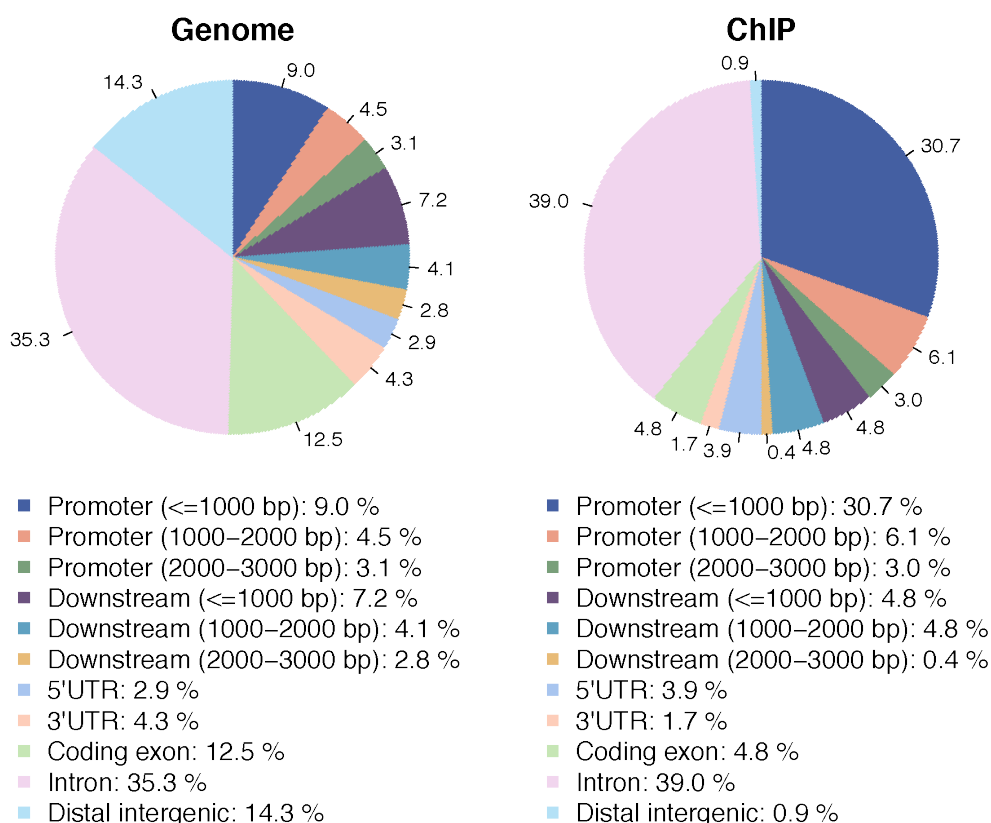


**Figure 3.12. Genomic distribution of Mondo-Mlx target sites.** (A) Genomic features in the genome background. (B) Genomic distribution of Mondo-Mlx-binding sites.

### **3.4.6 Motif searching analysis reveals the canonical ChoRE motif and a novel “GATAA” motif within putative Mondo-Mlx target sites**

It has been demonstrated that many glucose-regulated ChREBP/Mondo target genes contain the conserved ChoRE binding sites featured with two separate E boxes and five nucleotides in between. To determine whether the canonical Mondo binding motif also presented in our ChIP-seq dataset, motif searching was performed based on the sequences of 1,104 putative Mondo-Mlx target sites. It is worth noting that none of the motifs identified from the unfiltered data was centrally enriched at target sites in the analysis (data not shown). The motif searching based on the filtered binding sites showed a centrally enriched ChoRE motif at 398 target sites (Fig. 3.13A), again indicating that the identified peaks in our ChIP-seq presented those convincing peaks. Meanwhile, a novel DNA motif sequence “GATAA” was also identified at 289 Mondo-Mlx binding sites with more dispersed distribution within peaks compared to the ChoRE motif (Fig. 3.13B). It is interesting to clarify whether this putative “GATAA” motif was targeted solely by the Mondo-Mlx complex or co-existed in the same peak with ChoRE, which may provide an additional level of regulation by Mondo-Mlx to those genes. The comparison of the peak sets associated with these two motifs showed that 318 peaks contain the ChoRE element, 209 peaks contain the “GATAA” motif and 80 peaks have both (Fig. 3.13C). Next, to address whether the annotated genes associated with the peaks in each subset are functionally clustered distinctly, GO term analysis was performed. The results showed that genes with the “GATAA” motif were related to amino acid biosynthesis, while genes with the ChoRE motif were associated with fatty acid biosynthesis (Fig. 3.13D). Certainly, the binding of Mondo-Mlx to “GATAA” sites must be confirmed with experiments such as reporter assay or electrophoretic mobility shift assay (EMSA). It is of vital importance to study whether this region also serves as a regulatory binding site and how Mondo targets this motif to transduce regulation signaling.

### 3. GENOME-WIDE IDENTIFICATION OF TARGET GENES FOR MONDO-MLX COMPLEX IN THE FLY

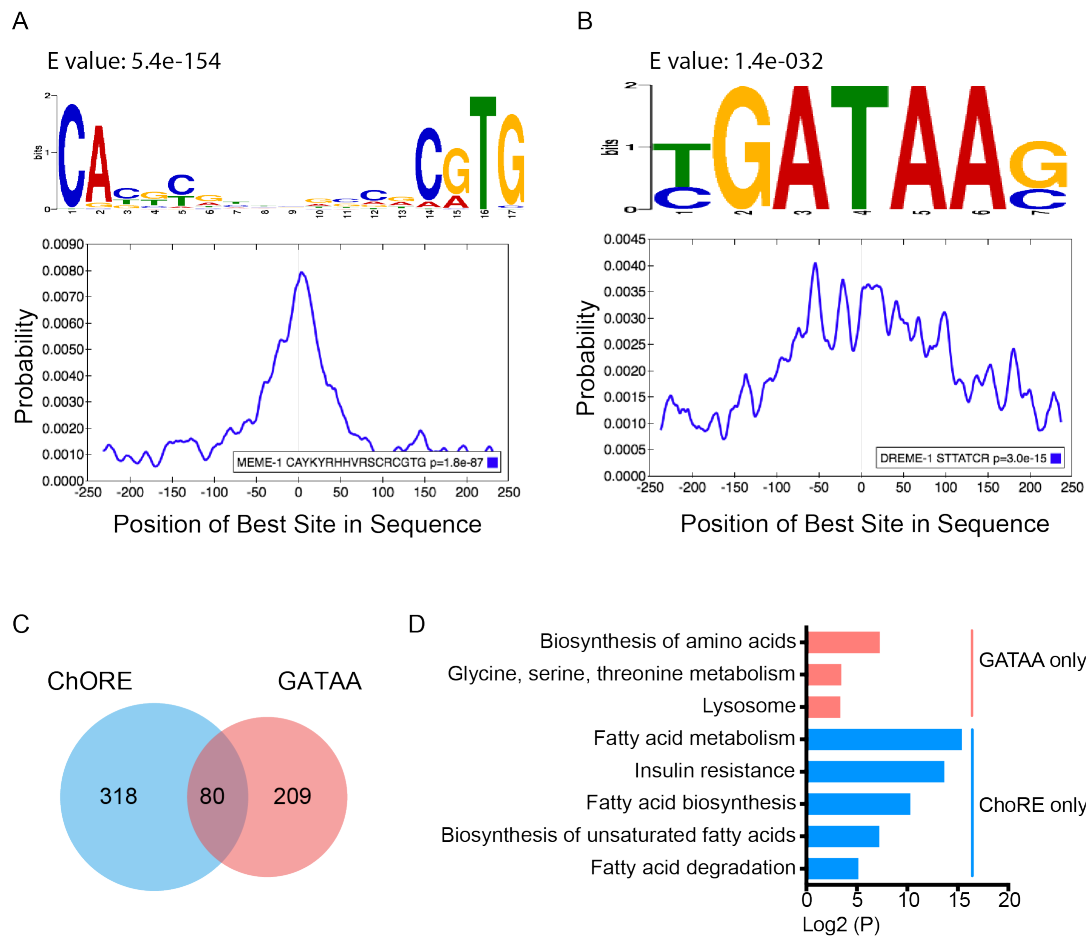


**Figure 3.13. Mondo-Mlx consensus binding sites predicted from the motif discovery program in MEME-ChIP.** Motifs found by de novo searching of Mondo-Mlx targets are the ChoRE element (A) and a novel motif (B). Plots of motif position as a function of distance from the peak summit are presented below. (C) A Venn diagram showing the overlap between ChoRE-contained peaks and TTATC-contained peaks. (D) GO term analysis on genes associated only with the ChoRE or GATAA motif.

#### 3.4.7 Mondo-Mlx's target genes are functionally clustered in metabolic pathways

To understand the potential function of Mondo-Mlx direct target genes, GO enrichment analysis regarding the biological process, molecular function and KEGG pathways was performed on those putative Mondo-Mlx targets (Fig. 3.14). Most of the functionally clustered KEGG pathways are related to metabolic pathways.

Moreover, several target genes were mapped in the pathways, such as “glycolysis and gluconeogenesis” (Fig. 3.15 A), “fatty acid metabolism” (Fig. 3.15 B), and “biosynthesis of amino acids” (Fig. 3.15 C); this reveals that these pathways are tightly regulated by Mondo-Mlx. This result is consistent with the role of *Drosophila* Mondo and mammalian ChREBP, which has been reported as a key metabolic regulator in the fly. Additionally, GO terms such as “sleep,” “long-term memory” and “olfactory learning” were among those associated with biological processes, suggesting that Mondo-Mlx may mediate these behaviors in the fly to control the overall energy balance. Fifty-four Mondo-Mlx target genes were shown to be involved in the oxidation-reduction process, which can be important during energy production and can maintain redox in cells to prevent oxidative stress. The GO terms regarding molecular function included “protein serine/threonine kinase activity,” “glucose transmembrane transporter activity,” “ATP binding” and “transcription factor activity”. Overall, the results suggest that Mondo-Mlx may have an extended function beyond metabolism.

#### **3.4.8 Mondo-Mlx is on top of a transcription cascade that targets several transcription factor genes**

It is noteworthy that 20 transcription factor genes were shown in the GO term analysis, and the canonical DNA binding motif was identified at all of these genes in the motif searching analysis (Figure. 3.16). The ChoRE sequences are shown in appendix table A3.2. In support of this observation, 12 out of 20 transcription factor genes displayed an altered expression in published Mondo-Mlx-dependent RNA-seq (60, 113). Interestingly, a decreased association of CTCF with its binding sites has been shown in the presence of aberrant metabolism (205). Our data also demonstrate the binding of Mondo-Mlx complex to the *hnf4* gene. In fact, Meng *et al.* have shown that the binding of HNF4 $\alpha$  to the *cis*-element of the ChREBP gene can activate the sugar-induced ChREBP transcription. This indicated a potential feedback loop between Mondo and HNF4 $\alpha$ . Taken together, it appears that Mondo may orchestrate a transcriptional cascade and regulate the transcription of various transcription factors.

3. GENOME-WIDE IDENTIFICATION OF TARGET GENES FOR MONDO-MLX COMPLEX  
IN THE FLY

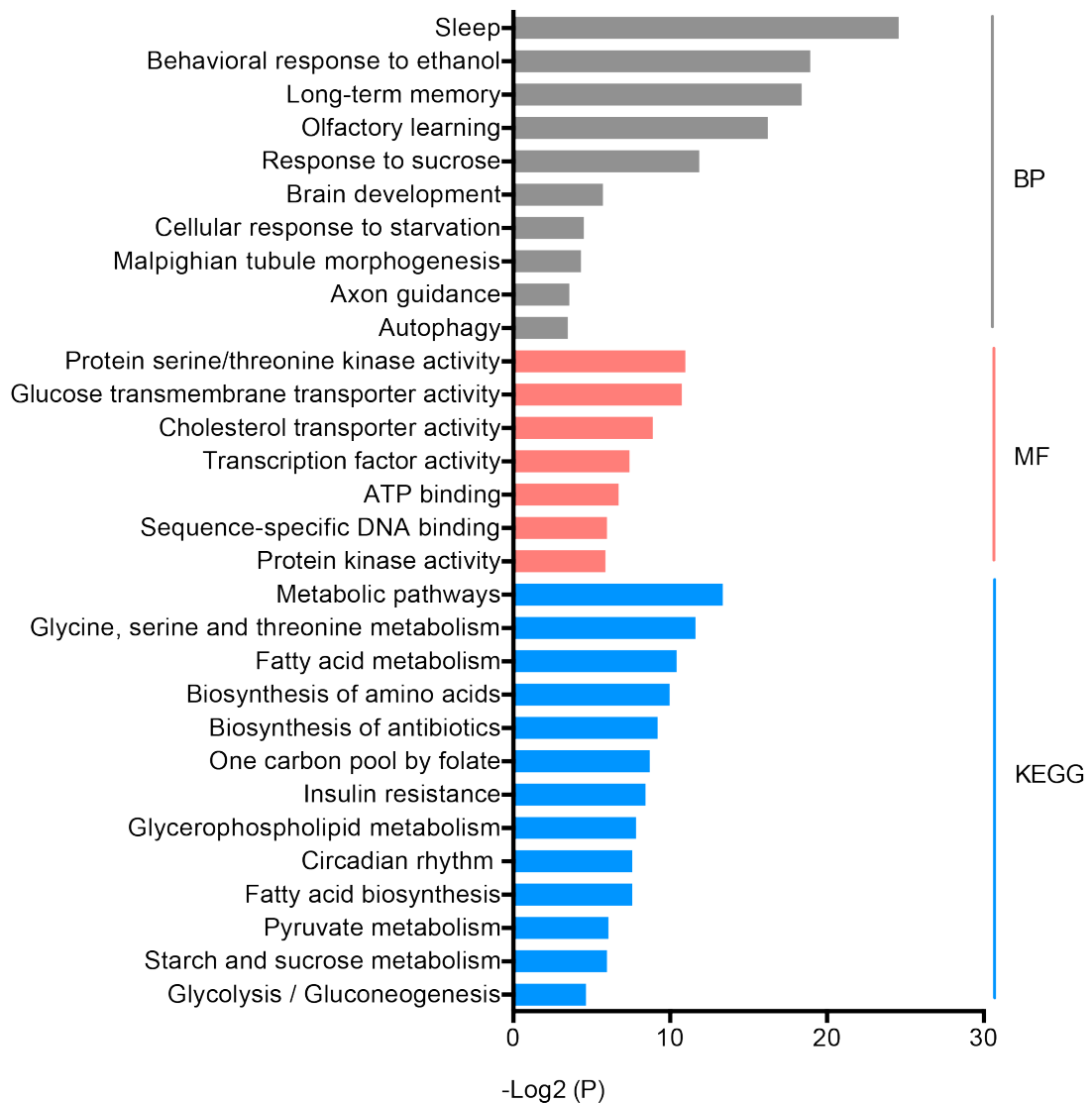
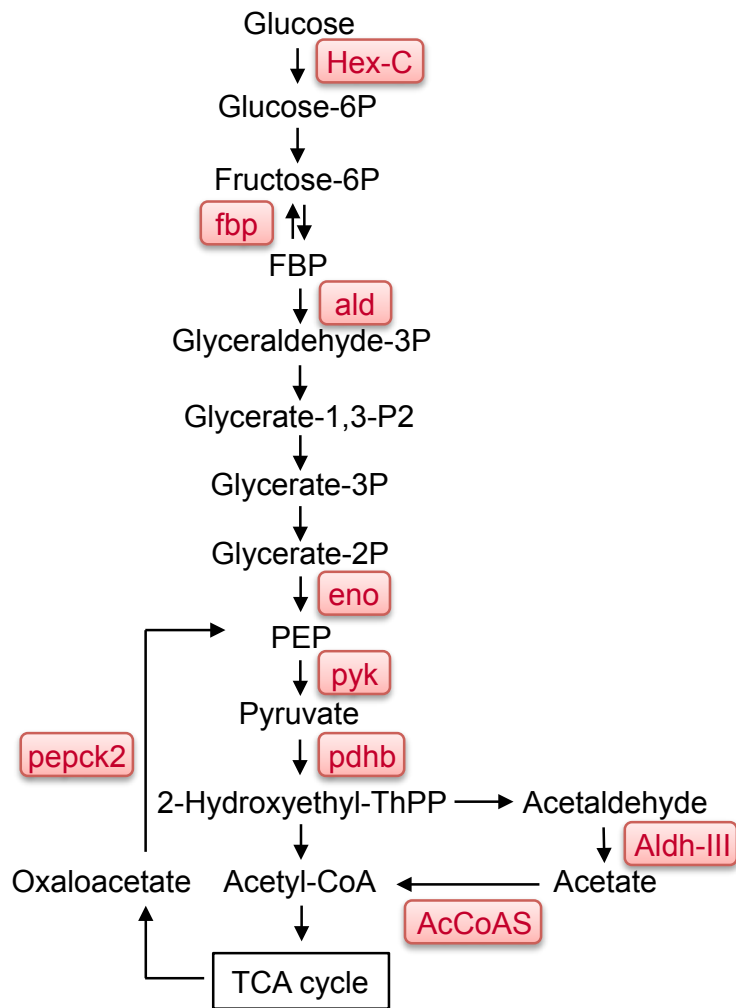


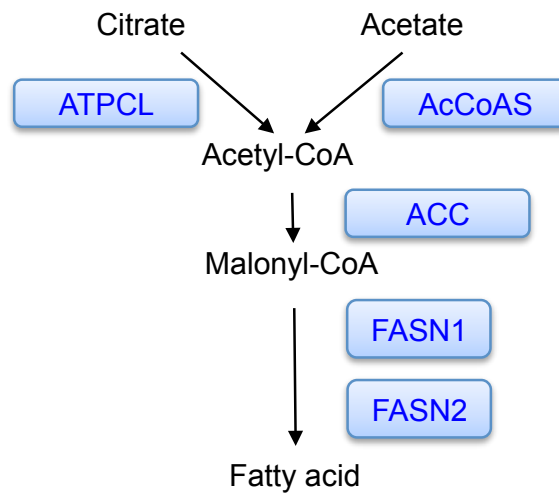
**Figure 3.14. GO term analysis on Mondo-Mlx targeted genes from DAVID.** Significantly enriched GO terms related to biological process (BP), molecular function (MF) and KEGG pathways (KEGG) are presented. Their  $-\log_2 P$ -values are plotted on the x-axis. Terms derived from the biological process are color-coded in gray, those associated with molecular function are depicted in red and those from KEGG pathways are shown in blue.

3. GENOME-WIDE IDENTIFICATION OF TARGET GENES FOR MONDO-MLX COMPLEX  
IN THE FLY

A



B



C

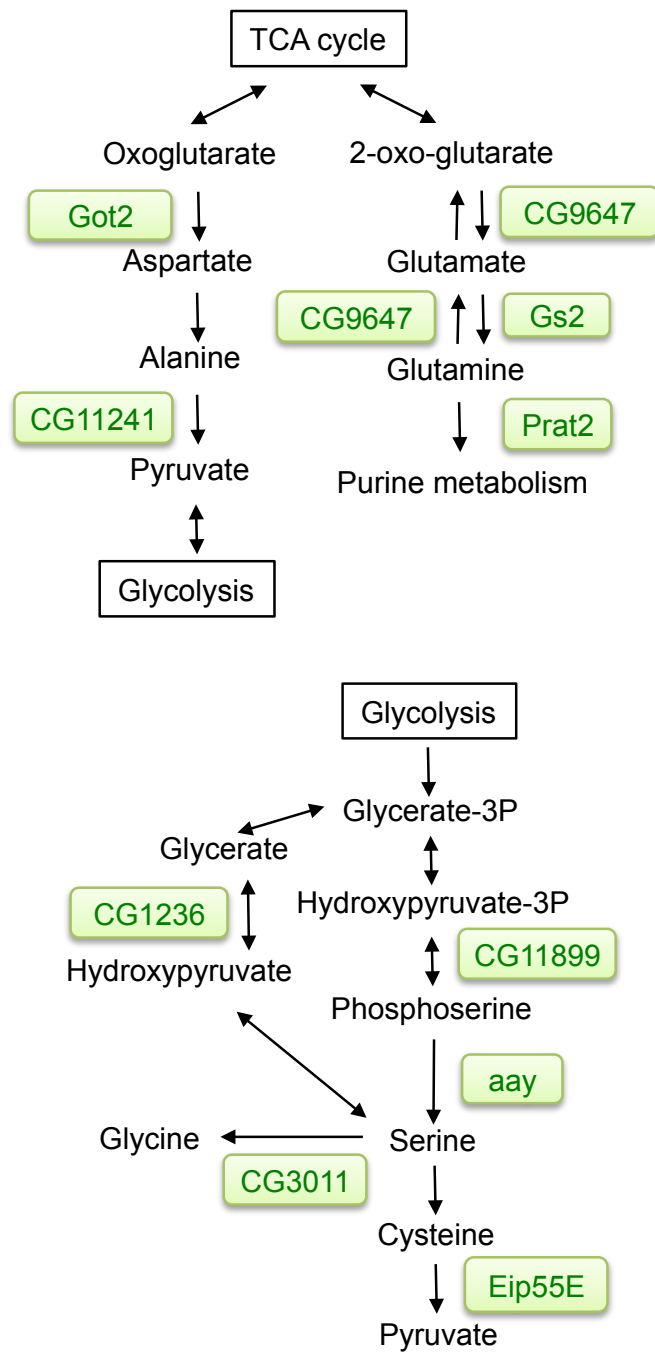


**Figure 3.15. Mondo-Mlx targeted genes involved in glycolysis, lipid synthesis and amino acid biosynthesis.** The identified Mondo targets are involved in the glycolysis pathway (A), the lipid synthesis pathway (B), and the amino acid biosynthesis pathway (C).

3. GENOME-WIDE IDENTIFICATION OF TARGET GENES FOR MONDO-MLX COMPLEX  
IN THE FLY

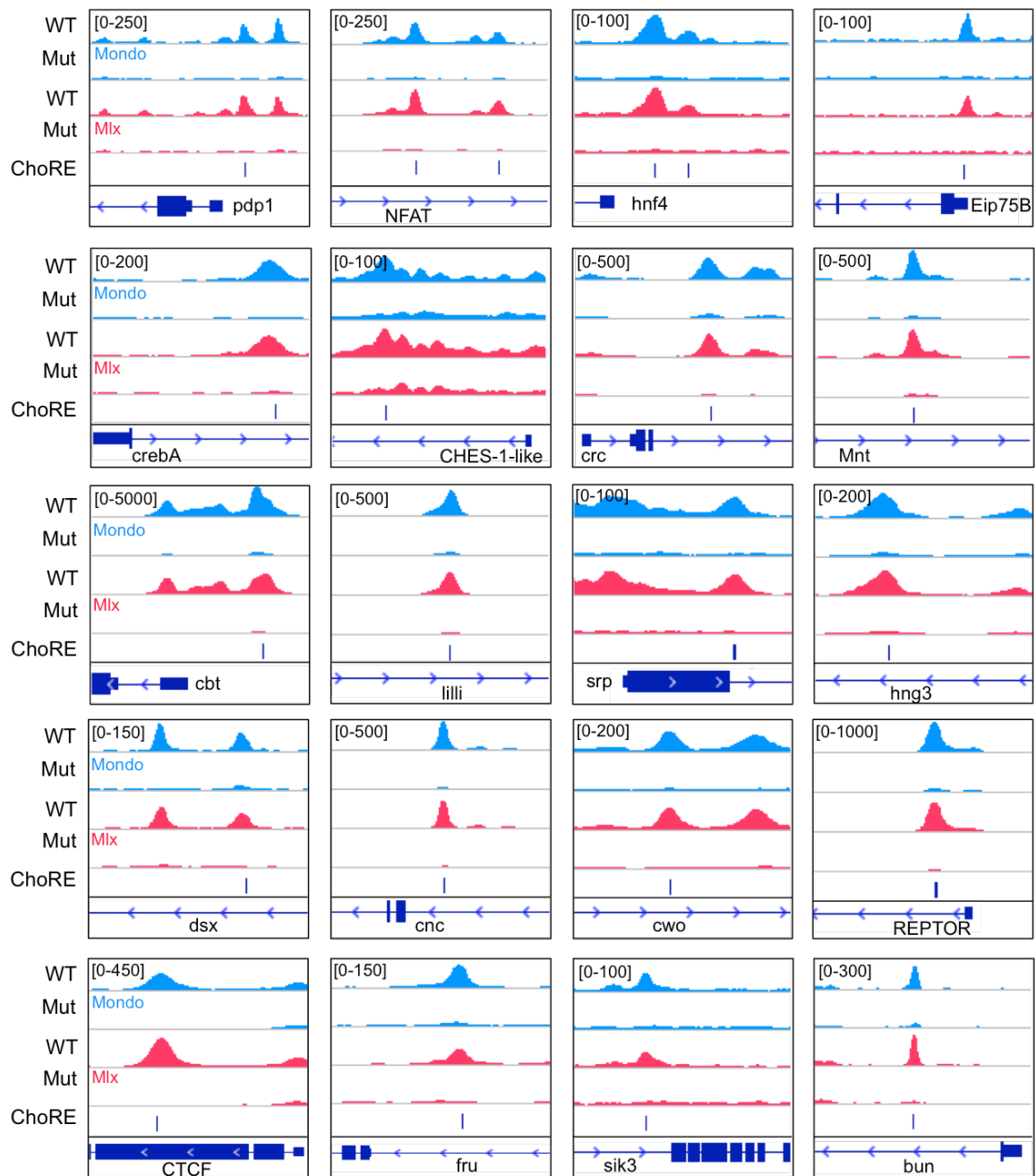


**Figure 3.16. Differential Mondo and Mlx peaks at the genes with transcription factor activity.** The peak profiles of Mondo-Mlx binding at genes with transcription factor activity binding are depicted. ChoRE element within these genes are identified and shown in the figure. The tracks in blue are the Mondo binding profile, and those in red present the Mlx binding profile.

### 3.4.9 Mondo regulates the recruitment and elongation of Pol II at the direct target genes

The recruitment, pausing, elongation and termination of RNA Pol II are important steps for gene transcription (198, 206). To determine how Mondo-Mlx regulates gene transcription via RNA Pol II, either by regulating RNA Pol II recruitment or by promoting elongation, RNA Pol II ChIP-seq was performed on WT and Mondo mutant flies that were cultured in the same setting as in the Mondo-Mlx ChIP-seq experiment. To evaluate the RNA Pol II ChIP-seq data, I compared Mondo mutant and WT RNA Pol II over promoters. In parallel, I also compared the RNA Pol II over the gene bodies in the two genotypes. Differential binding analysis revealed 66 regions with differential Pol II binding at the promoter of genes (Fig. 3.17A) and 100 regions identified with differential Pol II binding at the gene body (Fig. 3.17B).

To focus on Mondo, differential Pol II regions with Mondo-Mlx binding were identified. The average profiles show the distribution of Pol II in terms of reads per kilobase of transcript per million mapped reads (RPKM) at the promoters or gene bodies of Mondo-Mlx target genes in WT and Mondo mutants. Among these, nine Mondo-Mlx target genes have a decrease of the Pol II signal at the promoter (Fig. 3.17C), whereas four Mondo-Mlx target genes showed an increased Pol II signal at the promoter (Fig. 3.17E) in Mondo mutants. For genes displaying differential Pol II occupancy at the gene body, 43 genes had diminished Pol II occupancy (Fig. 3.17D), and eight genes had an increase of Pol II occupancy (Fig. 3.17F) in mutant flies. Changes in the Pol II profile at representative genes for each case are shown as in average profiles in Figure. 3.18. The diminished Pol II peak at the *CTCF* gene in Mondo mutants indicates a regulatory role of Mondo in Pol II recruitment, while an increase of RNA Pol II peak at the *mtp* gene in mutants suggests that Mondo represses the RNA Pol II recruitment (Fig. 3.18A). Opposing changes in Pol II occupancy were also observed across the gene body of the *AcCoAS* and *Fmo-2* genes, implying both the positive and negative regulation of Mondo in RNA Pol II elongation (Fig. 3.18B). Collectively, these results suggest that Mondo is capable of regulating gene transcription at the level of Pol II recruitment and Pol II elongation for some genes. In addition, the results provide the direct evidence indicating that Mondo functions as an activator or a repressor on gene transcription.

### 3. GENOME-WIDE IDENTIFICATION OF TARGET GENES FOR MONDO-MLX COMPLEX IN THE FLY

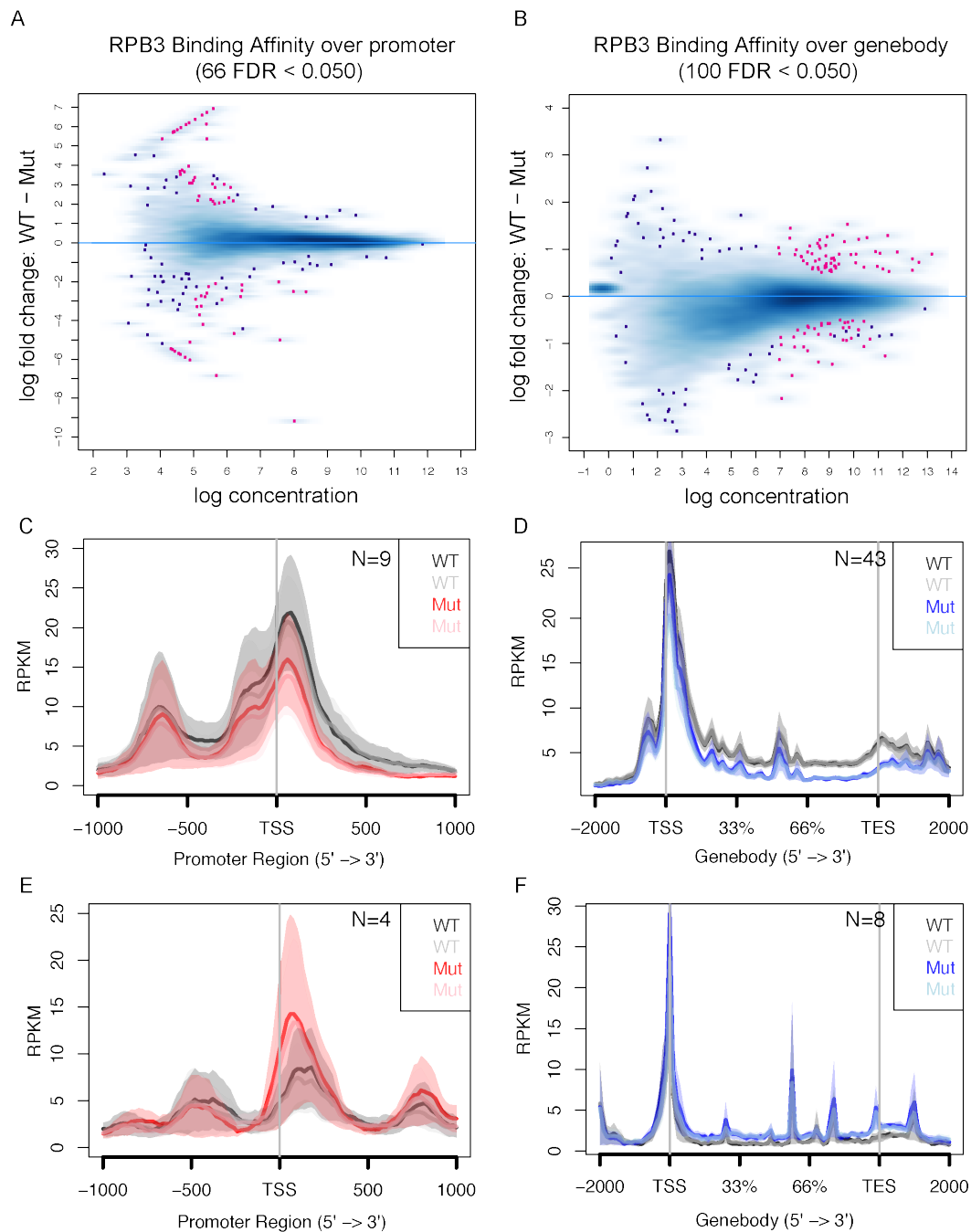


**Figure 3.17. Differential Pol II occupancy at the promoter and the gene body of the Mondo-targeted genes between WT and Mondo mutants.** Differential Pol II analysis between WT and Mondo mutants at the promoter (A) and the gene body (B). (FDR<0.05). Average profile with decreased Pol II occupancy in Mondo mutants at the promoter region (C) or gene body (D). Average profile with increased Pol II occupancy in Mondo mutants at the promoter region (E) or gene body (F).

3. GENOME-WIDE IDENTIFICATION OF TARGET GENES FOR MONDO-MLX COMPLEX  
IN THE FLY

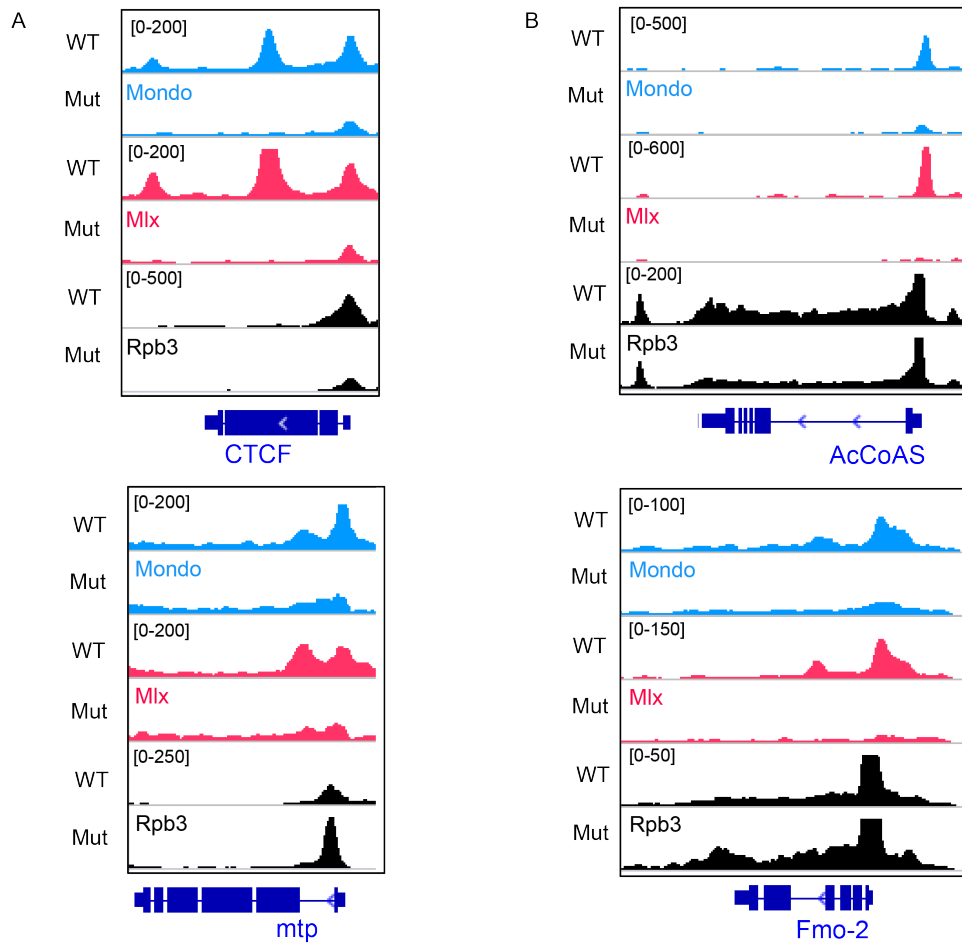


**Figure 3.18. Peak profile of Mondo, Mlx and RPB3 at the putative Mondo-Mlx target genes.** (A) Mondo-Mlx regulates Pol II recruitment at the *CTCF* and *mtp* genes. (B) Mondo-Mlx regulated Pol II elongation at *AcCoAS* and *Fmo-2* genes. The Mondo peak profile is depicted in blue, the Mlx peak profile in red and the RPB3 peak profile in black. The profiles ChIP-seq are shown in total tags normalized to  $1.00e+07$ . The normalization was performed by HOMER software. The tracks in blue stand for the Mondo binding profile, those in red present the Mlx binding profile, and those in black are the Rpb3 binding profile.

### 3.4.10 Correlation of Mondo binding and Mondo-dependent Pol II occupancy with RNA expression

To study the correlation between Mondo-Mlx binding and sugar-induced gene expression, I compared Mondo-Mlx putative target genes with DEGs identified in each cluster from the sugar-induced time-course transcriptome as shown in figure 3.3. As previously mentioned, genes are grouped in the same cluster based on its temporal expression pattern. Genes in cluster 1 are early-expressed genes, those in cluster 2 are late up-regulated genes, those in cluster 3 are down-regulated genes, those in cluster 4 are down-regulated genes and those in cluster 5 are circadian-dependent genes. Interestingly, Mondo targeted genes were observed to be more enriched in cluster 1 than in the other four clusters, suggesting that Mondo was able to quickly respond to sugar and regulated downstream effectors (Fig. 3.19).

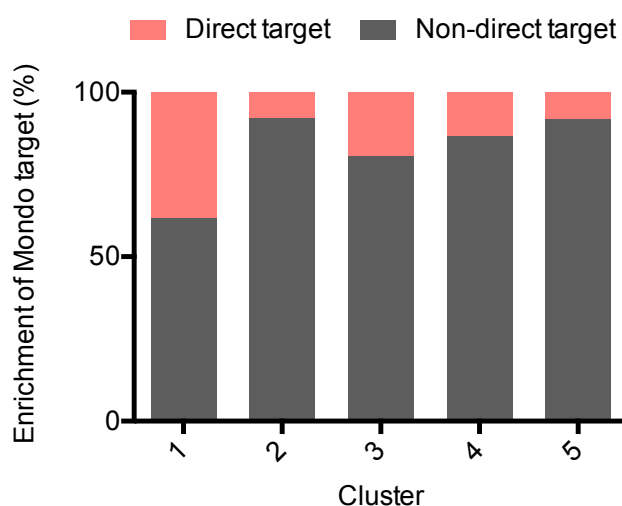


**Figure 3.19. Comparison of Mondo target genes with genes clustered based on the temporal expression profile.** The overlapping of putative Mondo-Mlx target genes with sugar-regulated genes in each cluster indicate that Mondo target genes were relatively enriched in early sugar-responsive genes (cluster 1).

Next, to determine the ability of Pol II ChIP-seq in identifying DEGs, differential Pol II binding genes were compared with sugar-induced DEGs as detected in the time-course sugar-induced transcriptome. The analysis was focused on the 43 genes that were shown with increased Pol II signals across gene body at which Mondo protein is present (Fig. 3.2D). Nineteen percent of the genes (eight out of 43) showed up-regulated expression at the mRNA level in response to sugar. The RNA expression profile and Pol II occupancy for the selected genes are shown in figure 3.20.

### 3. GENOME-WIDE IDENTIFICATION OF TARGET GENES FOR MONDO-MLX COMPLEX IN THE FLY

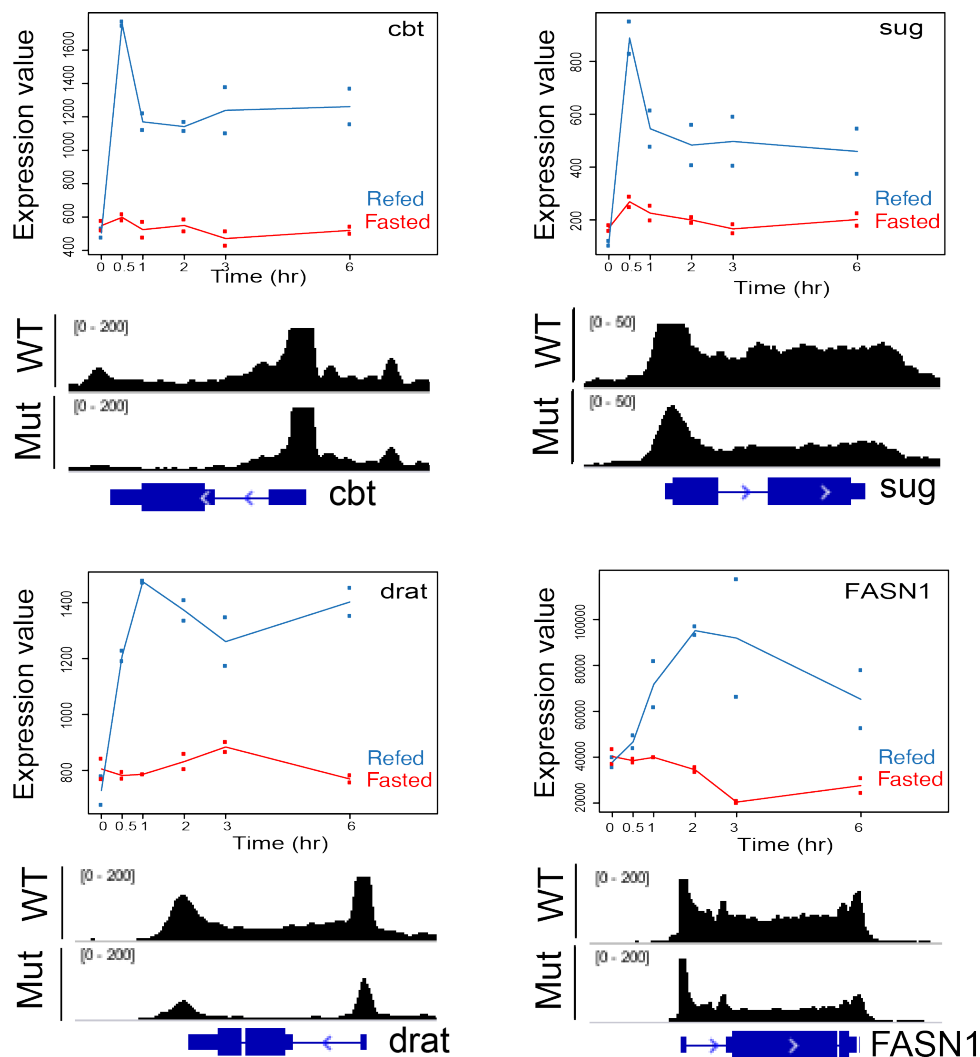


**Figure 3.20. Gene expression profile correlates with RNA Pol II binding at selected genes.** Temporal gene expression and Pol II occupancy at the *cbt*, *sug*, *drat*, and *fasn1* genes upon sucrose refeeding. The line in blue is the gene expression profile upon refeed states, while the line in red is the gene expression profile during starvation.

The percentage of Pol II differentially bound genes coupled with increased expression level could possibly be higher than was observed in the analysis. The mapped reads in time-course RNAseq were low; therefore, only genes with a higher expression in response to sugar can be detected. Moreover, in addition to regulation from TFs binding and Pol II-directed transcription, RNA levels are also affected by the RNA turnover rate. This may also explain the low overlapping between datasets. Nevertheless, this cross-dataset comparison allows us to analyze the transcription regulation of Mondo on specific genes.

#### **3.4.11 The comparison of Mondo-Mlx binding data with RNA expression data supports the role of Mondo as either a transcription activator or repressor**

To understand how Mondo-binding affects gene transcription, a cross-dataset comparison was performed between Mondo-Mlx ChIP-seq and published Mondo RNA-seq data (60), as well as Mlx RNA-seq data (113). The Mondo RNA-seq was performed on the dissected fat body from WT and Mondo RNAi flies at the wandering third instar larva stage upon 0.15M vs. 0.7M sucrose. The Mlx RNA-seq was done on WT and Mlx mutants at the early instar larvae stage while feeding on 10% yeast vs. 10% yeast + 20% sucrose food. Among the Mondo-Mlx-dependent DEGs, some are upregulated by sugar, while some are down-regulated, indicating that Mondo-Mlx can both activate or repress the gene expression. However, these sugar-regulated and Mondo-Mlx-dependent genes should include both direct and indirect Mondo-Mlx targets, and these genes' expression change may result from the regulation of a secondary effector. To determine whether Mondo-Mlx can directly activate or repress the gene transcription, DEGs from the Mlx-dependent and Mondo-dependent RNA-seq data were compared with the Mondo-Mlx targets identified in our ChIP-seq data. The overlapping with both sugar-upregulated and sugar-downregulated genes supports the notion that Mondo-Mlx primarily acts as an activator (Fig. 3.21A and 3.21C), but can also function as a repressor for some target genes (Fig. 3.21B and 3.21D).

3. GENOME-WIDE IDENTIFICATION OF TARGET GENES FOR MONDO-MLX COMPLEX  
IN THE FLY

---

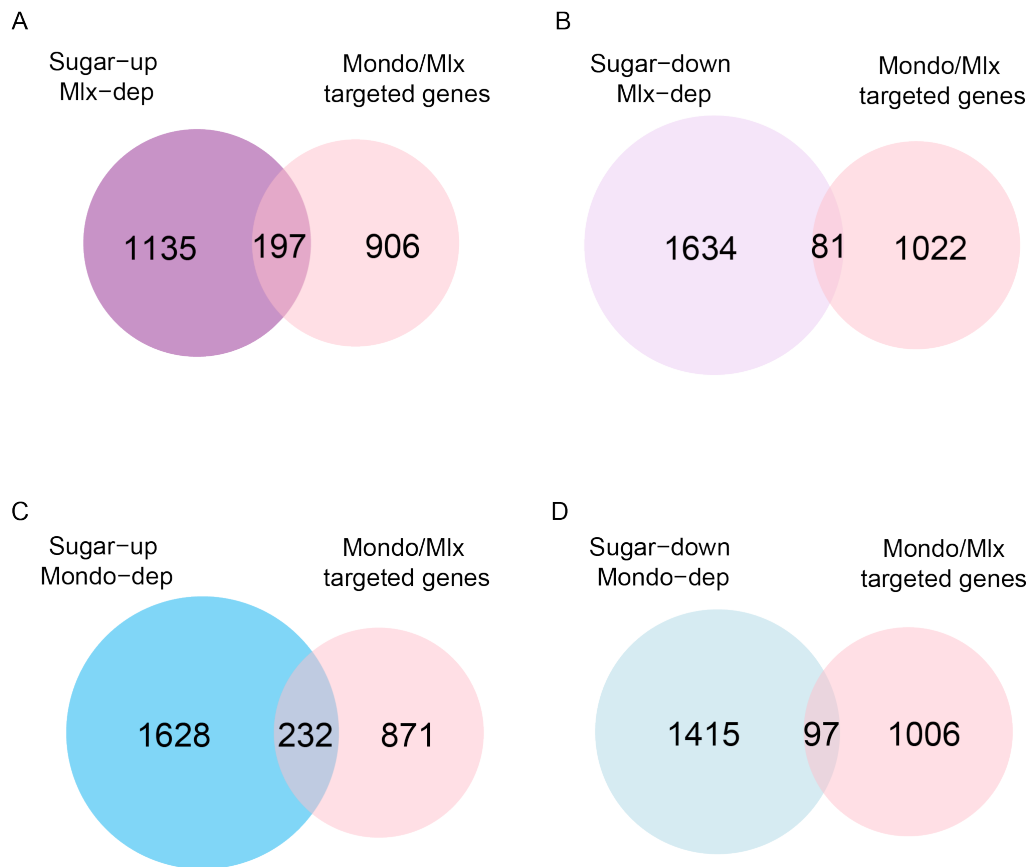


**Figure 3.21. Comparison of Mondo-Mlx target genes with sugar-regulated Mlx-dependent and Mondo-dependent genes identified in larvae.** 197 Mondo-Mlx target genes overlapped with sugar-up regulated Mlx-dependent genes (A), and 81 Mondo-Mlx target genes overlapped with sugar-down regulated Mlx-dependent genes identified in the whole larva (B). 232 Mondo-Mlx target genes overlapped with sugar-up regulated Mondo-dependent genes (C), while 97 Mondo-Mlx target genes overlapped with sugar-down regulated Mondo-dependent genes (D).

### 3.5 Discussion and future directions

The genome-wide sequencing data demonstrate that the Mondo-Mlx complex directly targets the genes involved in metabolic pathways such as glycolysis, *de novo* lipogenesis and amino acid metabolism. Overall, evidence from the viability assay (see chapter 2) and genomic data confirm that Mondo acts as a key metabolic regulator. Moreover, analysis of the Mondo-Mlx ChIP-seq reveals a putative novel DNA binding motif of Mondo, the “GATAA” motif. The results show that some identified target sites contain the canonical Mondo binding motif, the ChoRE motif and the contain the “GATAA” motif, while some target sites only contain the “GATAA” motif, suggesting the direct binding of Mondo-Mlx at the “GATAA” sites. It has been shown that the “GATAA” motif is bound by the GATA factor, as well as by DAF-16, the homolog of the FOXO transcription factor in *C. elegans*, which binds to the reverse complement of the “GATAA” motif. Moreover, in *C. elegans*, the GATA factor and FOXO transcription factor were shown to share binding sites at several metabolic genes. It is interesting to study whether Mondo actually binds to the “GATAA” motif and whether GATA factors assist the binding of Mondo to the target sites.

It is also intriguing to discover lines of evidence from GO term analysis, motif searching and expression data that suggest that Mondo is on the top of a transcription cascade by regulating the expression of several transcription factor genes. For example, the Mondo-Mlx complex was shown to target the *mnt* gene, which encodes a basic-helix-loop-helix-zipper transcription factor, which form heterodimers with the protein encoded by Max. This suggests the interplay between Mondo-Mlx network and Myc/Max/Mad network in the fly. Mondo-Mlx also targets the *hnf4a* gene, which encodes an important transcriptional regulator of glucose, fatty acid and cholesterol metabolism (207-209). This crosstalk allows cells to respond to nutrient input in a more delicate way. It is worth noting that many of the transcription factors targeted by Mondo-Mlx, such as PDP1 and CTCF, do not target metabolic genes, indicating that the function of the Mondo-Mlx-regulated network may extend beyond metabolism.

The first direct evidence indicating that Mondo can act as either a transcriptional activator or a repressor is also reported. By integrating the Mondo-Mlx ChIP-seq and Pol II ChIP-seq data, it was observed that Pol II occupancy was altered

in a Mondo-dependent manner at the promoter and/or the gene body of certain Mondo-Mlx-target genes. These data provide a direct readout of Mondo's role as a transcriptional activator or a repressor without concerns derived from the potential secondary effects on the gene expression. Our data also suggest that the Mondo-Mlx complex may regulate gene transcription mainly by regulating Pol II elongation because the percentage of Mondo target genes with altered Pol II occupancy at the gene body was higher than those with different Pol II binding levels at the promoter (51% vs. 20%). Moreover, increased Pol II levels at the gene body were observed in 84% (43 out of 51) of the Mondo target genes that are coupled with altered Pol II occupancy, suggesting that the Mondo-Mlx complex mainly acts as a transcriptional activator rather than a repressor.

However, it was also observed that very few Mondo target genes (64 out of 1,130) were coupled with either Pol II recruitment to the promoter or with Pol II elongation along the gene body, suggesting that Pol II-directed transcription may not rapidly respond to the binding of the Mondo-Mlx complex. It is worth noting that we address Mondo's role in gene transcription at the early sugar refeeding time point. Performing a time-course Mondo and Pol II ChIP-seq upon sugar refeeding will provide insight into sugar-induced Mondo-regulated transcription. Moreover, the mechanisms behind the Mondo-Mlx complex as an activator or repressor in gene transcription also merit further study. It would also be interesting to learn whether the binding of Mondo with different interacting partners, such as FOXO and HNF4, may result in different transcription outcomes.

3.6 Appendix

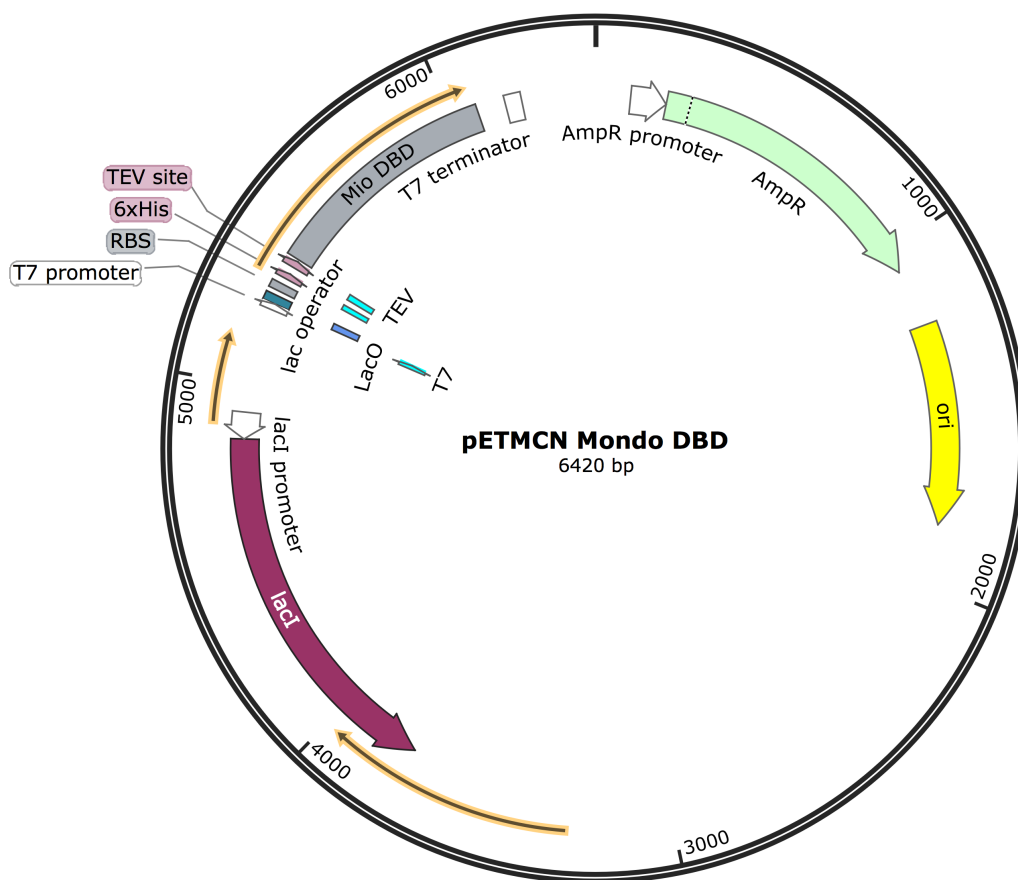
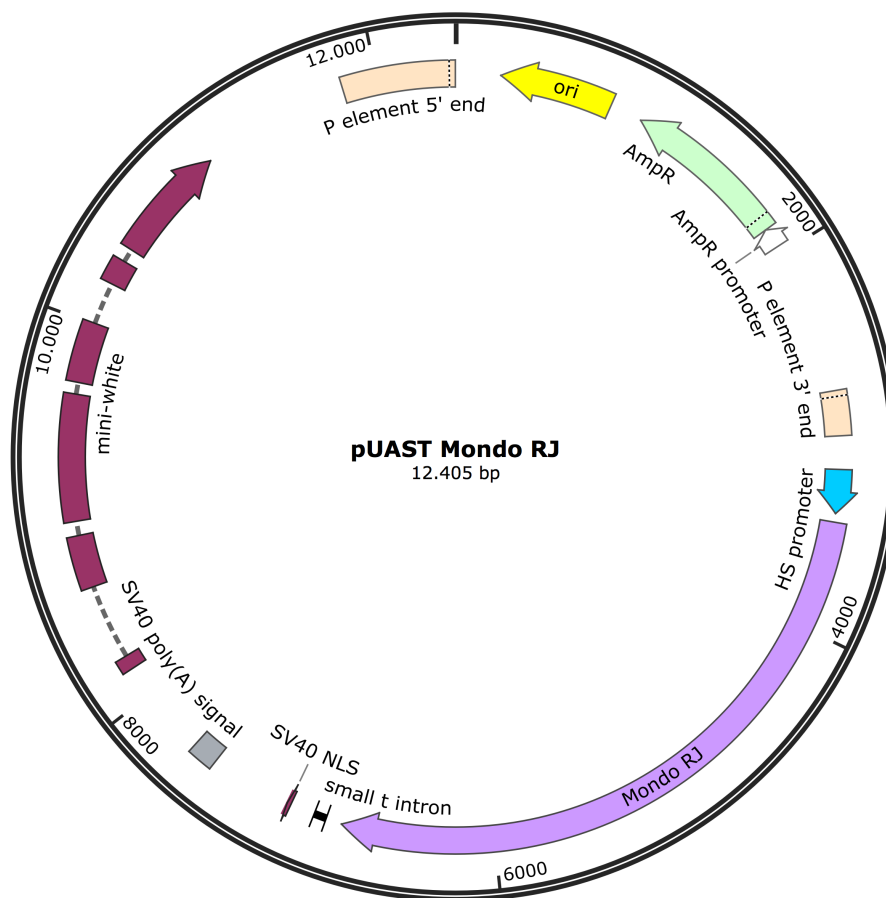


Figure A3.1. Map of expression plasmid pETMCN Mondo DBD

3. GENOME-WIDE IDENTIFICATION OF TARGET GENES FOR MONDO-MLX COMPLEX  
IN THE FLY

---



**Figure A3.2. Map of expression plasmid pUAST Mondo RJ**

3. GENOME-WIDE IDENTIFICATION OF TARGET GENES FOR MONDO-MLX COMPLEX  
IN THE FLY

---

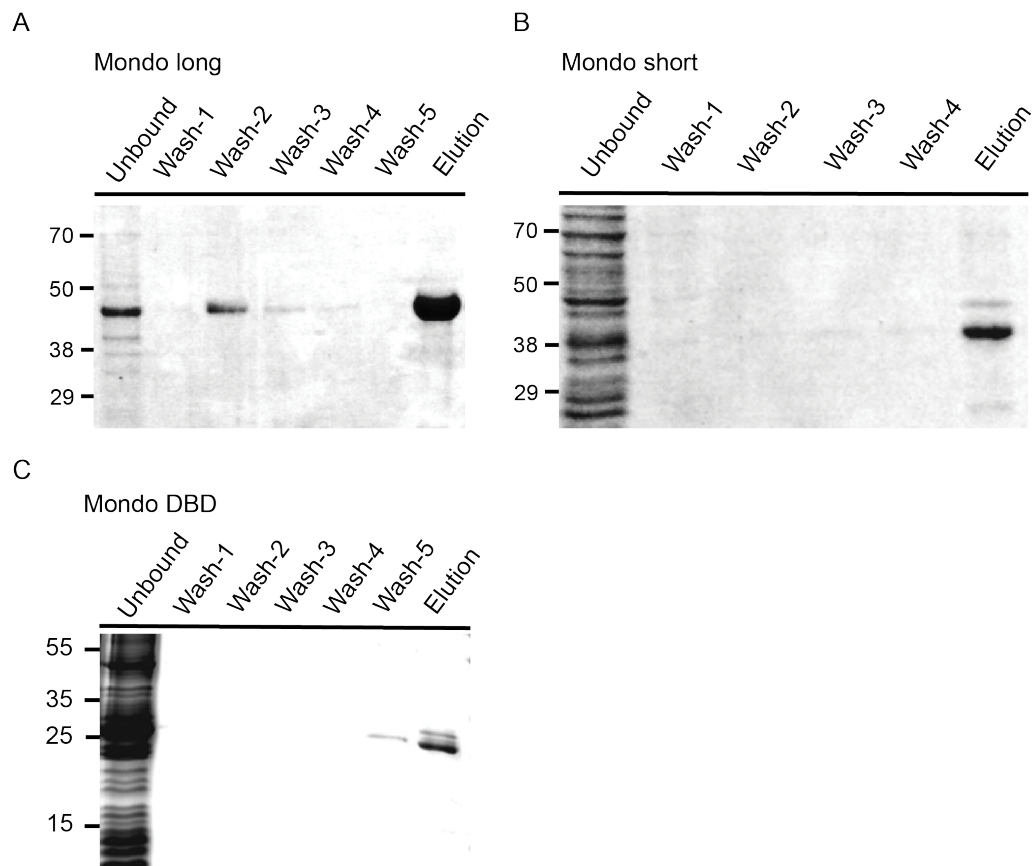


**Figure A3.3. The purification of recombinant Mondo proteins was tested on Coomassie-stained SDS-page.** Protein samples were saved from each purification step for the evaluation of purification efficiency. Coomassie-staining of SDS-pages with (A) Mondo long recombinant protein, (B) Mondo short recombinant protein and (C) Mondo DBD recombinant protein indicate the successful purification of each recombinant protein in the elution.

**Table A3.1 Primers used in ChIP-qPCR assays**

<b>Primer name</b>	<b>Primer sequence</b>	<b>Product size</b>
acc forward	CGAAAACGCCAGAAATTGAT	119
acc reverse	GCATCACGGAATGAAAACAA	
acc forward-negative	GCTGCTGACCTTGATTCCTA	107
acc reverse-negative	ACACACACGTTGGCAGCTAT	
cbt forward	GCGAAAGCAGGAGAGTATGG	100
cbt reverse	AATGCCTGCTTTTCGTGACT	
fas2+28 forward	GTGCTCTGCTTGCTGAGAGA	115
fas2+28 reverse	GCCACGACCGTTAACACATA	
ubx forward	TAGTCTTATCTGTATCTCGCTCTT A	83
ubx reverse	CAGAACCAAAGTGCCGATAACTC	

3. GENOME-WIDE IDENTIFICATION OF TARGET GENES FOR MONDO-MLX COMPLEX  
IN THE FLY

---

**Table A3.2. Mondo target genes with transcription factor activity are listed with the gene name and corresponding ChoRE sequence**

<b>Gene ID</b>	<b>ChoRE sequence</b>	<b>pvalue</b>	<b>qvalue</b>
pdp1	CACCTATCGGTACGTG	1.16E-50	0.0614
NFAT	CACGCGCACGTACGTG	2.87E-08	0.0103
hnf4	CACACGTTGTCCACATG	9.11E-06	0.0567
Eip75B	CCTGCTTTCGACGCGTG	6.38E-05	0.149
crebA	CCCGTACCCGGGGCGTG	3.84E-05	0.115
CHES-1-like	CATACGTTTTGCACATG	5.40E-05	0.138
crc	CACTCGCTTAACGCGTG	8.49E-07	0.025
Mnt	CAGGCGTTGGCAGCGTG	9.32E-08	0.0136
cbt	CACGCGTTGACCTCATG	5.50E-07	0.0219
lilli	CAGGCAGATGAAACGTG	8.08E-05	0.166
srp	CGCGCGACCGACGCGTG	3.00E-06	0.0363
hng3	CACTCGCCGAGAGGCTG	2.03E-05	0.0829
dsx	CACACGCGAGCAAAGTG	9.17E-05	0.175
cnc	CACGCCGTAAGAGAGTG	5.25E-06	0.0467
cwo	CACGGGAGGCAAACGTG	7.16E-05	0.156
REPTOR	CAGCCAACAGCCGCGTG	2.53E-06	0.0346
CTCF	CACTCCAATTCGGCATG	7.76E-05	0.162
fru	CACTCACTCTCCCCGTG	1.64E-06	0.0293
sik3	CATACA TGGTGC GCGTG	1.95E-05	0.0822
bun	CACGTGTTGGGGGCGTG	1.45E-07	0.0142

# Chapter 4

## Investigating Mondo function in the central nervous system of the fly

### 4.1 Summary

In this chapter, the tissue-specific function of Mondo is addressed in the fly brain via RNA-seq. Data from our previous tissue-specific Pol II ChIP-seq and RNA expression profiles from FlyAtlas indicate that *mondo* is expressed in the fly brain. To elucidate Mondo's role and its downstream regulatory network in the brain under different nutritional states, RNA-seq was performed on the dissected brains of WT and Mondo mutant flies that underwent either fasting or sugar refeeding. DEGs identified from the brain RNA-seq data are involved in metabolic pathways, oxidation-reduction process and sleep behaviors. It suggests that Mondo may have a function beyond metabolism in the fly brain, which would indicate a metabolic role of Mondo in the brain. Consistent with its role in sugar metabolism in the liver, Mondo also appears to regulate the expression of trehalose transporter (*tret1-1*) and trehalose-6-phosphate synthase 1 (*tps1*), which are important in trehalose metabolism in the fly. Mondo also regulates genes involved in amino acid (glycine, serine and glutamine) metabolism. To our surprise, the expression of these genes is only significantly changed upon starvation in a Mondo-dependent manner. In addition, a gene such as *aay*, a key enzyme in serine biosynthesis, has been shown to modulate sleep homeostasis. It would be intriguing to study how this brain-specific Mondo regulates the metabolism of sugar and amino acids and the corresponding physiological outcomes in the future.

## 4.2 Introduction

The brain is one of the most metabolically active organs in the organism. It mainly relies on circulating glucose as an energy source and stores a small amount of energy in the form of glycogen. The brain also utilizes substrates other than glucose in some circumstances to obtain energy. For example, ketone bodies are catabolized under prolonged starvation, and lactate is used as fuel during extensive physical activity. In addition to the quick metabolic adaptation to starvation, the brain also responds to nutrient fluctuation by mediating feeding and sleep behaviors, which play a major role in regulating energy homeostasis. Understanding the underlying molecular mechanisms of nutrient metabolism in either a nutrient-rich or nutrient-scarce state is thus an important research goal.

ChREBP, a key regulator in carbohydrate metabolism, has been reported to express in the CNS of murines and humans (133). Mondo expression has also been reported in the fly brain. Flies containing endogenously GFP-tagged Mondo present a GFP signal in the suboesophageal ganglion (SOG) in the fly brain (BrainTrap database). Tissue-specific RNA Pol II ChIP-seq data shows Pol II peaks at the *mondo* gene promoter not only in the fly fat body, but also in neurons and glia (210). Although evidence suggests that Mondo is expressed in the brain, its downstream effectors and associated function in the brain remain elusive. Docherty *et al.* have demonstrated that the downregulation of *mondo* in neurons leads to enhanced glycogen and triglyceride levels in the fly, while targeting *mondo* specifically in IPCs results in increased food intake of fly (155). Fat body-derived Mondo has been shown to promote feeding behavior, suggesting the crosstalk of Mondo signaling between the fat body and the brain (159).

To determine the function of Mondo in the brain, RNA-seq was performed on dissected fly brains of WT and Mondo mutant flies. The results reveal that Mondo is involved in metabolic pathways such as sucrose and glycerolipid metabolism. Mondo also regulates the *tret1-1* and *tps1* genes, which are essential in trehalose metabolism (10, 211). Moreover, Mondo regulates the metabolism of several amino acids, such as serine, glycine, and glutamine upon starvation, which may suggest a Mondo-directed metabolic switch in the fly brain in response to food scarcity. The results also

demonstrate that Mondo may potentially mediate sleep behaviors. It is important to understand whether Mondo controls serine levels in the fly brain and subsequently modulates sleep behavior during starvation, which may in turn balance the overall energy.

### **4.3 Methods**

#### **4.3.1 RNA-seq on the whole head and the fly brain**

Flies were anaesthetized with CO<sub>2</sub> or ice. The proboscis of the fly was removed with fine-tipped forceps and torn from the cuticle from the opening of proboscis. The rest of the cuticles attached to the brain were carefully removed. The dissected brains were immediately put into Trizol reagent, and samples were left on ice until the collection was finished. In total, 10 brains were collected, and the samples from males and females were equal. RNA was extracted by following the protocol mentioned in chapter four. The cNDA library and the details of the sequencing experiment are the same as described previously.

#### **4.3.2 Regulatory network analysis**

DEGs identified in the fly brain were analyzed for pathway enrichment by using the ClueGO and CluePedia plugins of Cytoscape.

## 4.4 Results

### 4.4.1 Evidence indicating Mondo expression in the fly brain

Mondo/ChREBP has been extensively studied in many metabolic tissues in the past two decades (75, 94, 98, 132, 148, 212), and is commonly known to be the key metabolic regulator. However, its role in the brain, the most metabolically active organ, remains unclear. In mice, ChREBP has been detected in the brain via *in situ* hybridization and northern blot assays (61, 133). Multiple lines of evidence also indicate that Mondo is expressed in the fly brain. First, the RNA-seq data from Flyatlas (213) indicates not only the predominant expression of Mondo in the Malpighian tube and the fat body, but also the moderate expression in the brain, midgut, hindgut, etc. (Fig. 4.1A). Second, our cell-type-specific Pol II ChIP-seq data demonstrate Pol II occupancy at the promoter region of the *mondo* gene in the fat body, as well as in neurons and glia (210), indicating that the *mondo* gene is transcribed in these three tissues (Fig.4.1B). Third, the brain image of an endogenously GFP-tagged Mondo fly line (refer to chapter 2; 214) displays a GFP signal in the SOG (Fig. 4.1C), a region of the fly brain that is considered a primary taste center responsible for feeding behavior (215, 216). From the functional perspective, Docherty *et al.* have shown that the pan-neuronal knockdown of Mondo increases overall triglyceride and glycogen levels but has no effect on food intake. Conversely, knockdown of the Mondo specifically in IPCs, the specialized neurons that produce and release ILPs to the hemolymph, alters food intake but has no effect on the global triglyceride and glycogen levels (155). Taken together, the expression profile and functional characterization of Mondo suggest that Mondo plays a role in CNS. To globally study Mondo's role in CNS, genome-wide approaches were used to determine its function and downstream effectors.

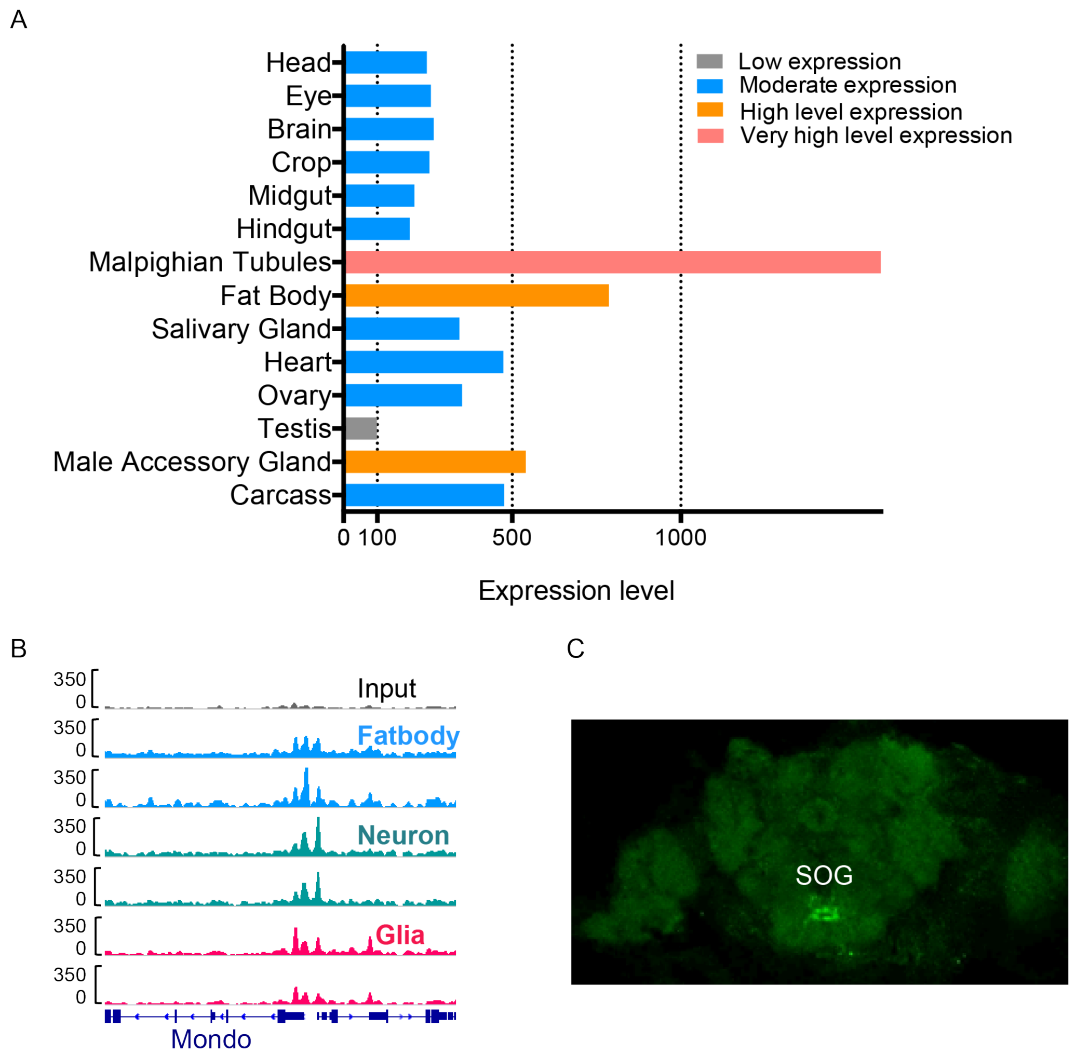


**Figure 4.1. Lines of evidence suggest Mondo expression in the fly brain.** (A) RNA-seq data from Flyatlas shows the *mondo* mRNA expression levels in different adult fly tissues (213). (B) A genome browser snapshot of Poll ChIP-seq data shows that Pol II is located at *mondo* promoter in the fat body, neuron and glia (210). (C) The brain image of the GFP-tagged Mondo fly shows Mondo expression in the SOG region of fly brain. The image was modified from the BrainTrap database (214).

#### 4.4.2 RNA-seq data confirm Mondo's expression and regulatory role on known target effector genes in the CNS

An RNA-seq experiment was performed on dissected brains from WT flies and Mondo<sup>K05106</sup> mutants to determine the Mondo-dependent regulatory network in the fly brain. The same feeding paradigm used in the ChIP-seq experiment mentioned in chapter 3 was applied. Flies were fasted for 21 hours and refed on sucrose for 1 hour before the dissection of their brains. The RT-qPCR results showed a reduced mRNA level of *mondo* and its target gene *cabut* in Mondo mutants compared with WT flies. This data provides additional evidence for the expression of *mondo* in the brain and the Mondo-dependent misregulation of *cbt* expression (Fig. 4.2A). RNA sequencing was performed on cDNA libraries prepared from the extracted brain RNA. After normalizing for batch effects, replicates of each group clustered well in PCA analysis, indicating sufficient reproducibility between replicates (Fig. 4.2B). RNA-seq data showed that a truncated Mondo transcript lacking the DNA binding domain was still transcribed in Mondo<sup>K05106</sup> mutants. Full-length was not detected in protein extracts from the Mondo<sup>K05106</sup> mutant with Mondo antibodies raised against the C-terminal DNA binding or N-terminal activation domains, as shown in Chapter 3 (Fig. 3.6). The downregulation of Mondo's known targets *cabut* and *dawdle* was observed in mutants, as well (Fig. 4. 2C). In addition, several Mondo target genes identified in the whole head Mondo-Mlx ChIP-seq, such as the *lip4*, *bmm* and *teq* genes, were shown to be downregulated in a Mondo-dependent manner in the brain RNA-seq data, suggesting that Mondo may suppress the expression of these genes directly or through a secondary effector in the brain (Fig. 4.2D).

4. INVESTIGATING MONDO FUNCTION IN THE CENTRAL NERVOUS SYSTEM  
OF THE FLY

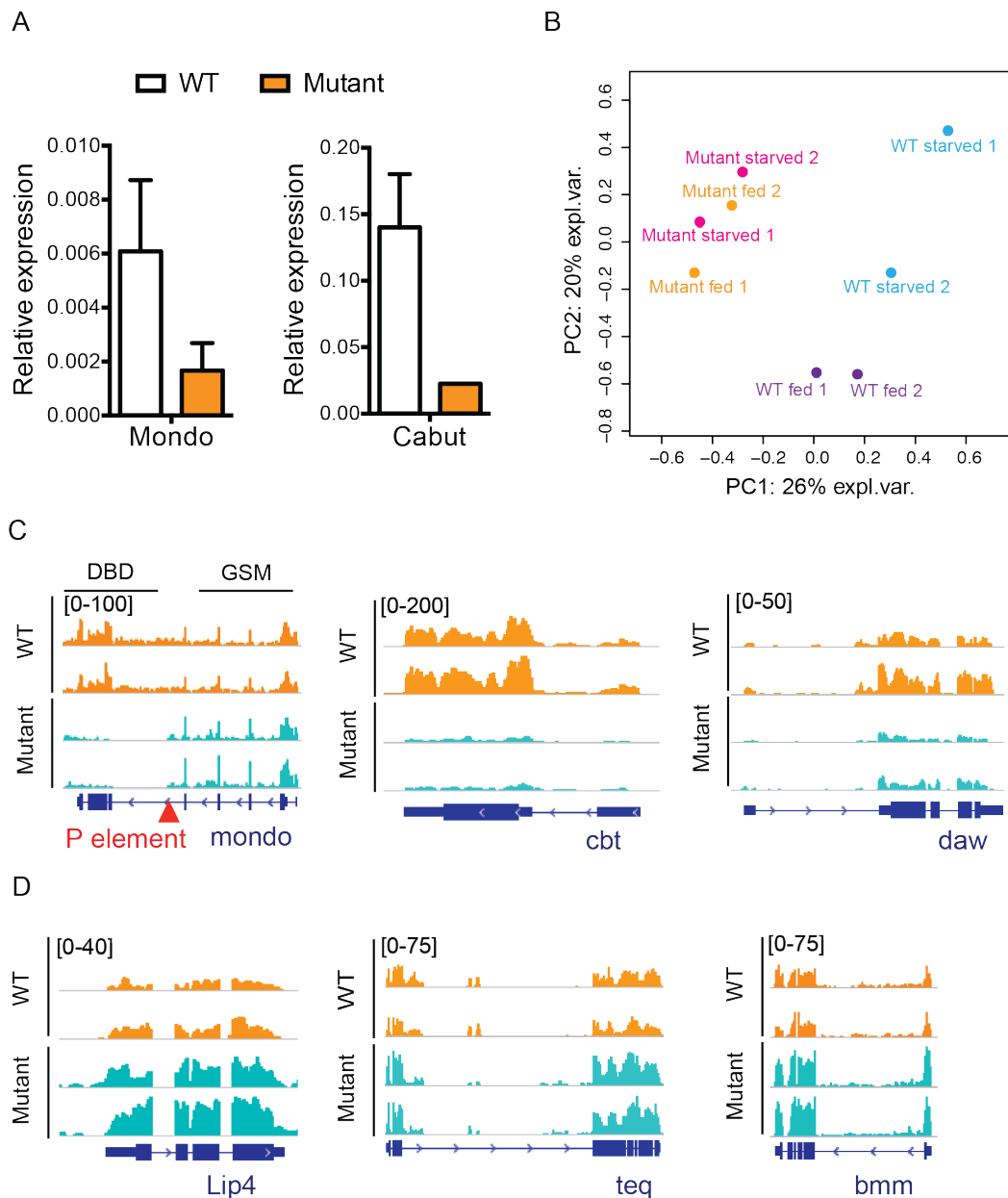


**Figure 4.2. RT-qPCR and RNA-seq indicate the expression of *mondo* and downstream effectors.** (A) *mondo* and *cbt* mRNA expression levels in the brains of WT flies and *Mondo* mutants were measured by RT-qPCR. The relative expression over *rp49* mRNA expression level is presented. (B) PCA analysis of replicates of data from groups of fed-WT, starved-WT, fed-mutant and starved-mutant groups after batch normalizing. (C) Genome browser snapshots show that the normalized read counts of *mondo*, *cbt* and *dawdle* mRNA are higher in WT flies compared to mutants. (D) Genome browser snapshots show that the normalized read counts of *lip4*, *teq* and *bmm* mRNA are lower in WT flies compared to mutants. RNA-seq data are presented

in biological replicates. The profiles of RNA-seq data are shown in total tags normalized to  $1.00e+07$ . The normalization was performed by HOMER software.

#### 4.4.3 Comparison of sugar-induced transcriptome from the brain and whole head

The differential expression analysis on the brain RNA-seq reveals that 64 genes were differentially regulated ( $FDR < 0.05$ ) in sugar-fed control flies compared with fasted control flies. To determine whether there were unique changes in gene expression in the brain compared to the whole head, DEGs in response to sugar were compared with the sugar-induced transcriptome from timecourse RNAseq data (Fig. 4.3). In total, 22% (14 out of 64) of DEGs in the brain were observed to overlap with genes that respond to sugar in the whole head. Biologically speaking, this suggests that a subset of genes specifically responds to sugar in the brain. Genes ( $N=10$ ) with oxidoreductase activity are observed to be enriched specifically in the brain. Interestingly, it seems that five of these 10 genes are downregulated during starvation in a Mondo-dependent manner (data not shown).

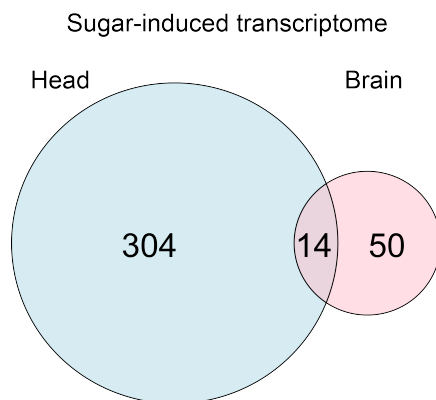


**Fig. 4.3. Comparison of sugar-induced transcriptome in the brain and whole head.** Venn diagram of sugar-induced transcriptome in the whole head (shown in blue) and in the brain (shown in pink). Fifty genes were shown to respond to sugar exclusively in the brain.

#### 4.4.4 Comparison of Mondo-dependent transcriptome in the brain with Mondo-Mlx target genes

To understand the correlation between Mondo-Mlx binding and subsequent action on gene transcription, the identified putative Mondo-Mlx direct targets were compared with the Mondo-dependent regulatory network determined from brain RNA-seq data. The comparison shows that 14% (31 out of 217) and 18% (20 out of 129) of the

DEGs identified upon starvation and sugar refeeding conditions, respectively, were also putative Mondo-Mlx targets, suggesting that Mondo may directly regulate these genes (Fig. 4.4). The comparison of Mondo-Mlx-regulated DEGs between starvation and sugar-refeeding conditions is shown in Table 4.1. Performing a Mondo ChIP specifically from the brain provides solid evidence to support the direct regulation of Mondo on these genes.

There may be several reasons for the poor overlapping of the genes between the two datasets. First, the binding of Mondo to the target gene may not immediately transmit regulation on gene transcription, which is supported by the low overlapping percentage between Mondo-Mlx ChIP-seq and Pol II-ChIP-seq shown in chapter 3. Only a few Mondo-Mlx target genes showed the altered Pol II occupancy while lacking Mondo, suggesting that the transcription machinery and the subsequent transcription do not respond to Mondo binding quickly. Second, the Mondo-Mlx ChIP-seq was done on the fly head instead of on neurons or glia cells; thus, the resolution of peaks at CNS-specific genes in the whole head ChIP-seq may be weaker. Taken together, it may not be necessary to observe a high correlation between these datasets. More importantly, this RNA-seq data shows several intriguing and potentially significant aspects of Mondo's function that are further discussed in the following sections.

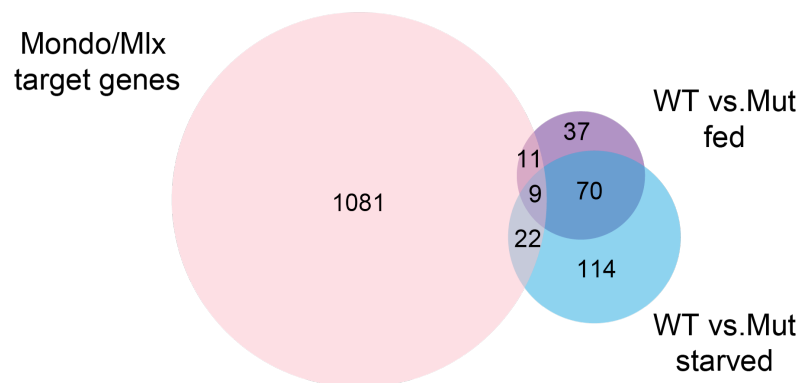


**Figure 4.4. Comparison of brain Mondo RNA-seq data with Mondo-Mlx ChIP-seq data.** The overlapping of Mondo-Mlx target genes (shown in pink), Mondo-dependent transcriptome upon starvation (shown in blue) and the sugar refeeding condition (shown in purple).

**Table 4.1. Mondo-dependent DEGs in the brain under sugar-refeeding, starvation or under both conditions**

Genes only differentially expressed in refeed condition	Genes only differentially expressed in starved condition	Genes differentially expressed in both conditions
lip4, beat-1b, CG14688, aralar1, odc1, CG31324, CG31688, gk2, teq, elB, CR45973	cbt, mondo, cyp6g1, tret1-1, pncr009:3L, CG5830, bmm, tps1, bgm	CG3011, irc, CG11089, CG13868, CG10924, CG2233, hex-c, sardh, CG5835, hn, CG3376, wdp, ork, gs2, lsd-2, CG10960, CG6910, aay, prat2, pelo, sh, muc

#### 4.4.5 Functional clustering of DEGs suggests that CNS-Mondo may be involved in the oxidation-reduction process, metabolic pathways and sleep behavior

To explore the possible function of Mondo in the brain in response to sugar, regulatory network analysis was performed on DEGs identified from the data generated on the sugar-refeeding condition. The analysis reveals that Mondo may have functions associated with “monooxygenase activity,” “glycerolipid,” “sugar transporter,” “sleep” and “starch and sucrose metabolism” (Fig. 4.5). Approximately 12% (14 out of 118) and 12.7% (23 out of 180) of DEGs were shown to have oxidoreductase activity upon the refeed condition and starved condition, respectively (Table 4.2). In support of this observation, 6.4% (70 out of 1091) of putative Mondo/Mlx direct target genes were also shown to possess the oxidoreductase activity in the whole head Mondo ChIP-seq (data not shown). The regulation of Mondo on oxidoreductase has also been reported in fly larvae (113). Although several genome-wide studies suggest that Mondo may control oxidation-reduction reactions via regulating the expression of oxidoreductase, the physiological outcomes remain unclear and require further study.

The results also demonstrate that Mondo may potentially mediate sleep behaviors, as 5.1% (six out of 118) and 4.4% (eight out of 180) of DEGs identified in either the refeed or starved condition were shown to functionally cluster with the GO term “sleep” (Table 4.3). Consistent with this, 2.7% (29 out of 1,091) of putative targets identified in ChIP-seq from the whole head were also clustered with the GO

term “sleep” (Fig. 3.14). In our analysis, genes such as *bmm* and *CG4500* have already been shown to control sleep homeostasis, which is defined as the increase in sleep following sleep deprivation (217). It is interesting to note that these genes are involved in lipid metabolism and storage. That is, *bmm* is known to be homologous with the human adipocyte triglyceride lipase, while *CG4500* is a long-chain fatty acid-CoA ligase. It remains to be determined whether Mondo mediates sleep homeostasis though regulating lipid levels in the brain. In conclusion, functional clustering analysis indicates that brain-specific Mondo may act not only as a metabolic regulator in the brain, but may also have a function beyond metabolism, for example, concerning regulation in sleep behaviors.

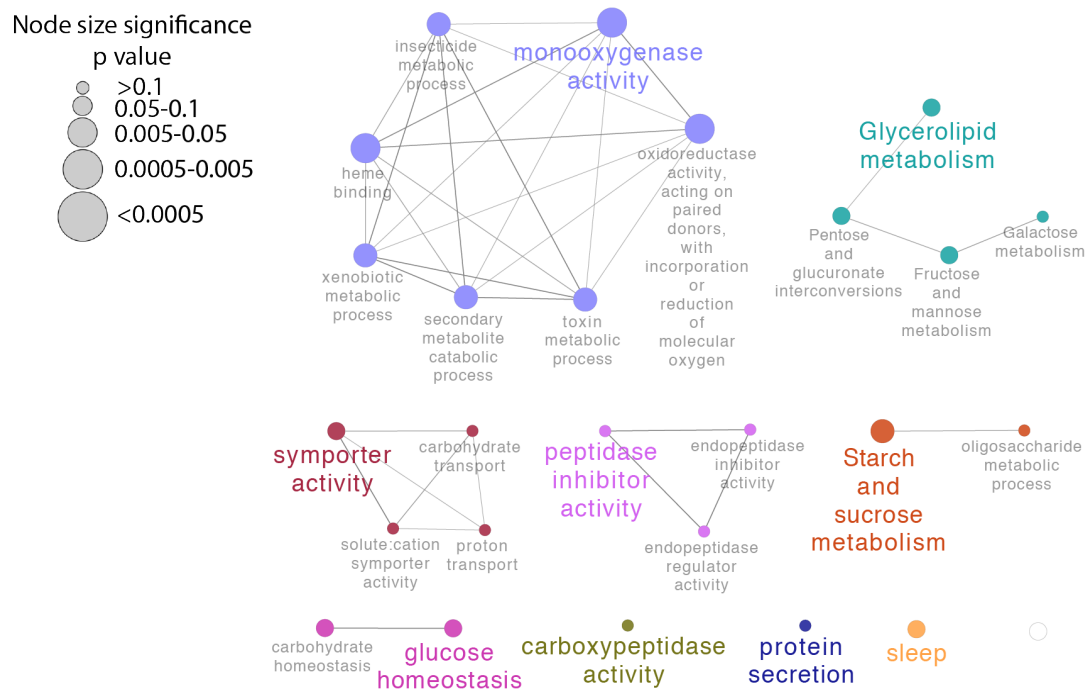


**Figure 4.5. Mondo-dependent regulatory network upon sugar refeeding in the brain.** DEGs regulated by Mondo involved in oxidoreductase, glycerolipid, sucrose metabolism, and sleep, as well as in glycine, serine and threonine metabolism. Regulatory network analysis was done with the cytoscape and ClueGO tool.

**Table 4.2 Oxidoreductase-associated DEGs identified from brain RNA-seq data**

Oxidoreductase-associated DEGs identified upon refeed condition	Oxidoreductase-associated DEGs identified upon starved condition
cyp12a5, CG14688, cyp9h1, CG17691, cyp6a13, CG31075, CG3999, CG8046, cyp6w1, cyp6g1, cyp28a5, cyp6a2, ppo2, sodh-2	CG17896, CG3999, CG5065, CG910, CG8302, CG8345, CG8453, CG8687, CG8864, cyp4e1, cyp6a2, cyp9b2, hn, irc, nmdmc, nd4, nd5, ppo2, sardh, sodh-2, zw, cox2, pug

**Table 4.3 Sleep-associated DEGs identified from brain RNA-seq data**

Sleep-associated DEGs identified upon refeed condition	Sleep-associated DEGs identified upon starved condition
amy-p, CG10383, mondo, cyp6g1, bmm, cbt	CG10383, CG13868, CG4500, CG8453, aay, bmm, cbt, mondo

#### 4.4.6 CNS-Mondo regulates the expression of sugar transporter in the brain

CNS-Mondo also seems to regulate the expression of the sugar transporter gene, trehalose transporter 1-1 (*tret1-1*), in the brain. Unexpectedly, the Mondo-dependent downregulation of *tret 1-1* was observed upon sugar refeeding (Fig. 4.6A). Consistent with this result, our whole head Pol II-ChIP-seq also showed less Pol II occupancy at the gene body of *tret 1-1* in WT flies compared with mutants (Fig. 4.6C). This indicates that Mondo negatively controls the trehalose transport into the brain, which may help maintain the steady state of carbohydrate homeostasis.

A higher expression of trehalose-6-phosphate synthase 1 (*tps1*) gene was observed in WT flies compared to the mutant upon sugar-refeeding (Fig. 4.6B), which is also consistent with Pol II occupancy at the gene body of *tps1* (Fig. 4.6D). This indicates that Mondo may inhibit the sugar uptake and glycolysis by down-regulating these two genes in the brain. Studying the physiological meaning and the underlying molecular mechanisms will lead us to a better understanding of how Mondo maintains carbohydrate homeostasis.

4. INVESTIGATING MONDO FUNCTION IN THE CENTRAL NERVOUS SYSTEM  
OF THE FLY

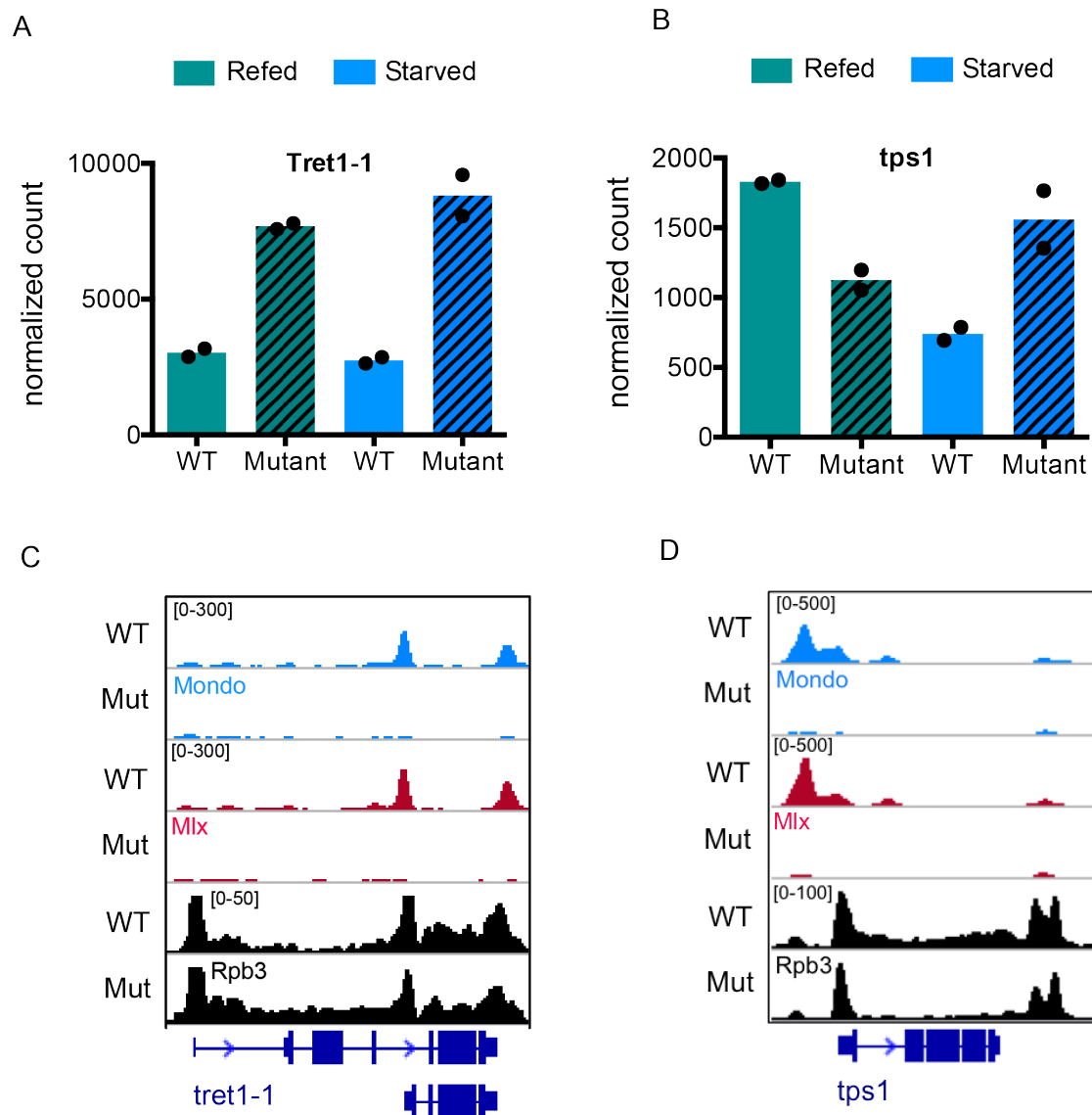


**Figure 4.6. CNS-Mondo regulates the expression of *tret1-1* and *tps1* in the brain.** mNRA expression profile of *tret1-1* (A) and *tps1* (B) in brain Mondo RNA-seq data in WT and Mondo mutants upon sugar refeeding. Deseq2-derived normalized read counts of *tret1-1* and *tps1* are depicted below the profile. The peak profile of Mondo, Mlx and Pol II at *tret1-1* (C) and *tps1* (D). The profiles of ChIP-seq are shown in total tags normalized to 1.00e+07. The normalization was performed by HOMER software.

#### **4.4.7 The metabolism of glycine, serine, glutamine and purine may be regulated in a Mondo-dependent manner in the fly brain upon starvation**

Strikingly, GO term analysis on DEGs exclusively expressed in either condition revealed that pathways regarding amino acid metabolism and nucleotide (purine) metabolism were solely enriched under the starvation condition, but not under the sucrose-refeeding condition (Fig. 4.7). The genes involved in the pathway “glycine and serine metabolic pathway” are the *astray* (*aay*), serine pyruvate aminotransferase (*spat*), *CG11899* and *CG3011* genes (Fig. 4.8A). Except for *spat*, these three genes are identified as direct targets of Mondo in our whole-head Mondo ChIP-seq data. Mondo exerts an inhibitory effect on the expression of these genes, particularly upon starvation (Fig. 4.8B). Specifically, the downregulation of *aay*, a phosphoserine phosphatase involved in serine biosynthesis, by Mondo upon starvation was observed. Interestingly, the depletion of *aay* has been reported to reduce starvation-induced sleep suppression as a result of altered serine metabolism in the fly brain (218). It is important to understand whether Mondo controls serine levels in the fly brain and further mediates sleep behavior during starvation, which may in turn balance overall energy.

Genes such as glutamine synthase 2 (*gs2*), phosphoribosylamidotransferase 2 (*prat2*) and *ade2* that are involved in “glutamine metabolic pathway” and “purine metabolism” are also downregulated by Mondo upon starvation (Fig. 4.9). *Gs2* encodes an enzyme that converts glutamate to glutamine. *Prat2* encodes a type-2 glutamine amidotransferase that controls the *de novo* synthesis of the precursor for purine nucleotides required for energy transfer and cell signaling. Collectively, this analysis indicates a distinct role of Mondo in the brain upon different nutrient states. It is also the first genome-wide data that probe Mondo’s function upon starvation in the brain.

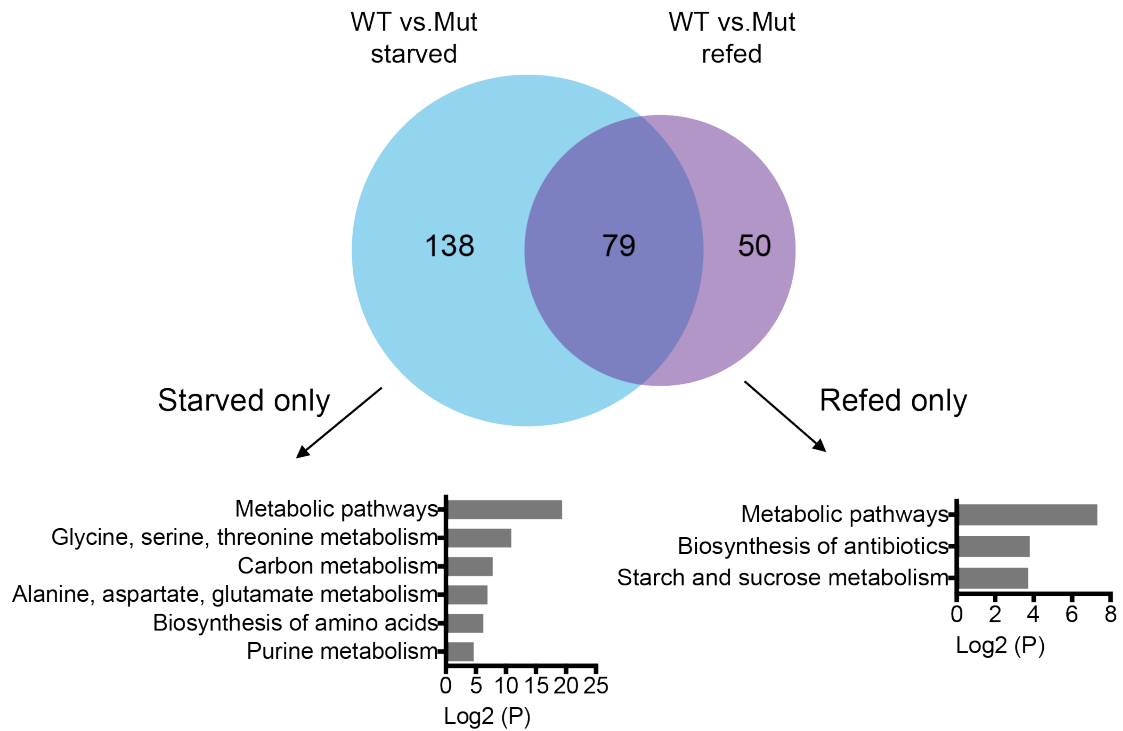


**Figure 4.7. Comparison of Mondo-dependent DEGs between the starvation condition and the sugar-refeeding condition.** Venn diagram of brain Mondo-dependent transcriptome upon the starved condition (shown in blue) and the sugar refeeding (shown in purple) condition. GO terms that were enriched only upon the starvation condition or the sugar-refed condition are shown below the Venn diagram with  $-\log_2(P)$  plotted at the x-axis.

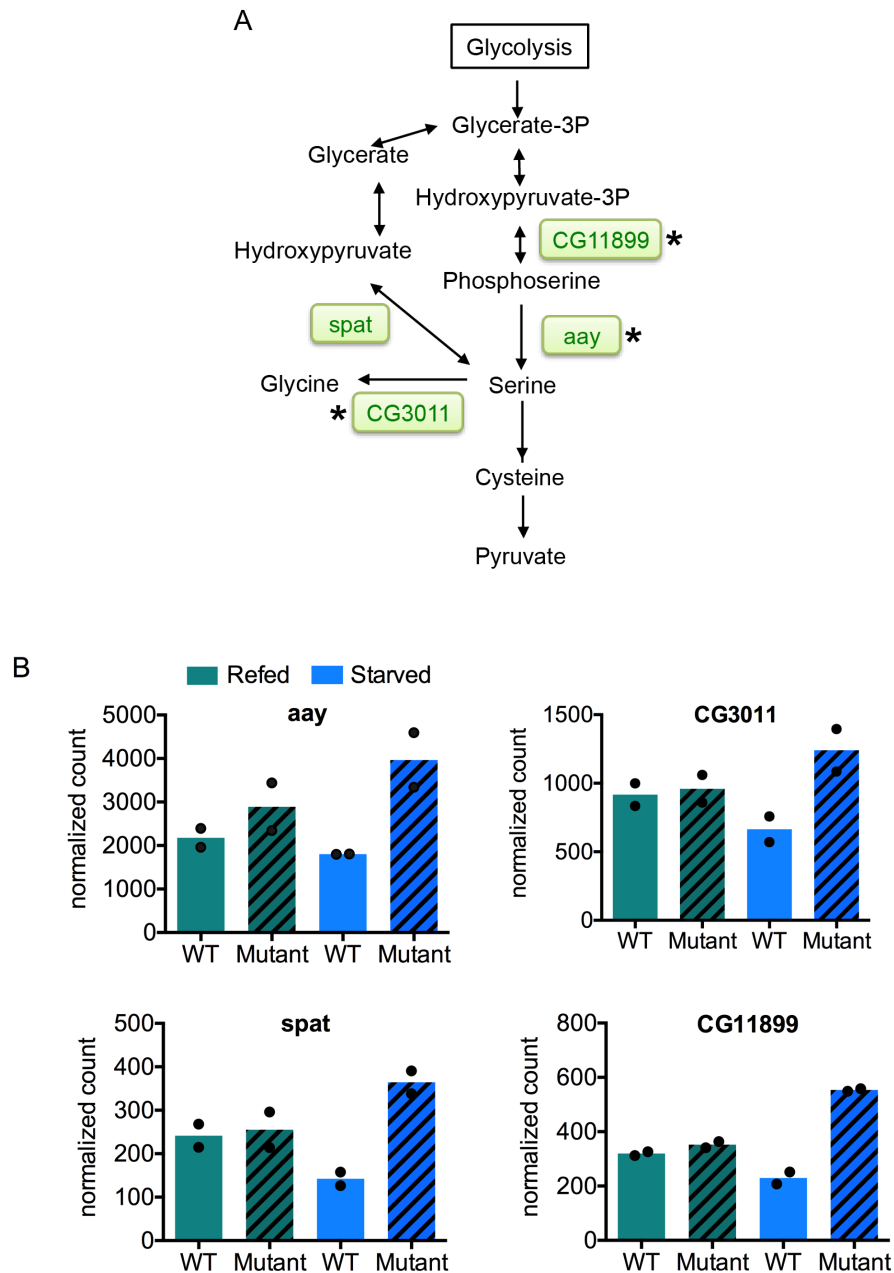


**Figure 4.8. Mondo-dependent DEGs are involved in glycine and serine metabolism in the brain** (A) Mondo-regulated genes encoding enzymes involved in the glycine and serine metabolic pathways are shown in green text. (B) The expression of the genes in the brain Mondo RNA-seq data in WT and Mondo mutants upon the sugar refeeding and starved conditions. \*: Indicates Mondo-targeted genes that were shown in both the whole head ChIP-seq and brain RNA-seq data.

4. INVESTIGATING MONDO FUNCTION IN THE CENTRAL NERVOUS SYSTEM  
OF THE FLY

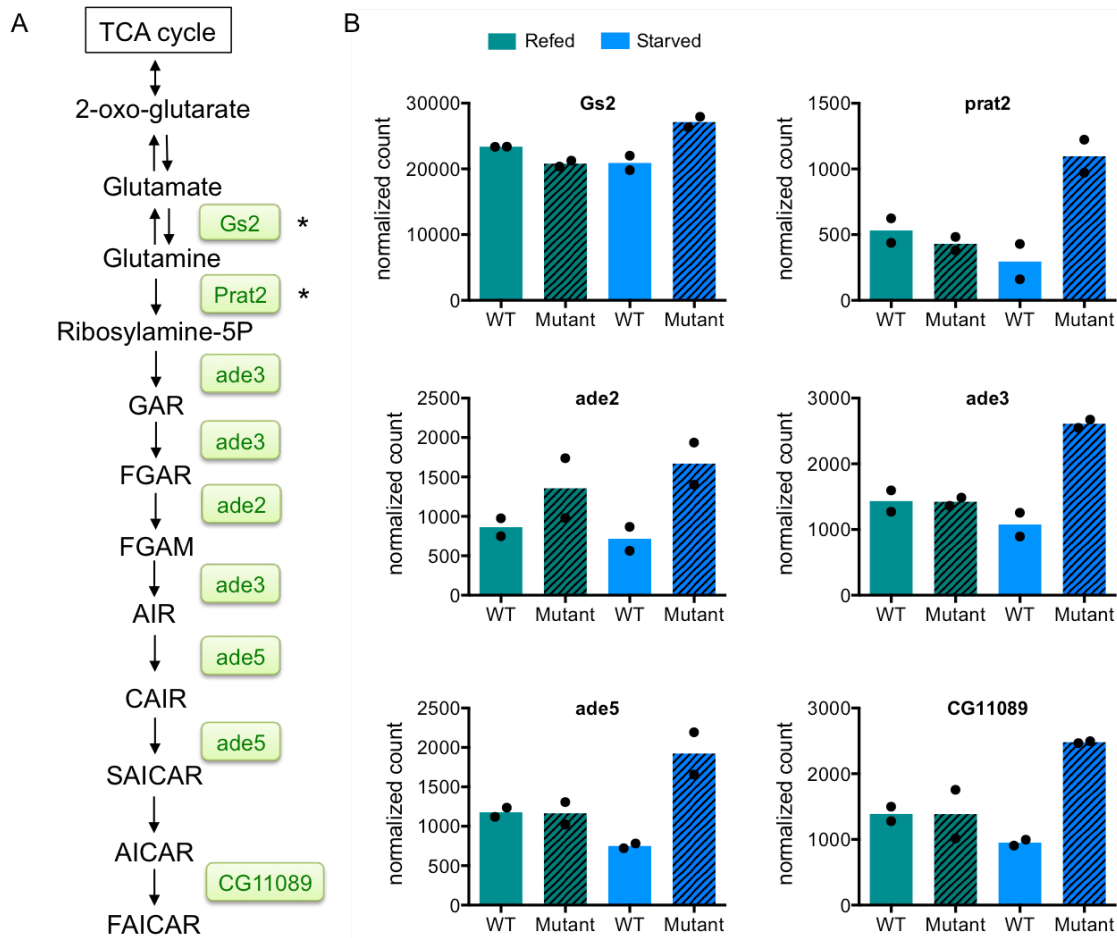


**Figure 4.9. Mondo-dependent DEGs are involved in glutamine and purine metabolism in the brain.** (A) Mondo-regulated genes encoding enzymes in the glutamate metabolism and purine synthesis are shown in the green text. (B) Expression of the genes in the brain Mondo RNA-seq data in WT and Mondo mutants upon the sugar refeeding and starved conditions. \*: Indicates Mondo-targeted genes that were shown in both the whole head ChIP-seq and brain RNA-seq data. GAR: 5-phosphoribosyl-glycinamide. FGAR: 5-phosphoribosyl-N-formylglycinamide. FGAM: 5-phosphoribosyl-N-formylglycinamide. AIR: 5-phosphoribosyl-5-aminoimidazole. CAIR: 5-phosphoribosyl-5-amino-imidazole-4-carboxylate. SAICAR: 5-amino-4-imidazole-N-succinocarboxamide ribonucleotide. AICAR: 5-amino-4-imidazolecarboxamide ribonucleotide. FAICAR: 5-phosphoribosyl-4-carboxamide-5-formamidoimidazole.

#### 4.5 Discussion and future directions

Our brain-RNA-seq data and Pol II ChIP-seq data show that Mondo may be involved in trehalose transport by repressing the expression of the trehalose transporter gene *tret1-1*. It has been shown that trehalose, the main circulating carbohydrate in flies, is taken up and catabolized in the glial cells to provide energy to the brain (222). Given that a high glucose level has adverse impacts on brain function (219-221), materials are selectively transported through the blood-brain barrier to maintain the glucose level in the steady state in the brain. This may suggest that Mondo could serve as a glucose sensor to reduce the expression of *tret1-1* upon high circulating trehalose to maintain the steady state of the glucose level in the brain.

In addition to the metabolic function, our data also suggest a role of Mondo in sleep behaviors. Mondo-regulated genes such as *CG4500* and *bmm* have been reported to be involved in modulating sleep homeostasis via regulating lipid deposit. However, *CG4500* and *bmm* display opposing effects in sleep recovery after sleep deprivation (217, 223). This indicates that Mondo may act as an upstream regulator to balance the energy expense overall. Additionally, Mondo may also mediate starvation-induced sleep suppression by regulating the expression of genes such as *aay*, *spat*, *CG3001* and *CG11899*, which are involved in serine metabolism. It has been shown that the serine level in the fly brain controls starvation-induced sleep suppression (218). Moreover, the pan-neuronal knockdown of the *aay* gene, a rate-limiting enzyme in serine biosynthesis, has been shown to suppress starvation-induced sleep suppression. Overall, these data suggest that Mondo, particularly brain-specific Mondo, may regulate sleep behaviors via reprogramming lipid and serine metabolism in the fly brain (Fig. 4.10), though fat body-specific Mondo has been shown to have no influence on starvation-induced sleep suppression (159). Performing sleep behavior assays with Mondo mutants may help address the potential regulatory role of Mondo in sleep behaviors. In addition, measuring the alteration in sleep patterns with Mondo mutants along with tissue-specific rescue experiments will help unravel whether Mondo has a function in mediating sleep behaviors.

Overall, our RNA-seq data suggest that Mondo is expressed in the fly brain and has multiple extended functions beyond metabolism. However, one concern is

that the glucose level in the brain is not within the glucose range for the activation of ChREBP by high glucose (224, 225). The way Mondo is activated in the brain deserves further investigation.

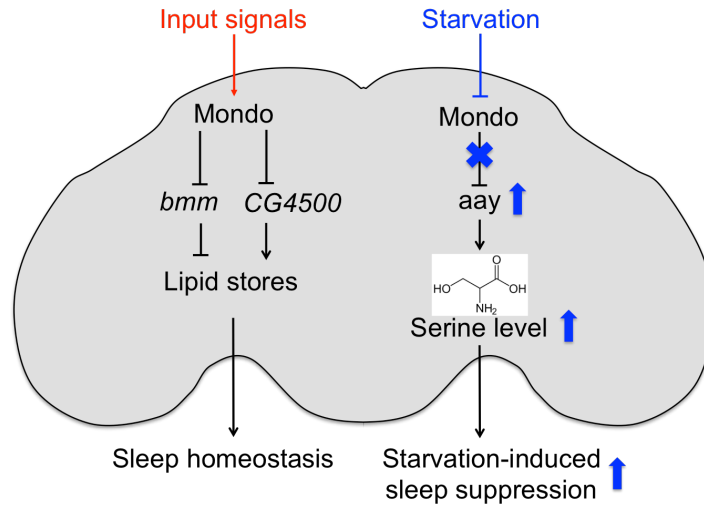


**Figure 4.10. Hypothesized Mondo-dependent regulation on the genes involved in lipid and serine metabolism and subsequent outcome in sleep behaviors.** Genes involved in lipid metabolism such as *bmm* and *CG4500*, as well as the genes involved in serine metabolism such as *aay*, are downregulated by Mondo in the brain during starvation. The graph depicts the regulation of Mondo on these genes observed in our analysis and the published evidence of these genes in sleep behaviors.

# Chapter 5

## Perspectives

My PhD project broadly addresses the role of Mondo from different aspects. In chapter 2, I have demonstrated the physiological role of Mondo on the survival rate at different stages of the life cycle, on different types of sugar diet and different nutritional states. Next, in chapter 3, the downstream effectors of Mondo-Mlx were identified globally with genome-wide approaches. Lastly, in chapter 4, the tissue-specific role of Mondo was addressed in the fly brain.

In the past decade, ChREBP has been shown as a key metabolic regulator in mammals (61,90,113,226). Consistent with the mammalian data, Mondo is required for flies to survive on a high sugar diet. Interestingly, I have also observed that Mondo is essential for flies to survive starvation if they were previously fed on yeast-only (protein-based) food but not on yeast+sucrose food. This nutrient-dependent phenotype is the first evidence implying an extended role of Mondo in metabolic adaptation in response to starvation. However, to study the underlying mechanisms of this phenotype, several works still need to be done (Fig. 5.1). First of all, this phenotype should be validated with CRISPR-Mondo mutant, which is believed to be a null Mondo mutant fly line. Second, metabolic indicators such as biomass, glucose levels, glycogen levels, and TG contents need to be measured to better characterize the metabolic profiles upon different nutritional states in the absence or presence of Mondo. Third, MS-based metabolomics can be performed to elucidate the overall alteration in metabolism profiles dependent on Mondo upon starvation.

Besides determining the Mondo-regulated physiological outcomes in the fly, identification of direct target genes of Mondo-Mlx has been another major focus of my project. ChIP-seq data reveals that Mondo-Mlx not only regulates the genes involved in metabolic pathways but also directly controls a wide range of transcription factors, which overall constitute a large transcription cascade. Consistently, the laboratory of Hietakangas has discovered the regulatory role of Mlx on specific transcription factors genes such as *sugarbabe* and *cbt*, that are presented in the analysis (227). Moreover, these downstream effectors contain the canonical

ChoRE motif within identified Mondo binding sites (see chapter 3, Fig.3.16), which also supports the Mondo-dependent regulation on these genes. These downstream transcription factors have been shown to play different roles in several biological processes including sugar metabolism, development, and circadian rhythm...etc. Functional characterization of these effectors allows further understanding of the physiological role of Mondo in the fly.

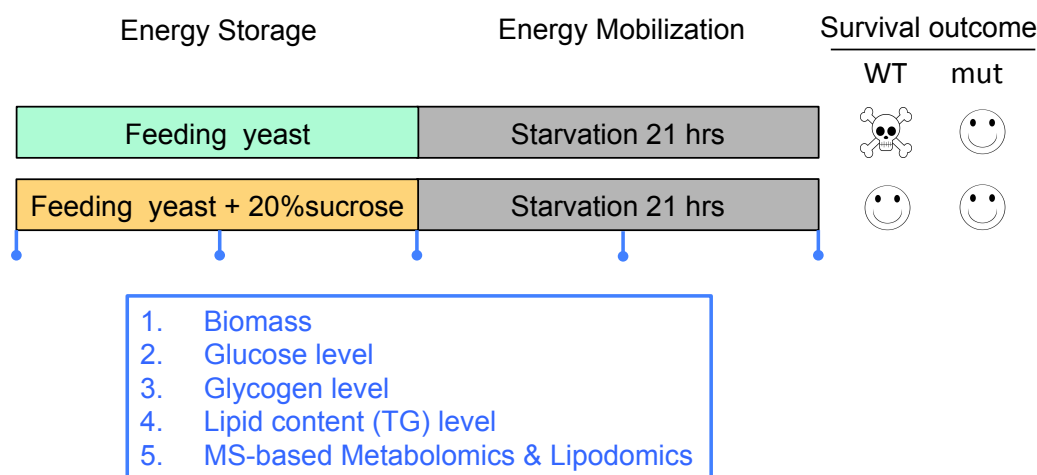


**Figure 5.1. Measuring metabolic profiles across different time points.** Our data suggest that flies fed on yeast-only (protein-based) food require Mondo to survive starvation. To study how Mondo is involved in the metabolism of amino acids upon starvation, general indices for energy storage and mobilization such as biomass, glucose levels, glycogen levels, lipid content can be measured during feeding on yeast-only food and yeast+sucrose food and during starvation. MS-based metabolomics and lipidomics can be performed to explore the Mondo-dependent metabolic profiles under each condition. TG: Triglycerides.

In addition, in the motif searching analysis, a novel motif “GATAA” besides the canonical ChoRE motif was discovered to be centrally-enriched within Mondo-Mlx binding sites (see chapter 3, Fig. 3.13B). It is known that the “GATAA” motif is targeted by GATA factors. Meanwhile, the “GATAA” motif is reverse complement of the DAF-16-associated element (DAE), CTTATCA. It has been shown that GATA factor and DAF-16, the homolog of FOXO transcription factor in *C. elegans* share binding sites on several metabolic genes in worms. It is interesting to learn apart from

Mlx, whether Mondo interacts with another interacting partner such as FOXO to bind to genes containing this “GATAA” motif. To address this question, reporter assays in combination with mutated binding sites (Fig. 5.2A) or electrophoretic mobility shift assay (EMSA) can be used to elucidate the binding fidelity of Mondo at this motif. Alternatively, performing Mondo ChIP-qPCR on flies introduced with mutation at identified “GATAA” sites can also validate the binding of Mondo at this specific motif *in vivo* if limitations exist *in vitro* assays (Fig. 5.2B).

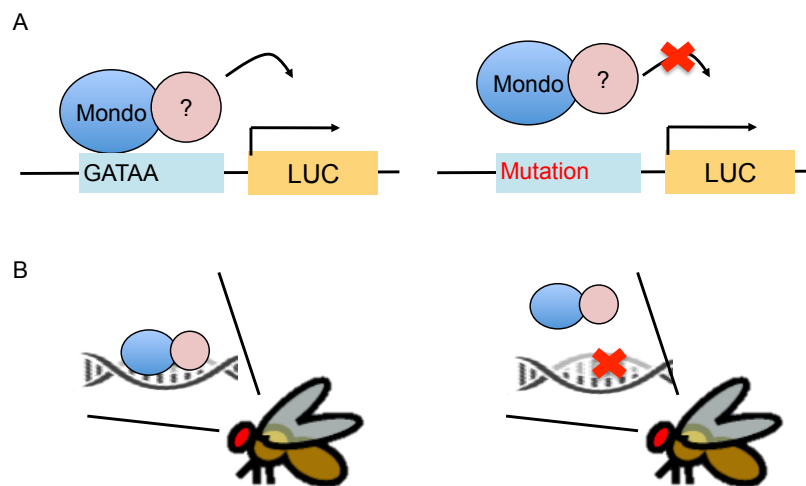


**Figure 5.2** *In vitro* and *in vivo* assays allow the investigation of the interaction between TF and DNA binding sites. (A) Promoter/enhancer activity reporter assay can be performed to validate the binding of Mondo at the “GATAA” motif. (B) Genome editing can be introduced into the “GATAA” motif for assessing the contribution of the motif to the binding of Mondo.

The current model suggests that the transcription activity of Mondo protein family is turned on by direct binding of G6P to the LID domain. To validate this model in the fly, CRISPR-Mondo mutants can be utilized. CRISPR-Mondo mutant needs to be transformed into a Mondo-GAL4 driver fly line by replacing the original cassette with GAL4 fragment. Moreover, to functionally characterize the protein domains of Mondo *in vivo*, one can cross GAL4 Mondo null mutant with different UAS Mondo mutant flies such as G6P binding deficient mutant or domain deletion mutant to see if Mondo mutant proteins are able to rescue the sugar intolerance phenotype.

When deep dive into the tissue-specific function of Mondo in the fly brain, Mondo is shown to be involved in metabolic pathways and also have function beyond

metabolism such as sleep behavior. The brain-specific RNAseq data reveals that Mondo regulates the expression of *bmm* and *CG4500* genes which have been shown to associate with sleep homeostasis response (223). In addition, Mondo seems to regulate *aay* gene which has been reported to mediate starvation-induced sleep suppression via regulating serine level in the fly brain (218). To investigate whether brain-specific Mondo controls sleep behavior, firstly, sleep behaviors of WT flies and *mondo* mutants that can be measured with a *Drosophila* activity monitor (DAM) system (Fig. 5.3). If misregulated sleep behaviors are observed with *mondo* mutants, a rescue experiment can be performed by expressing *mondo* or the downstream genes such as *bmm*, *CG4500*, and *aay* genes in the Mondo mutants to validate the involvement of Mondo in the sleep behavior.

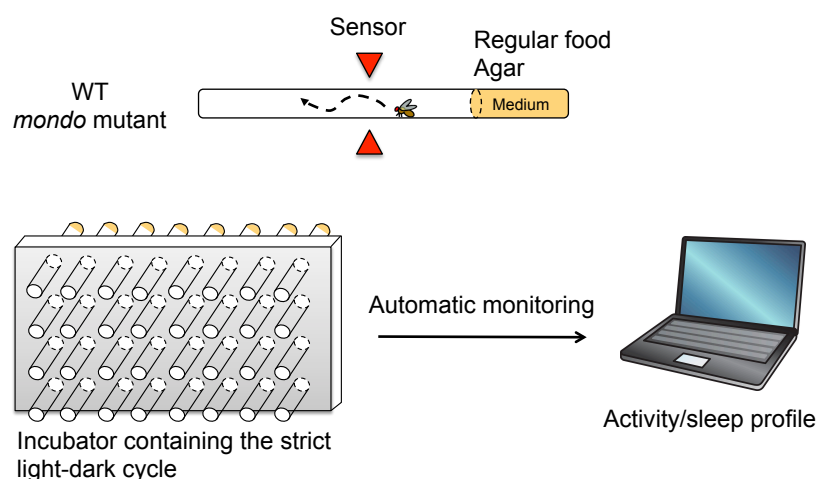


**Figure 5.3 Graphic representation of fly activity monitor system.** Sleep behavior can be analyzed using DAM system. WT and Mondo mutants tested on regular or starvation medium within the DAM to measure sleep.

Last but not the least, to better understand the role of Mondo in the fly brain, the detailed expression pattern of Mondo in the brain needs to be characterized. It is of great importance to identify the expression profile, and cell types where Mondo is expressed in the brain. It allows speculation of the potential role of Mondo in the fly brain based on the characterized function of the cell types or the specific brain regions.

# Abbreviations

RBCs : red blood cells

SGLT1: sodium/glucose cotransporter

Gr: gustatory receptor

GCK: glucokinase

GLUT: glucose transporter

GPR: G protein-coupled receptors

GLP1: glucagon-like peptide-1

ChREBP: carbohydrate response element binding protein

AMPK: AMP-activated protein kinase

GCN2: general control nonderepressible 2

eIF2 $\alpha$ : eukaryotic translation initiator factor 2  $\alpha$

mTORC1: mechanistic target of rapamycin complex 1

SESN2: Sestrin2

LRS: Leucyl-tRNA synthetase

FLCN: Folliculin

TXNIP: thioredoxin-interacting protein

CCHa2: CCHamide-2

IPCs: insulin producing cells

Upd2: Unpaired 2

dILPs: insulin-like peptides

sAKH: adipokinetic hormone

CC: Corpora cardiaca

Dh44: diuretic hormone 44 neuropeptide

CIF: calorie-induced secreted factor

PI3K: phosphatidylinositol 3-kinase

SREBP-1c: sterol regulatory element-binding transcription factor-1c

PKB: protein kinase B

FOXO: Forkhead box O

InR: insulin receptor

HNF1a: hepatocyte nuclear factor 1a

## ABBREVIATIONS

---

PDX1: pancreatic duodenal homeobox 1  
HNF4a: hepatocyte nuclear factor 4a  
ChoRE: carbohydrate response element  
PPARs: peroxisome proliferator-activated receptors  
SRE: sterol regulatory element  
ACC: acetyl-CoA carboxylase  
FAS: fatty acid synthase  
SCD1: stearoyl-CoA desaturase 1  
G6PD: glucose-6-phosphate dehydrogenase  
LXR a: liver X receptor a  
ATF4: activating transcription factor 4  
GS: glutamine synthase  
GRE: glucocorticoid response element  
bHLH/LZ : basic helix-loop-helix leucine zipper  
*L-PK: L-type pyruvate kinase*  
GSM: Glucose sensing module  
MCR: Mondo conserved regions  
LID: low glucose inhibitory domain  
GRACE: glucose-response activation conserved element  
DCD: cytoplasmic localization domain  
ARRDC4: arrestin domain-containing 4  
G6P: Glucose-6-phosphate  
F-2,6-BP : fructose-2,6-bisphosphate  
Xu5P : Xylulose 5-phosphate  
HAT : histone acetyltransferase  
SIK2: Salt-inducible kinase 2  
NES: nuclear export signals  
NLS: nuclear import signal  
AMP: adenosine monophosphate  
gRNAs: guiding RNA  
PPRE : proliferator response element  
SIK3: Salt-Inducible Kinase 3

## ABBREVIATIONS

---

PPP: pentose phosphate pathway  
DNL: *de novo* lipogenesis  
PTM: post-translational modification  
ROS: reactive oxygen species  
TG: triglycerides  
WAT: white adipose tissue  
BAT: brown adipose tissue  
T3: triiodothyronine  
ROR: RAR-related orphan receptor  
CNS: central nervous system  
FGF21: fibroblast growth factor 21  
Sb: stubble bristles  
Ser: serrated wings  
sgRNA: single strand guide RNA  
PFA: paraformaldehyde  
PBS: phosphate-buffered saline  
HDR: homology-directed repair  
HFCS: high-fructose corn syrup  
RMCE: recombinase-mediated cassette exchange  
TSS: transcription start site  
TFs: transcription factors  
PCR: polymerase chain reaction  
IPTG: isopropyl  $\beta$ -D-1-thiogalactopyranoside  
ChIP: chromatin immunoprecipitation  
Dm6: *Drosophila* genome release 6  
GO: gene ontology  
DEGs: differentially expressed genes  
RNA Pol II: RNA polymerase II  
PCA: principle component analysis  
*tret1-1*: trehalose transporter  
*tps1*: trehalose-6-phosphate synthase 1  
SOG: subesophageal ganglion

## ABBREVIATIONS

---

ILPs: insulin-like peptides

*aay*: *astray*

*spat*: *serine pyruvate aminotransferase*

GAR: 5-phosphoribosyl-glycinamide

FGAR: 5-phosphoribosyl-N-formylglycinamide

FGAM: 5-phosphoribosyl-N-formylglycinamide

AIR: 5-phosphoribosyl-5-aminoimidazole

CAIR: 5-phosphoribosyl-5-amino-imidazole-4-carboxylate

SAICAR: 5-amino-4-imidazole-N-succinocarboxamide ribonucleotide

AICAR: 5-amino-4-imidazolecarboxamide ribonucleotide

FAICAR: 5-phosphoribosyl-4-carboxamide-5-formamidoimidazole

DAE: DAF-16-associated element

EMSA: electrophoretic mobility shift assay

DAM: *Drosophila* activity monitor

# List of Figures and Tables

Table 1.1 Conservation of metabolic tissues between flies and mammals.....	7
Figure 1.1. Model of the bHLH/LZ region of two ChREBP/Mlx heterodimers binding to a tandem E box DNA element.....	12
Figure 1.2. Structural domains of human Mondo and Mlx proteins and fly Mondo.....	13
Figure 1.3. Protein functional domains are conserved in the fly and human.....	15
Figure 1.4. The model of Mondo/ChREBP regulation in response to glucose.....	18
Figure 1.5. Regulatory network composed of interplay between ChREBP/Mondo and other nutrient-induced factors and the downstream effector.....	21
Figure 1.6. Metabolic adjustment upon fed and starvation states.....	25
Figure 1.7. ChREBP functions as a central metabolic coordinator in various cell types .....	26
Figure 2.1. Mondo <sup>K05106</sup> mutant fly is not viable on high sugar food.....	40
Figure 2.2 Generating CRISPR/Cas9 <i>mondo</i> knockout fly .....	41
Figure 2.3. Flies require Mondo and Mlx to survive on high-sugar food.....	43
Figure 2.4. Mondo knockdown flies are not viable on high-glucose and high-fructose food .....	45
Fig 2.5. Adult Mondo mutant has a reduced life span when fed a high sucrose only diet.....	46
Figure 2.6. Flies deprived of sugar require Mondo to survive upon starvation.....	47
Figure 2.7. Functional characterization of N-terminal and C-terminal GFP-tagged Mondo protein in the fly .....	49
Figure 2.8. GFP expression in the fat body-GAL4 driven H2B-GFP fly and the N-terminal tagged GFP-Mondo fly.....	50
Figure 2.9. Investigating the sugar-dependent viability of flies by knocking down Mondo in the fat body, neuron and glia .....	51
Figure 3.1. PCA analysis shows the reproducibility of biological replicates and the correlative relationships between each condition in the RNA-seq experiment.....	71
Figure 3.2. Hierarchical clustering of the time-course sugar-induced transcriptome.....	73
Figure 3.3 Clustering of the time-course <i>Drosophila</i> transcriptome profiling based on the gene expression differences between sugar-refeeding and starvation groups.....	74
Figure 3.4. Expressing Mondo protein domains as antigens to raise Mondo-specific antibodies .....	75
Figure 3.5. Assessing the sensitivity of Mondo antibodies on the serial titration of recombinant proteins.....	76

Figure 3.6. Western blot analysis on fly protein extracts with Mondo antibodies ....	77
Figure 3.7. The efficiency of Mondo-ChIP experiment with three Mondo antibodies is evaluated with qPCR .....	79
Figure 3.8. Mondo is most active at 1 hour sugar-refeeding time point.....	80
Figure 3.9. Mondo-Mlx ChIP-qPCR on WT and Mondo mutant flies.....	82
Figure 3.10. PCA analysis and Mondo-Mlx peak profile at known target sites.....	84
Figure 3.11. Differential binding analysis of Mondo and Mlx targeted site.....	85
Figure 3.12. Genomic distribution of Mondo-Mlx target sites.....	86
Figure 3.13. Mondo-Mlx consensus binding sites predicted from the motif discovery program in MEME-ChIP .....	88
Figure 3.14. GO term analysis on Mondo-Mlx targeted genes from DAVID.....	90
Figure 3.15. Mondo-Mlx targeted genes involved in glycolysis, lipid synthesis and amino acid biosynthesis .....	91
Figure 3.16. Differential Mondo and Mlx peaks at the genes with transcription factor activity .....	93
Figure 3.17. Differential Pol II occupancy at the promoter and the gene body of the Mondo-targeted genes between WT and Mondo mutants .....	95
Figure 3.18. Peak profile of Mondo, Mlx and RPB3 at the putative Mondo-Mlx target genes .....	96
Figure 3.19. Comparison of Mondo target genes with genes clustered based on the temporal expression profile.....	97
Figure 3.20. Gene expression profile correlates with RNA Pol II binding at selected genes.....	98
Figure 3.21. Comparison of Mondo-Mlx target genes with sugar-regulated Mlx-dependent and Mondo-dependent genes identified in larvae.....	100
Figure A3.1. Map of expression plasmid pETMCN Mondo DBD.....	103
Figure A3.2. Map of expression plasmid pUAST Mondo RJ.....	104
Figure A3.3. The purification of recombinant Mondo proteins was tested on coomassie-stained SDS-page .....	105
Table A3.1 Primers used in ChIP-qPCR assays .....	106
Table A3.2. Mondo target genes with transcription factor activity are listed with the gene name and corresponding ChoRE sequence .....	107
Figure 4.1. Lines of evidence suggest Mondo expression in the fly brain .....	112
Figure 4.2. RT-qPCR and RNA-seq indicate the expression of <i>mondo</i> and downstream effectors .....	114
Figure 4.3. Comparison of sugar-induced transcriptome in the brain and the whole head.....	115
Figure 4.4. Comparison of brain Mondo RNA-seq data with Mondo-Mlx ChIP-seq data .....	116
Table 4.1 Mondo-dependent DEGs in the brain under sugar-refeeding, starvation or under both conditions .....	117

Figure 4.5. Mondo-dependent regulatory network upon sugar refeeding  
in the brain ..... 118

Table 4.2 Oxidoreductase-associated DEGs identified from brain RNA-seq data.... 119

Table 4.3 Sleep-associated DEGs identified from brain RNA-seq data..... 119

Figure 4.6. CNS-Mondo down-regulates the expression of *tret1-1* and *tps1* in the  
brain ..... 120

Figure 4.7. Comparison of Mondo-dependent DEGs between the starvation condition  
and the sugar-refeeding condition..... 122

Figure 4.8. Mondo-dependent DEGs are involved in glycine and serine metabolism  
in the brain ..... 123

Figure 4.9. Mondo-dependent DEGs are involved in glutamine and purine  
metabolism in the brain..... 124

Figure 4.10. Hypothesized Mondo-dependent regulation on the genes involved in  
lipid and serine metabolism and subsequent outcome in sleep behaviors ..... 126

Figure 5.1. Measuring metabolic profiles across different time points ..... 128

Figure 5.2 *In vitro* and *in vivo* assays allow the investigation of interaction between  
TF and DNA binding sites ..... 129

Figure 5.3 Graphic representation of fly activity monitor system..... 130

# Bibliography

1. Dus M, Min S, Keene AC, Lee GY, Suh GSB. Taste-independent detection of the caloric content of sugar in *Drosophila*. *Proc Natl Acad Sci USA*. 2011 Jul 12;108(28):11644–9.
2. de Araujo IE, Oliveira-Maia AJ, Sotnikova TD, Gainetdinov RR, Caron MG, Nicolelis MAL, et al. Food reward in the absence of taste receptor signaling. *Neuron*. 2008 Mar 27;57(6):930–41.
3. Fontana L, Partridge L, Longo VD. Extending healthy life span--from yeast to humans. *Science*. 2010 Apr 16;328(5976):321–6.
4. Chantranupong L, Wolfson RL, Sabatini DM. Nutrient-Sensing Mechanisms across Evolution. *Cell*. Elsevier Inc; 2015 Mar 26;161(1):67–83.
5. Nelson G, Hoon MA, Chandrashekar J, Zhang Y, Ryba NJ, Zuker CS. Mammalian sweet taste receptors. *Cell*. 2001 Aug 10;106(3):381–90.
6. Margolskee RF, Dyer J, Kokrashvili Z, Salmon KSH, Ilegems E, Daly K, et al. T1R3 and gustducin in gut sense sugars to regulate expression of Na<sup>+</sup>-glucose cotransporter 1. *Proceedings of the National Academy of Sciences*. National Academy of Sciences; 2007 Sep 18;104(38):15075–80.
7. Marella S, Fischler W, Kong P, Asgarian S, Rueckert E, Scott K. Imaging taste responses in the fly brain reveals a functional map of taste category and behavior. *Neuron*. 2006 Jan 19;49(2):285–95.
8. Miyamoto T, Chen Y, Slone J, Amrein H. Identification of a *Drosophila* glucose receptor using Ca<sup>2+</sup> imaging of single chemosensory neurons. Meyerhof W, editor. *PLoS ONE*. Public Library of Science; 2013;8(2):e56304.
9. Slone J, Daniels J, Amrein H. Sugar receptors in *Drosophila*. *Current Biology*. 2007 Oct 23;17(20):1809–16.
10. Matsuda H, Yamada T, Yoshida M, Nishimura T. Flies without Trehalose. *J Biol Chem*. 2015 Jan 8;290(2):1244–55.
11. Kawahito S, Kitahata H, Oshita S. Problems associated with glucose toxicity: role of hyperglycemia-induced oxidative stress. *World J Gastroenterol*. Baishideng Publishing Group Inc; 2009 Sep 7;15(33):4137–42.
12. Isabel G, Martin JR, of SCAJ, 2004. Ablation of AKH-producing neuroendocrine cells decreases trehalose levels and induces behavioral changes in *Drosophila*. [researchgatenet](http://researchgatenet)
13. Lee G, Park JH. Hemolymph Sugar Homeostasis and Starvation-Induced Hyperactivity Affected by Genetic Manipulations of the Adipokinetic Hormone-Encoding Gene in *Drosophila melanogaster*. *Genetics*. Genetics; 2004 May 1;167(1):311–23.

14. Rulifson EJ, Kim SK, Nusse R. Ablation of Insulin-Producing Neurons in Flies: Growth and Diabetic Phenotypes. *Science*. American Association for the Advancement of Science; 2002 May 10;296(5570):1118–20.
15. Mueckler M, Thorens B. The SLC2 (GLUT) family of membrane transporters. *Mol Aspects Med*. 2013 Apr;34(2-3):121–38.
16. Ugrankar R, Berglund E, Akdemir F, Tran C, Kim MS, Noh J, et al. *Drosophila* glucose screening identifies Ck1alpha as a regulator of mammalian glucose metabolism. *Nature Communications*. Nature Publishing Group; 14:6:1–10.
17. Fahy E, Cotter D, Sud M, Subramaniam S. Lipid classification, structures and tools. *Biochimica et Biophysica Acta (BBA) - Molecular and Cell Biology of Lipids*. 2011 Nov;1811(11):637–47.
18. Ruvolo PP. Intracellular signal transduction pathways activated by ceramide and its metabolites. *Pharmacol Res*. 2003 May;47(5):383–92.
19. Maceyka M, Harikumar KB, Milstien S, Spiegel S. Sphingosine-1-phosphate signaling and its role in disease. *Trends Cell Biol*. 2012 Jan;22(1):50–60.
20. Briscoe CP, Tadayyon M, Andrews JL, Benson WG, Chambers JK, Eilert MM, et al. The orphan G protein-coupled receptor GPR40 is activated by medium and long chain fatty acids. *J Biol Chem*. American Society for Biochemistry and Molecular Biology; 2003 Mar 28;278(13):11303–11.
21. Edfalk S, Steneberg P, Edlund H. Gpr40 is expressed in enteroendocrine cells and mediates free fatty acid stimulation of incretin secretion. *Diabetes*. American Diabetes Association; 2008 Sep;57(9):2280–7.
22. Hirasawa A, Tsumaya K, Awaji T, Katsuma S, Adachi T, Yamada M, et al. Free fatty acids regulate gut incretin glucagon-like peptide-1 secretion through GPR120. *Nat Med*. Nature Publishing Group; 2005 Jan;11(1):90–4.
23. Holst JJ. Incretin hormones and the satiation signal. *Int J Obes (Lond)*. Nature Publishing Group; 2013 Sep;37(9):1161–8.
24. Sato S, Jung H, Nakagawa T, Pawlosky R, Takeshima T, Lee W-R, et al. Metabolite Regulation of Nuclear Localization of Carbohydrate Response Element-binding Protein (ChREBP). Role of AMP as an Allosteric Inhibitor. *J Biol Chem*. American Society for Biochemistry and Molecular Biology; 2016 Mar 16;291(20):jbc.M115.708982–10527.
25. Kawaguchi T, Osatomi K, Yamashita H, Kabashima T, Uyeda K. Mechanism for fatty acid “sparing” effect on glucose-induced transcription: regulation of carbohydrate-responsive element-binding protein by AMP-activated protein kinase. *J Biol Chem*. American Society for Biochemistry and Molecular Biology; 2002 Feb 8;277(6):3829–35.
26. Bjordal M, Arquier N, Kniazeff J, Pin JP, Léopold P. Sensing of amino acids in a dopaminergic circuitry promotes rejection of an incomplete

- diet in *Drosophila*. *Cell*. 2014 Jan 30;156(3):510–21.
27. Wang S, Tsun ZY, Wolfson RL, Shen K, Wyant GA, Plovanich ME, et al. Lysosomal amino acid transporter SLC38A9 signals arginine sufficiency to mTORC1. *Science*. 2015 Jan 8;347(6218):188–94.
  28. Singh SR, Liu W, Hou S. The adult *Drosophila* Malpighian tubules are maintained by multipotent stem cells. *Comparative Biochemistry and Physiology, Part A*. 2008;3 Supplement(150):S133.
  29. Colombani J, Raisin S, Pantalacci S, Radimerski T, Montagne J, Léopold P. A nutrient sensor mechanism controls *Drosophila* growth. *Cell*. 2003 Sep 19;114(6):739–49.
  30. Sano H, Nakamura A, Texada MJ, Truman JW, Ishimoto H, Kamikouchi A, et al. The Nutrient-Responsive Hormone CChamide-2 Controls Growth by Regulating Insulin-like Peptides in the Brain of *Drosophila melanogaster*. Taghert PH, editor. *PLoS Genet. Public Library of Science*; 2015 May 28;11(5):e1005209.
  31. Farooqi IS, Bullmore E, Keogh J, Gillard J, O'Rahilly S, Fletcher PC. Leptin Regulates Striatal Regions and Human Eating Behavior. *Science. American Association for the Advancement of Science*; 2007 Sep 7;317(5843):1355–5.
  32. Rajan A, Perrimon N. *Drosophila* Cytokine Unpaired 2 Regulates Physiological Homeostasis by Remotely Controlling Insulin Secretion. *Cell*. *Cell Press*; 2012 Sep 28;151(1):123–37.
  33. Gutierrez E, Wiggins D, Fielding B, Gould AP. Specialized hepatocyte-like cells regulate *Drosophila* lipid metabolism. *Nature*. 2006 Nov 29;445(7125):275–80.
  34. Brogiolo W, Stocker H, Ikeya T, Rintelen F, Fernandez R, Hafen E. An evolutionarily conserved function of the *Drosophila* insulin receptor and insulin-like peptides in growth control. *Current Biology. Cell Press*; 2001 Feb 20;11(4):213–21.
  35. Grönke S, Clarke D-F, Broughton S, Andrews TD, Partridge L. Molecular Evolution and Functional Characterization of *Drosophila* Insulin-Like Peptides. Rulifson E, editor. *PLoS Genet. Public Library of Science*; 2010 Feb 26;6(2):e1000857.
  36. Bai H, Kang P, Tatar M. *Drosophila* insulin-like peptide-6 (*dilp6*) expression from fat body extends lifespan and represses secretion of *Drosophila* insulin-like peptide-2 from the brain. *Aging Cell. Wiley/Blackwell* (10.1111); 2012 Dec 1;11(6):978–85.
  37. Miguel-Aliaga I, Thor S, Gould AP. Postmitotic Specification of *Drosophila* Insulinergic Neurons from Pioneer Neurons. Nusse R, editor. *PLoS Biol. Public Library of Science*; 2008 Mar 11;6(3):e58.
  38. Ikeya T, Galic M, Belawat P, Nairz K, Hafen E. Nutrient-Dependent Expression of Insulin-like Peptides from Neuroendocrine Cells in the CNS Contributes to Growth Regulation in *Drosophila*. *Current Biology*.

- Cell Press; 2002 Aug 6;12(15):1293–300.
39. Post S, Tatar M. Nutritional Geometric Profiles of Insulin/IGF Expression in *Drosophila melanogaster*. Min K-J, editor. PLoS ONE. Public Library of Science; 2016 May 12;11(5):e0155628.
  40. Géminard C, Rulifson EJ, Léopold P. Remote Control of Insulin Secretion by Fat Cells in *Drosophila*. *Cell Metabolism*. Cell Press; 2009 Sep 2;10(3):199–207.
  41. Kim J, Neufeld TP. Dietary sugar promotes systemic TOR activation in *Drosophila* through AKH-dependent selective secretion of Dilp3. *Nature Communications*. Nature Publishing Group; 2015 Apr 17;6(1):6846.
  42. Kim SK, Rulifson EJ. Conserved mechanisms of glucose sensing and regulation by *Drosophila corpora cardiaca* cells. *Nature*. Nature Publishing Group; 2004 Sep 1;431(7006):316–20.
  43. Song W, Cheng D, Hong S, Sappe B, Hu Y, Wei N, et al. Midgut-Derived Activin Regulates Glucagon-like Action in the Fat Body and Glycemic Control. *Cell Metabolism*. Elsevier Inc; 2017 Feb 7;25(2):386–99.
  44. Staubli F, Jørgensen TJD, Cazzamali G, Williamson M, Lenz C, Søndergaard L, et al. Molecular identification of the insect adipokinetic hormone receptors. *Proceedings of the National Academy of Sciences*. National Academy of Sciences; 2002 Mar 19;99(6):3446–51.
  45. Ugrankar R, Theodoropoulos P, Akdemir F, Henne WM, Graff JM. Circulating glucose levels inversely correlate with *Drosophila* larval feeding through insulin signaling and SLC5A11. *Communications Biology*. Springer US; 2018 Aug 7;:1–15.
  46. Fujita M, Tanimura T. *Drosophila* evaluates and learns the nutritional value of sugars. *Curr Biol*. 2011 May 10;21(9):751–5.
  47. Dus M, Lai JS-Y, Gunapala KM, Min S, Tayler TD, Hergarden AC, et al. Nutrient Sensor in the Brain Directs the Action of the Brain-Gut Axis in *Drosophila*. *Neuron*. 2015 Jul 1;87(1):139–51.
  48. Xu X, So J-S, Park J-G, Lee A-H. Transcriptional Control of Hepatic Lipid Metabolism by SREBP and ChREBP. *Semin Liver Dis*. 2013 Nov 12;33(04):301–11.
  49. Schmoll D, Walker KS, Alessi DR, Grempler R, Burchell A, Guo S, et al. Regulation of Glucose-6-phosphatase Gene expression by protein kinase B $\alpha$  and the forkhead transcription factor FKHR. Evidence for insulin response unit-dependent and-independent effects of insulin on promoter activity. *J Biol Chem*. American Society for Biochemistry and Molecular Biology; 2000 Nov 17;275(46):36324–33.
  50. Unterman TG. Regulation of Hepatic Glucose Metabolism by FoxO Proteins, an Integrated Approach. In: *Forkhead FOXO Transcription Factors in Development and Disease*. Elsevier; 2018. pp. 119–47. (Current Topics in Developmental Biology; vol. 127).

51. Puig O, Marr MT, Ruhf ML, Tjian R. Control of cell number by Drosophila FOXO: downstream and feedback regulation of the insulin receptor pathway. *Genes Dev. Cold Spring Harbor Lab*; 2003 Aug 15;17(16):2006–20.
52. Senokuchi T, Liang C-P, Seimon TA, Han S, Matsumoto M, Banks AS, et al. Forkhead transcription factors (FoxOs) promote apoptosis of insulin-resistant macrophages during cholesterol-induced endoplasmic reticulum stress. *Diabetes. American Diabetes Association*; 2008 Nov;57(11):2967–76.
53. Zhang X, Tang N, Hadden TJ, Rishi AK. Akt, FoxO and regulation of apoptosis. *BBA - Molecular Cell Research. Elsevier B.V*; 2011 Nov 1;1813(11):1978–86.
54. Sedding DG. FoxO transcription factors in oxidative stress response and ageing – a new fork on the way to longevity? *Biological Chemistry*. 389(3):1359.
55. Puig O, Tjian R. Transcriptional feedback control of insulin receptor by dFOXO/FOXO1. *Genes Dev. Cold Spring Harbor Lab*; 2005 Oct 15;19(20):2435–46.
56. Shih DQ, Screenan S, Munoz KN, Lou Philipson, Pontoglio M, Yaniv M, et al. Loss of HNF-1 $\alpha$  Function in Mice Leads to Abnormal Expression of Genes Involved in Pancreatic Islet Development and Metabolism. *Diabetes. American Diabetes Association*; 2001 Nov 1;50(11):2472–80.
57. Waeber G, Thompson N, Nicod P, Bonny C. Transcriptional activation of the GLUT2 gene by the IPF-1/STF-1/IDX-1 homeobox factor. *Molecular Endocrinology*. 1996 Nov;10(11):1327–34.
58. Ahlgren U, Jonsson J, Jonsson L, Simu K, Edlund H. beta-cell-specific inactivation of the mouse *Ipfl/Pdx1* gene results in loss of the beta-cell phenotype and maturity onset diabetes. *Genes Dev. Cold Spring Harbor Laboratory Press*; 1998 Jun 15;12(12):1763–8.
59. Song M-Y, Wang J, Ka S-O, Bae EJ, Park B-H. Insulin secretion impairment in *Sirt6* knockout pancreatic  $\beta$  cells is mediated by suppression of the FoxO1-Pdx1-Glut2 pathway. *Nature Publishing Group. Nature Publishing Group*; 2016 Jul 26;6(1):30321.
60. Musselman LP, Fink JL, Ramachandran PV, Patterson BW, Okunade AL, Maier E, et al. Role of Fat Body Lipogenesis in Protection against the Effects of Caloric Overload in *Drosophila*. *J Biol Chem*. 2013 Mar 22;288(12):8028–42.
61. Iizuka K, Bruick RK, Liang G, Horton JD, Uyeda K. Deficiency of carbohydrate response element-binding protein (ChREBP) reduces lipogenesis as well as glycolysis. *Proceedings of the National Academy of Sciences*. 2004 May 11;101(19):7281–6.
62. Kliewer SA, Forman BM, Blumberg B, Ong ES, Borgmeyer U, Mangelsdorf DJ, et al. Differential expression and activation of a family of murine peroxisome proliferator-activated receptors. *Proceedings of the*

- National Academy of Sciences. National Academy of Sciences; 1994 Jul 19;91(15):7355–9.
63. Martin G, Schoonjans K, Lefebvre AM, Staels B, Auwerx J. Coordinate regulation of the expression of the fatty acid transport protein and acyl-CoA synthetase genes by PPARalpha and PPARgamma activators. *J Biol Chem. American Society for Biochemistry and Molecular Biology*; 1997 Nov 7;272(45):28210–7.
  64. Rakhshandehroo M, Hooiveld G, Müller M, KERSTEN S. Comparative Analysis of Gene Regulation by the Transcription Factor PPAR $\alpha$  between Mouse and Human. Laudet V, editor. *PLoS ONE. Public Library of Science*; 2009 Aug 27;4(8):e6796.
  65. Kersten S. Peroxisome proliferator activated receptors and obesity. *European Journal of Pharmacology. Elsevier*; 2002 Apr 12;440(2-3):223–34.
  66. Escher P, Braissant O, Basu-Modak S, Michalik L, Wahli W, Desvergne B. Rat PPARs: quantitative analysis in adult rat tissues and regulation in fasting and refeeding. *Endocrinology*. 2001 Oct;142(10):4195–202.
  67. Ravnskjaer K, Frigerio F, Boergesen M, Nielsen T, Maechler P, Mandrup S. PPARdelta is a fatty acid sensor that enhances mitochondrial oxidation in insulin-secreting cells and protects against fatty acid-induced dysfunction. *J Lipid Res*. 2010 Jun;51(6):1370–9.
  68. Dressel U, Allen TL, Pippal JB, Rohde PR, Lau P, Muscat GEO. The peroxisome proliferator-activated receptor beta/delta agonist, GW501516, regulates the expression of genes involved in lipid catabolism and energy uncoupling in skeletal muscle cells. *Molecular Endocrinology*. 2003 Dec;17(12):2477–93.
  69. Leonardini A, Laviola L, Perrini S, Natalicchio A, Giorgino F. Cross-Talk between PPARgamma and Insulin Signaling and Modulation of Insulin Sensitivity. *PPAR Res. Hindawi*; 2009;2009(10):818945–12.
  70. Yang XY, Wang LH, Farrar WL. A Role for PPARgamma in the Regulation of Cytokines in Immune Cells and Cancer. *PPAR Res. Hindawi*; 2008;2008(4-5):961753–12.
  71. Palanker L, Tennessen JM, Lam G, Thummel CS. Drosophila HNF4 Regulates Lipid Mobilization and  $\beta$ -Oxidation. *Cell Metabolism. Cell Press*; 2009 Mar 4;9(3):228–39.
  72. Linden AG, Li S, Choi HY, Fang F, Fukasawa M, Uyeda K, et al. Interplay between ChREBP and SREBP-1c Coordinates Postprandial Glycolysis and Lipogenesis in Livers of Mice. *J Lipid Res. American Society for Biochemistry and Molecular Biology*; 2018 Jan 15;59(3):jlr.M081836–487.
  73. Miserez AR, Muller PY, Barella L, Barella S, Staehelin HB, Leitersdorf E, et al. Sterol-regulatory element-binding protein (SREBP)-2 contributes to polygenic hypercholesterolaemia. *Atherosclerosis. Elsevier*; 2002 Sep 1;164(1):15–26.

74. Ferre P, Foufelle F. SREBP-1c transcription factor and lipid homeostasis: clinical perspective. *Horm Res. Karger Publishers*; 2007;68(2):72–82.
75. Linden AG, Li S, Choi HY, Fang F, Fukasawa M, Uyeda K, et al. Interplay between ChREBP and SREBP-1c Coordinates Postprandial Glycolysis and Lipogenesis in Livers of Mice. *J Lipid Res. American Society for Biochemistry and Molecular Biology*; 2018 Jan 15;59(3):jlr.M081836–487.
76. Repa JJ, Liang G, Ou J, Bashmakov Y, Lobaccaro JM, Shimomura I, et al. Regulation of mouse sterol regulatory element-binding protein-1c gene (SREBP-1c) by oxysterol receptors, LXRalpha and LXRbeta. *Genes Dev. Cold Spring Harbor Laboratory Press*; 2000 Nov 15;14(22):2819–30.
77. Ye J, Kumanova M, Hart LS, Sloane K, Zhang H, De Panis DN, et al. The GCN2-ATF4 pathway is critical for tumour cell survival and proliferation in response to nutrient deprivation. *The EMBO Journal. EMBO Press*; 2010 Jun 16;29(12):2082–96.
78. Baird TD, Wek RC. Eukaryotic initiation factor 2 phosphorylation and translational control in metabolism. *Adv Nutr.* 2012 May 1;3(3):307–21.
79. Kilberg MS, Shan J, Su N. ATF4-dependent transcription mediates signaling of amino acid limitation. *Trends in Endocrinology & Metabolism.* 2009 Nov;20(9):436–43.
80. Zhao E, Ding J, Xia Y, Liu M, Ye B, Choi J-H, et al. KDM4C and ATF4 Cooperate in Transcriptional Control of Amino Acid Metabolism. *CellReports. The Authors*; 2016 Jan 26;14(3):506–19.
81. Avisar N, Shifan L, Ben-Dror I, Havazelet N, Vardimon L. A silencer element in the regulatory region of glutamine synthetase controls cell type-specific repression of gene induction by glucocorticoids. *J Biol Chem.* 1999 Apr 16;274(16):11399–407.
82. Ben-Dror I, Havazelet N, Vardimon L. Developmental control of glucocorticoid receptor transcriptional activity in embryonic retina. *Proceedings of the National Academy of Sciences.* 1993 Feb 1;90(3):1117–21.
83. Kersten S, Mandara S, Escher P, Gonzalez FJ, Tafuri S, Desvergne B, et al. The peroxisome proliferator-activated receptor  $\alpha$  regulates amino acid metabolism. *The FASEB Journal. Federation of American Societies for Experimental Biology*; 2001 Sep 1;15(11):1971–8.
84. Billin AN, Eilers AL, Coulter KL, Logan JS, Ayer DE. MondoA, a novel basic helix-loop-helix-leucine zipper transcriptional activator that constitutes a positive branch of a max-like network. *Molecular and Cellular Biology. American Society for Microbiology (ASM)*; 2000 Dec;20(23):8845–54.
85. Yamashita H, Takenoshita M, Sakurai M, Bruick RK, Henzel WJ, Shillinglaw W, et al. A glucose-responsive transcription factor that regulates carbohydrate metabolism in the liver. *Proceedings of the*

- National Academy of Sciences. National Academy of Sciences; 2001 Jul 31;98(16):9116–21.
86. Li MV, Chen W, Pongvarin N, Imamura M, Chan L. Glucose-mediated transactivation of carbohydrate response element-binding protein requires cooperative actions from Mondo conserved regions and essential trans-acting factor 14-3-3. *Molecular Endocrinology*. 2008 Jul;22(7):1658–72.
87. McFerrin LG, Atchley WR. A novel N-terminal domain may dictate the glucose response of Mondo proteins. Uversky VN, editor. *PLoS ONE*. Public Library of Science; 2012;7(4):e34803.
88. McFerrin LG, Atchley WR. Evolution of the Max and Mlx Networks in Animals. *Genome Biology and Evolution*. 2011 Aug 22;3(5461):915–37.
89. Imamura M, Chang BH-J, Kohjima M, Li M, Hwang B, Taegtmeier H, et al. MondoA deficiency enhances sprint performance in mice. *Biochem J*. 2nd ed. Portland Press Limited; 2014 Nov 15;464(1):35–48.
90. Jois T, Chen W, Howard V, Harvey R, Youngs K, Thalmann C, et al. Deletion of hepatic carbohydrate response element binding protein (ChREBP) impairs glucose homeostasis and hepatic insulin sensitivity in mice. *Molecular Metabolism*. Elsevier; 2017 Nov 1;6(11):1381–94.
91. Ahn B, Soundarapandian MM, Sessions H, Peddibhotla S, Roth GP, Li J-L, et al. MondoA coordinately regulates skeletal myocyte lipid homeostasis and insulin signaling. *Journal of Clinical Investigation*. 2016 Sep 1;126(9):3567–79.
92. Zhang P, Kumar A, Katz LS, Li L, Paulynice M, Herman MA, et al. Induction of the ChREBP $\beta$  Isoform Is Essential for Glucose-Stimulated  $\beta$ -Cell Proliferation. *Diabetes*. 2015 Dec;64(12):4158–70.
93. Li MV, Chang B, Imamura M, Pongvarin N, Chan L. Glucose-Dependent Transcriptional Regulation by an Evolutionarily Conserved Glucose-Sensing Module. *Diabetes*. 2006 Apr 26;55(5):1179–89.
94. Herman MA, Peroni OD, Villoria J, Schön MR, Abumrad NA, Blüher M, et al. A novel ChREBP isoform in adipose tissue regulates systemic glucose metabolism. *Nature*. Nature Publishing Group; 2012 Apr 10;484(7394):333–8.
95. Jing G, Chen J, Xu G, Shalev A. Islet ChREBP- $\beta$ ; is increased in diabetes and controls ChREBP- $\alpha$ ; and glucose-induced gene expression via a negative feedback loop. *Molecular Metabolism*. Elsevier GmbH; 2016 Dec 1;5(12):1208–15.
96. Davies MN, O'Callaghan BL, Towle HC. Activation and repression of glucose-stimulated ChREBP requires the concerted action of multiple domains within the MondoA conserved region. *American Journal of Physiology-Endocrinology and Metabolism*. 2010 Oct;299(4):E665–74.
97. Kawaguchi T, Takenoshita M, Kabashima T, Uyeda K. Glucose and cAMP regulate the L-type pyruvate kinase gene by phosphorylation/dephosphorylation of the carbohydrate response element

- binding protein. *Proceedings of the National Academy of Sciences*. 2001 Nov 20;98(24):13710–5.
98. Guinez C, Filhoulaud G, Rayah-Benhamed F, Marmier S, Dubuquoy C, Dentin R, et al. O-GlcNAcylation Increases ChREBP Protein Content and Transcriptional Activity in the Liver. *Diabetes*. 2011 Apr 27;60(5):1399–413.
99. Bricambert J, Miranda J, Benhamed F, Girard J, Postic C, Dentin R. Salt-inducible kinase 2 links transcriptional coactivator p300 phosphorylation to the prevention of ChREBP-dependent hepatic steatosis in mice. *Journal of Clinical Investigation*. 2010 Dec 1;120(12):4316–31.
100. Du J, Chen Q, Takemori H, Xu H. SIK2 Can be Activated by Deprivation of Nutrition and It Inhibits Expression of Lipogenic Genes in Adipocytes. *Obesity*. John Wiley & Sons, Ltd; 2008 Mar 1;16(3):531–8.
101. Fukasawa M, Ge Q, Wynn RM, Ishii S, Uyeda K. Coordinate regulation/localization of the carbohydrate responsive binding protein (ChREBP) by two nuclear export signal sites: Discovery of a new leucine-rich nuclear export signal site. *Biochemical and Biophysical Research Communications*. 2010 Jan;391(2):1166–9.
102. Nakagawa T, Ge Q, Powlosky R, Wynn RM, Veech RL, Uyeda K. Metabolite regulation of nucleo-cytosolic trafficking of carbohydrate response element binding protein (ChREBP): role of ketone bodies. *J Biol Chem*. American Society for Biochemistry and Molecular Biology; 2013 Aug 5;288(39):jbc.M113.498550–28367.
103. Ge Q, Nakagawa T, Wynn RM, Chook YM, Miller BC, Uyeda K. Importin-alpha protein binding to a nuclear localization signal of carbohydrate response element-binding protein (ChREBP). *J Biol Chem*. American Society for Biochemistry and Molecular Biology; 2011 Aug 12;286(32):28119–27.
104. Kooner JS, Chambers JC, Aguilar-Salinas CA, Hinds DA, Hyde CL, Warnes GR, et al. Genome-wide scan identifies variation in MLXIPL associated with plasma triglycerides. *Nat Genet*. Nature Publishing Group; 2008 Feb;40(2):149–51.
105. Nakayama K, Yanagisawa Y, Ogawa A, Ishizuka Y, Munkhtulga L, Charupoonphol P, et al. High prevalence of an anti-hypertriglyceridemic variant of the MLXIPL gene in Central Asia. *J Hum Genet*. Nature Publishing Group; 2011 Dec;56(12):828–33.
106. Barry WE, Thummel CS. The *Drosophila* HNF4 nuclear receptor promotes glucose-stimulated insulin secretion and mitochondrial function in adults. *eLife*. 2016 May 17;5:306.
107. Chavalit T, Rojvirat P, Muangsawat S, Jitrapakdee S. Hepatocyte nuclear factor 4 $\alpha$  regulates the expression of the murine pyruvate carboxylase gene through the HNF4-specific binding motif in its proximal promoter. *Biochimica et Biophysica Acta (BBA) - Gene Regulatory Mechanisms*. 2013 Oct;1829(10):987–99.

108. Pongvarin N, Chang B, Imamura M, Chen J, Moolsuwan K, Sae-Lee C, et al. Genome-Wide Analysis of ChREBP Binding Sites on Male Mouse Liver and White Adipose Chromatin. *Endocrinology*. 2015 Jun;156(6):1982–94.
109. Adamson AW, Suchankova G, Rufo C, Nakamura MT, Teran-Garcia M, Clarke SD, et al. Hepatocyte nuclear factor-4 $\alpha$  contributes to carbohydrate-induced transcriptional activation of hepatic fatty acid synthase. *Biochemical Journal*. Portland Press Limited; 2006 Oct 15;399(2):285–95.
110. Burke SJ, Collier JJ, Scott DK. cAMP opposes the glucose-mediated induction of the L-PK gene by preventing the recruitment of a complex containing ChREBP, HNF4 $\alpha$ , and CBP. *The FASEB Journal*. 2009 Sep;23(9):2855–65.
111. Meng J, Feng M, Dong W, Zhu Y, Li Y, Zhang P, et al. Identification of HNF-4 $\alpha$  as a key transcription factor to promote ChREBP expression in response to glucose. *Nature Publishing Group*. Nature Publishing Group; 2016 Mar 22;6:1–14.
112. Teesalu M, Rovenko BM, Hietakangas V. Salt-Inducible Kinase 3 Provides Sugar Tolerance by Regulating NADPH/NADP<sup>+</sup> Redox Balance. *Current Biology*. Elsevier Ltd; 2017 Feb 6;27(3):458–64.
113. Mattila J, Havula E, Suominen E, Teesalu M, Surakka I, Hynynen R, et al. Mondo-Mlx Mediates Organismal Sugar Sensing through the Gli-Similar Transcription Factor Sugarbabe. *CellReports*. The Authors; 2015 Oct 13;13(2):350–64.
114. Horton JD, Goldstein JL, Brown MS. SREBPs: activators of the complete program of cholesterol and fatty acid synthesis in the liver. *Journal of Clinical Investigation*. American Society for Clinical Investigation; 2002 May 1;109(9):1125–31.
115. Ferre P, Foufelle F. Hepatic steatosis: a role for de novo lipogenesis and the transcription factor SREBP - 1c. *Diabetes Obes Metab*. John Wiley & Sons, Ltd (10.1111); 2010 Oct 1;12(Pt 2):83–92.
116. Shimomura I, Shimano H, Horton JD, Goldstein JL, Brown MS. Differential expression of exons 1a and 1c in mRNAs for sterol regulatory element binding protein-1 in human and mouse organs and cultured cells. *Journal of Clinical Investigation*. American Society for Clinical Investigation; 1997 Mar 1;99(5):838–45.
117. Ido-Kitamura Y, Sasaki T, Kobayashi M, Kim H-J, Lee Y-S, Kikuchi O, et al. Hepatic FoxO1 Integrates Glucose Utilization and Lipid Synthesis through Regulation of ChREBP O-Glycosylation. *Kulkarni R, editor. PLoS ONE*. 2012 Oct 8;7(10):e47231–7.
118. Kibbe C, Chen J, Xu G, Jing G, Shalev A. FOXO1 Competes with Carbohydrate Response Element-binding Protein (ChREBP) and Inhibits Thioredoxin-interacting Protein (TXNIP) Transcription in Pancreatic Beta Cells. *J Biol Chem*. 2013 Aug 9;288(32):23194–202.

---

BIBLIOGRAPHY

---

119. Zhou J, Chng W-J. Roles of thioredoxin binding protein (TXNIP) in oxidative stress, apoptosis and cancer. *Mitochondrion*. Elsevier; 2013 May 1;13(3):163–9.
120. Hong K, Xu G, Grayson TB, Shalev A. Cytokines Regulate  $\beta$ -Cell TXNIP via Distinct Mechanisms and Pathways. *J Biol Chem*. American Society for Biochemistry and Molecular Biology; 2016 Feb 8;291(16):jbc.M115.698365–439.
121. Chau GC, Im DU, Kang TM, Bae JM, Kim W, Pyo S, et al. mTOR controls ChREBP transcriptional activity and pancreatic  $\beta$  cell survival under diabetic stress. *J Cell Biol*. 2017 Jul 3;216(7):2091–105.
122. Chaves VE, Frasson D, Martins-Santos MES, Navegantes LCC, Galban VD, Garófalo MAR, et al. Fatty acid synthesis and generation of glycerol-3-phosphate in brown adipose tissue from rats fed a cafeteria diet. *Can J Physiol Pharmacol*. 2008 Jul;86(7):416–23.
123. Adeva MM, Calviño J, Souto G, Donapetry C. Insulin resistance and the metabolism of branched-chain amino acids in humans. *Amino Acids*. 2012 Jul;43(1):171–81.
124. Fujita S, Rasmussen BB, Cadenas JG, Grady JJ, Volpi E. Effect of insulin on human skeletal muscle protein synthesis is modulated by insulin-induced changes in muscle blood flow and amino acid availability. *American Journal of Physiology-Endocrinology and Metabolism*. 2006 Oct;291(4):E745–54.
125. Proud CG. Regulation of protein synthesis by insulin. *Biochem Soc Trans*. Portland Press Limited; 2006 Apr;34(Pt 2):213–6.
126. Felig P, Marliss E, Pozefsky T, Cahill GF. Amino acid metabolism in the regulation of gluconeogenesis in man. *Am J Clin Nutr*. 1970 Jul;23(7):986–92.
127. Ruderman NB. Muscle amino acid metabolism and gluconeogenesis. *Annu Rev Med*. Annual Reviews 4139 El Camino Way, P.O. Box 10139, Palo Alto, CA 94303-0139, USA; 1975;26(1):245–58.
128. Ross BD, Hems R, Krebs HA. The rate of gluconeogenesis from various precursors in the perfused rat liver. *Biochemical Journal*. 1967 Mar;102(3):942–51.
129. Laffel L. Ketone bodies: a review of physiology, pathophysiology and application of monitoring to diabetes. *Diabetes Metab Res Rev*. John Wiley & Sons, Ltd; 1999 Nov;15(6):412–26.
130. Boyd ME, Albright EB, Foster DW, McGarry JD. In vitro reversal of the fasting state of liver metabolism in the rat. Reevaluation of the roles of insulin and glucose. *Journal of Clinical Investigation*. American Society for Clinical Investigation; 1981 Jul;68(1):142–52.
131. Geisler CE, Hepler C, Higgins MR, Renquist BJ. Hepatic adaptations to maintain metabolic homeostasis in response to fasting and refeeding in mice. *Nutrition & Metabolism* 2005 2:1. BioMed Central;

- 2016;13(1):62–13.
132. Dentin R, Benhamed F, Hainault I, Fauveau V, Foufelle F, Dyck JRB, et al. Liver-Specific Inhibition of ChREBP Improves Hepatic Steatosis and Insulin Resistance in ob/ob Mice. *Diabetes*. 2006 Jul 27;55(8):2159–70.
  133. Cairo S, Merla G, Urbinati F, Ballabio A, Reymond A. WBSR14, a gene mapping to the Williams-Beuren syndrome deleted region, is a new member of the Mlx transcription factor network. *Human Molecular Genetics*. 2001 Apr;10:617–27.
  134. Søberg S, Sandholt CH, Jespersen NZ, Toft U, Madsen AL, Holstein-Rathlou von S, et al. FGF21 Is a Sugar-Induced Hormone Associated with Sweet Intake and Preference in Humans. *Cell Metabolism*. Elsevier Inc; 2017 May 2;25(5):1045–6.
  135. Talukdar S, Owen BM, Song P, Hernandez G, Zhang Y, Zhou Y, et al. FGF21 Regulates Sweet and Alcohol Preference. *Cell Metabolism*. Elsevier; 2016 Feb 9;23(2):344–9.
  136. Brewer M, Lange D, Baler R, Anzulovich A. SREBP-1 as a Transcriptional Integrator of Circadian and Nutritional Cues in the Liver. *Journal of Biological Rhythms*. Sage PublicationsSage CA: Thousand Oaks, CA; 2016 Jun 29;20(3):195–205.
  137. Saely CH, Geiger K, Drexel H. Brown versus white adipose tissue: a mini-review. *GER. Karger Publishers*; 2012;58(1):15–23.
  138. Eissing L, Scherer T, Tödter K, Knippschild U, Greve JW, Buurman WA, et al. De novo lipogenesis in human fat and liver is linked to ChREBP- $\beta$  and metabolic health. *Nature Communications*. Nature Publishing Group; 2013 Feb 26;4(1):1528.
  139. Nuotio-Antar AM, Pongvarin N, Li M, Schupp M, Mohammad M, Gerard S, et al. FABP4-Cre Mediated Expression of Constitutively Active ChREBP Protects Against Obesity, Fatty Liver, and Insulin Resistance. *Endocrinology*. 2015 Nov;156(11):4020–32.
  140. Hurtado del Pozo C, Vesperinas-García G, Rubio M-Á, Corripio-Sánchez R, Torres-García AJ, Obregon M-J, et al. ChREBP expression in the liver, adipose tissue and differentiated preadipocytes in human obesity. *Biochimica et Biophysica Acta (BBA) - Molecular and Cell Biology of Lipids*. Elsevier; 2011 Dec 1;1811(12):1194–200.
  141. Witte N, Muenzner M, Rietscher J, Knauer M, Heidenreich S, Nuotio-Antar AM, et al. The Glucose Sensor ChREBP Links De Novo Lipogenesis to PPAR $\gamma$  Activity and Adipocyte Differentiation. *Endocrinology*. 2015 Nov;156(11):4008–19.
  142. Iizuka K, Wu W, Horikawa Y, Saito M, Takeda J. Feedback looping between ChREBP and PPAR $\alpha$  in the regulation of lipid metabolism in brown adipose tissues. *Endocrine Journal*. The Japan Endocrine Society; 2013;60(10):1145–53.

143. Katz LS, Xu S, Ge K, Scott DK, Gershengorn MC. T3 and Glucose Coordinately Stimulate ChREBP-Mediated Ucp1 Expression in Brown Adipocytes From Male Mice. *Endocrinology*. 2017 Oct 25;159(1):557–69.
144. Seale P, Conroe HM, Estall J, Kajimura S, Frontini A, Ishibashi J, et al. Prdm16 determines the thermogenic program of subcutaneous white adipose tissue in mice. *J Clin Invest*. American Society for Clinical Investigation; 2011 Jan;121(1):96–105.
145. Stanford KI, Middelbeek RJW, Townsend KL, An D, Nygaard EB, Hitchcox KM, et al. Brown adipose tissue regulates glucose homeostasis and insulin sensitivity. *J Clin Invest*. American Society for Clinical Investigation; 2013 Jan;123(1):215–23.
146. Soggia A, Flosseau K, Ravassard P, Szinnai G, Scharfmann R, Guillemain G. Activation of the transcription factor carbohydrate-responsive element-binding protein by glucose leads to increased pancreatic beta cell differentiation in rats. *Diabetologia*. Springer-Verlag; 2012 Jul 5;55(10):2713–22.
147. Gao N, Le Lay J, Qin W, Doliba N, Schug J, Fox AJ, et al. Foxa1 and Foxa2 Maintain the Metabolic and Secretory Features of the Mature  $\beta$ -Cell. *Molecular Endocrinology*. Oxford University Press; 2010 Aug 1;24(8):1594–604.
148. Metukuri MR, Zhang P, Basantani MK, Chin C, Stamateris RE, Alonso LC, et al. ChREBP Mediates Glucose-Stimulated Pancreatic  $\beta$ -Cell Proliferation. *Diabetes*. American Diabetes Association; 2012 May 11;61(8):DB\_110802–2015.
149. Schmidt SF, Madsen JGS, Frafjord KØ, Poulsen LLC, Salö S, Boergesen M, et al. Integrative Genomics Outlines a Biphasic Glucose Response and a ChREBP-ROR $\gamma$  Axis Regulating Proliferation in  $\beta$  Cells. *CellReports*. ElsevierCompany; 2016 Aug 30;16(9):2359–72.
150. Noordeen NA, Meur G, Rutter GA, Leclerc I. Glucose-Induced Nuclear Shuttling of ChREBP Is Mediated by Sorcin and Ca<sup>2+</sup> Ions in Pancreatic  $\beta$ -Cells. *Diabetes*. American Diabetes Association; 2012 Jan 31;61(3):DB\_101329–585.
151. Jones HF, Butler RN, Brooks DA. Intestinal fructose transport and malabsorption in humans. *American Journal of Physiology-Gastrointestinal and Liver Physiology*. American Physiological Society Bethesda, MD; 2011 Feb 1;300(2):G202–6.
152. Heizer WD, Southern S, McGovern S. The Role of Diet in Symptoms of Irritable Bowel Syndrome in Adults: A Narrative Review. *Journal of the American Dietetic Association*. Elsevier; 2009 Jul 1;109(7):1204–14.
153. Oh A-R, Sohn S, Lee J, Park J-M, Nam KT, Hahm K-B, et al. ChREBP deficiency leads to diarrhea-predominant irritable bowel syndrome. *Metabolism*. W.B. Saunders; 2018 Aug 1;85:286–97.

154. Zhao Q, Che X, Zhang H, Fan P, Tan G, Liu L, et al. Thioredoxin-interacting protein links endoplasmic reticulum stress to inflammatory brain injury and apoptosis after subarachnoid haemorrhage. *Journal of Neuroinflammation* 2017 14:1. BioMed Central; 2017 Dec 1;14(1):104.
155. Docherty JEB, Manno JE, McDermott JE, DiAngelo JR. Mio acts in the *Drosophila* brain to control nutrient storage and feeding. *Gene*. 2015 Sep 1;568(2):190–5.
156. Talukdar S, Zhou Y, Li D, Rossulek M, Dong J, Somayaji V, et al. A Long-Acting FGF21 Molecule, PF-05231023, Decreases Body Weight and Improves Lipid Profile in Non-human Primates and Type 2 Diabetic Subjects. *Cell Metabolism*. Cell Press; 2016 Mar 8;23(3):427–40.
157. Havula E, Teesalu M, Hyötyläinen T, Seppälä H, Hasygar K, Auvinen P, et al. Mondo/ChREBP-Mlx-Regulated Transcriptional Network Is Essential for Dietary Sugar Tolerance in *Drosophila*. Rulifson E, editor. *PLoS Genet*. 2013 Apr 4;9(4):e1003438–13.
158. Iizuka K, Miller B, Uyeda K. Deficiency of carbohydrate-activated transcription factor ChREBP prevents obesity and improves plasma glucose control in leptin-deficient (*ob/ob*) mice. *American Journal of Physiology-Endocrinology and Metabolism*. American Physiological Society; 2006 Aug 1;291(2):E358–64.
159. Sassu ED, McDermott JE, Keys BJ, Esmaili M, Keene AC, Birnbaum MJ, et al. Mio/dChREBP coordinately increases fat mass by regulating lipid synthesis and feeding behavior in *Drosophila*. *Biochemical and Biophysical Research Communications*. Academic Press; 2012 Sep 14;426(1):43–8.
160. Stoeckman AK, Ma L, Towle HC. Mlx Is the Functional Heteromeric Partner of the Carbohydrate Response Element-binding Protein in Glucose Regulation of Lipogenic Enzyme Genes. *J Biol Chem*. 2004 Apr 2;279(15):15662–9.
161. Ma L, Sham YY, Walters KJ, Towle HC. A critical role for the loop region of the basic helix-loop-helix/leucine zipper protein Mlx in DNA binding and glucose-regulated transcription. *Nucleic Acids Research*. 2006 Dec 7;35(1):35–44.
162. Zhang Y, Xie Y, Berglund ED, Coate KC, He TT, Katafuchi T, et al. The starvation hormone, fibroblast growth factor-21, extends lifespan in mice. *eLife*. eLife Sciences Publications Limited; 2012 Oct 15;1:e00065.
163. Kramer JM, Davidge JT, Lockyer JM, Staveley BE. Expression of *Drosophila* FOXO regulates growth and can phenocopy starvation. *BMC Dev Biol*. BioMed Central; 2003 Jul 5;3(1):5.
164. Iroz A, Montagner A, Benhamed F, Levavasseur F, Polizzi A, Anthony E, et al. A Specific ChREBP and PPAR $\alpha$  Cross-Talk Is Required for the Glucose-Mediated FGF21 Response. *CellReports*. ElsevierCompany; 2017 Oct 10;21(2):403–16.

165. Boynton S, Tully T. *latheo*, a new gene involved in associative learning and memory in *Drosophila melanogaster*, identified from P element mutagenesis. *Genetics*. Genetics Society of America; 1992 Jul;131(3):655–72.
166. Dauwalder B, Tsujimoto S, Moss J, Mattox W. The *Drosophila* takeout gene is regulated by the somatic sex-determination pathway and affects male courtship behavior. *Genes Dev*. 2002 Nov 15;16(22):2879–92.
167. Sepp KJ, Schulte J, Auld VJ. Peripheral Glia Direct Axon Guidance across the CNS/PNS Transition Zone. *Developmental Biology*. Academic Press; 2001 Oct 1;238(1):47–63.
168. Zhang X, Koolhaas WH, Schnorrer F. A versatile two-step CRISPR- and RMCE-based strategy for efficient genome engineering in *Drosophila*. *G3 (Bethesda)*. 2014 Oct 15;4(12):2409–18.
169. Böttcher R, Hollmann M, Merk K, Nitschko V, Obermaier C, Philippou-Massier J, et al. Efficient chromosomal gene modification with CRISPR/cas9 and PCR-based homologous recombination donors in cultured *Drosophila* cells. *Nucleic Acids Research*. Oxford University Press; 2014 Jun 17;42(11):e89–9.
170. Bellen HJ, Levis RW, Liao G, He Y, Carlson JW, Tsang G, et al. The BDGP gene disruption project: single transposon insertions associated with 40% of *Drosophila* genes. *Genetics*. Genetics; 2004 Jun;167(2):761–81.
171. Watanabe K, Toba G, Koganezawa M, Yamamoto D. Gr39a, a highly diversified gustatory receptor in *Drosophila*, has a role in sexual behavior. *Behav Genet*. 2011 Sep;41(5):746–53.
172. Zhang X, Ferreira IRS, Schnorrer F. A simple TALEN-based protocol for efficient genome-editing in *Drosophila*. *Methods*. Elsevier Inc; 2014 Aug 15;69(1):32–7.
173. Goran MI, Ulijaszek SJ, Ventura EE. High fructose corn syrup and diabetes prevalence: a global perspective. *Glob Public Health*. 2013;8(1):55–64.
174. Freeman CR, Zehra A, Ramirez V, Wiers CE, Volkow ND, Wang G-J. Impact of sugar on the body, brain, and behavior. *Front Biosci (Landmark Ed)*. 2018 Jun 1;23:2255–66.
175. Archer E. In Defense of Sugar: A Critique of Diet-Centrism. *Prog Cardiovasc Dis*. 2018 Jun;61(1):10–9.
176. Chong MF-F, Fielding BA, Frayn KN. Mechanisms for the acute effect of fructose on postprandial lipemia. *Am J Clin Nutr*. 2007 Jun;85(6):1511–20.
177. Baena M, Sangüesa G, Dávalos A, Latasa M-J, Sala-Vila A, Sánchez RM, et al. Fructose, but not glucose, impairs insulin signaling in the three major insulin-sensitive tissues. *Nature Publishing Group*. Nature Publishing Group; 2016 May 10;:1–15.

178. Janevski M, Ratnayake S, Siljanovski S, McGlynn MA, Cameron-Smith D, Lewandowski P. Fructose containing sugars modulate mRNA of lipogenic genes ACC and FAS and protein levels of transcription factors ChREBP and SREBP1c with no effect on body weight or liver fat. *Food Funct. The Royal Society of Chemistry*; 2012 Feb;3(2):141–9.
179. Rovenko BM, Kubrak OI, Gospodaryov DV, Yurkevych IS, Sanz A, Lushchak OV, et al. Restriction of glucose and fructose causes mild oxidative stress independently of mitochondrial activity and reactive oxygen species in *Drosophila melanogaster*. *Comp Biochem Physiol, Part A Mol Integr Physiol*. 2015 Sep;187:27–39.
180. Lushchak OV, Gospodaryov DV, Rovenko BM, Yurkevych IS, Perkhulya NV, Lushchak VI. Specific dietary carbohydrates differentially influence the life span and fecundity of *Drosophila melanogaster*. *J Gerontol A Biol Sci Med Sci*. 2014 Jan;69(1):3–12.
181. Blanc E, Alves RLAO-GC, Yang M, He X, Linford NJ, Hoddinott MP, et al. A holidic medium for *Drosophila melanogaster*. *Nature Methods. Nature Publishing Group*; 2013 Nov 17;1–8.
182. Lowe N, Rees JS, Roote J, Ryder E, Armean IM, Johnson G, et al. Analysis of the expression patterns, subcellular localisations and interaction partners of *Drosophila* proteins using a pigP protein trap library. *Development*. 2014 Oct 7;141(20):3994–4005.
183. Fraser RB, Waite SL, Wood KA, Martin KL. Impact of hyperglycemia on early embryo development and embryopathy: in vitro experiments using a mouse model. *Human Reproduction*. 2007 Oct 18;22(12):3059–68.
184. Jeong Y-S, Kim D, Lee YS, Kim H-J, Han J-Y, Im S-S, et al. Integrated Expression Profiling and Genome-Wide Analysis of ChREBP Targets Reveals the Dual Role for ChREBP in Glucose-Regulated Gene Expression. Ahuja SK, editor. *PLoS ONE*. 2011 Jul 21;6(7):e22544–15.
185. Noordeen NA, Khera TK, Sun G, Longbottom ER, Pullen TJ, da Silva Xavier G, et al. Carbohydrate-responsive element-binding protein (ChREBP) is a negative regulator of ARNT/HIF-1beta gene expression in pancreatic islet beta-cells. *Diabetes*. 2010 Jan;59(1):153–60.
186. Bartok O, Teesalu M, Ashwall-Fluss R, Pandey V, Hanan M, Rovenko BM, et al. The transcription factor Cabut coordinates energy metabolism and the circadian clock in response to sugar sensing. *The EMBO Journal*. 2015 Jun 2;34(11):1538–53.
187. Langmead B, Trapnell C, Pop M, Salzberg SL. Ultrafast and memory-efficient alignment of short DNA sequences to the human genome. *Genome Biol. BioMed Central*; 2009;10(3):R25.
188. Stark R, version GBRP, 2011. DiffBind: differential binding analysis of ChIP-Seq peak data. *bioconductorstatistiktu-dortmundde*
189. Shin H, Liu T, Manrai AK, Liu XS. CEAS: cis-regulatory element annotation system. *Bioinformatics*. 2009 Aug 18;25(19):2605–6.

BIBLIOGRAPHY

---

190. Bailey TL, Johnson J, Grant CE, Noble WS. The MEME Suite. *Nucleic Acids Research*. 2015 Jun 30;43(W1):W39–W49.
191. de Hoon MJL, Imoto S, Nolan J, Miyano S. Open source clustering software. *Bioinformatics*. 2004 Jun 12;20(9):1453–4.
192. Saldanha AJ. Java Treeview--extensible visualization of microarray data. *Bioinformatics*. 2004 Nov 22;20(17):3246–8.
193. Ishii S, Iizuka K, Miller BC, Uyeda K. Carbohydrate response element binding protein directly promotes lipogenic enzyme gene transcription. *Proceedings of the National Academy of Sciences*. National Academy of Sciences; 2004 Nov 2;101(44):15597–602.
194. Savla U, Benes J, Zhang J, Jones RS. Recruitment of Drosophila Polycomb-group proteins by Polycomblike, a component of a novel protein complex in larvae. *Development*. The Company of Biologists Ltd; 2008 Mar 1;135(5):813–7.
195. Ma L, Robinson LN, Towle HC. ChREBP•Mlx Is the Principal Mediator of Glucose-induced Gene Expression in the Liver. *J Biol Chem*. 2006 Sep 22;281(39):28721–30.
196. Glass CK, Rosenfeld MG. The coregulator exchange in transcriptional functions of nuclear receptors. *Genes Dev*. Cold Spring Harbor Lab; 2000 Jan 15;14(2):121–41.
197. McKenna NJ, Lanz RB, O'Malley BW. Nuclear Receptor Coregulators: Cellular and Molecular Biology. *Endocr Rev*. Oxford University Press; 1999 Jun 1;20(3):321–44.
198. Muse GW, Gilchrist DA, Nechaev S, Shah R, Parker JS, Grissom SF, et al. RNA polymerase is poised for activation across the genome. *Nat Genet*. 2007 Dec;39(12):1507–11.
199. Zeitlinger J, Stark A, Kellis M, Hong J-W, Nechaev S, Adelman K, et al. RNA polymerase stalling at developmental control genes in the Drosophila melanogaster embryo. *Nat Genet*. 2007 Dec;39(12):1512–6.
200. Guenther MG, Levine SS, Boyer LA, Jaenisch R, Young RA. A chromatin landmark and transcription initiation at most promoters in human cells. *Cell*. 2007 Jul 13;130(1):77–88.
201. Hsu HT, Chen HM, Yang Z, Wang J, Lee NK, Burger A, et al. Recruitment of RNA polymerase II by the pioneer transcription factor PHA-4. *Science*. American Association for the Advancement of Science; 2015 Jun 19;348(6241):1372–6.
202. Fuda NJ, Guertin MJ, Sharma S, Danko CG, Martins AL, Siepel A, et al. GAGA Factor Maintains Nucleosome-Free Regions and Has a Role in RNA Polymerase II Recruitment to Promoters. Lieb JD, editor. *PLoS Genet*. Public Library of Science; 2015 Mar 27;11(3):e1005108.
203. Rahl PB, Lin CY, Seila AC, Flynn RA, McCuine S, Burge CB, et al. c-Myc Regulates Transcriptional Pause Release. *Cell*. Cell Press; 2010 Apr

- 30;141(3):432–45.
204. Thompson KS, Towle HC. Localization of the carbohydrate response element of the rat L-type pyruvate kinase gene. *J Biol Chem.* 1991 May 15;266(14):8679–82.
205. Flavahan WA, Drier Y, Liau BB, Gillespie SM, Venteicher AS, Stemmer-Rachamimov AO, et al. Insulator dysfunction and oncogene activation in IDH mutant gliomas. *Nature.* Nature Publishing Group; 2016 Jan 7;529(7584):110–4.
206. Core LJ, Lis JT. Paused Pol II captures enhancer activity and acts as a potent insulator. *Genes Dev.* Cold Spring Harbor Lab; 2009 Jul 15;23(14):1606–12.
207. Jiang G, Nepomuceno L, Hopkins K, Sladek FM. Exclusive homodimerization of the orphan receptor hepatocyte nuclear factor 4 defines a new subclass of nuclear receptors. *Molecular and Cellular Biology.* 1995 Sep;15(9):5131–43.
208. Odom DT, Zizlsperger N, Gordon DB, Bell GW, Rinaldi NJ, Murray HL, et al. Control of pancreas and liver gene expression by HNF transcription factors. *Science.* 2004 Feb 27;303(5662):1378–81.
209. Martinez-Jimenez CP, Kyrmizi I, Cardot P, GONZALEZ FJ, Talianidis I. Hepatocyte nuclear factor 4 $\alpha$  coordinates a transcription factor network regulating hepatic fatty acid metabolism. *Molecular and Cellular Biology.* American Society for Microbiology Journals; 2010 Feb;30(3):565–77.
210. Schauer T, Schwalie PC, Handley A, Margulies CE, Flicek P, Ladurner AG. CAST-ChIP Maps Cell-Type-Specific Chromatin States in the *Drosophila* Central Nervous System. *CellReports.* Elsevier; 2013 Oct 17;5(1):271–82.
211. Yoshida M, Matsuda H, Kubo H, Nishimura T. Molecular characterization of *Tps1* and *Treh* genes in *Drosophila* and their role in body water homeostasis. *Nature Publishing Group.* Nature Publishing Group; 2016 Jul 21;:1–12.
212. Heidenreich S, Witte N, Weber P, Goehring I, Tolkachov A, Loeffelholz C, et al. Retinol saturase coordinates liver metabolism by regulating ChREBP activity. *Nature Communications.* Springer US; 2017 Aug 23;:1–10.
213. Chintapalli VR, Wang J, Dow JAT. Using FlyAtlas to identify better *Drosophila melanogaster* models of human disease. *Nat Genet.* Nature Publishing Group; 2007 Jun;39(6):715–20.
214. Knowles-Barley S, Longair M, Armstrong JD. BrainTrap: a database of 3D protein expression patterns in the *Drosophila* brain. *Database (Oxford).* 2010 Jul 6;2010:baq005.
215. Wang Z, Singhvi A, Kong P, Scott K. Taste representations in the *Drosophila* brain. *Cell.* 2004 Jun 25;117(7):981–91.

216. Sun F, Wang Y, Zhou Y, Van Swinderen B, Gong Z, Liu L. Identification of neurons responsible for feeding behavior in the *Drosophila* brain. *Sci China Life Sci. Science China Press*; 2014 Apr;57(4):391–402.
217. Thimman MS, Suzuki Y, Seugnet L, Gottschalk L, Shaw PJ. The Perilipin Homologue, Lipid Storage Droplet 2, Regulates Sleep Homeostasis and Prevents Learning Impairments Following Sleep Loss. Hardin PE, editor. *PLoS Biol.* 2010 Aug 31;8(8):e1000466–13.
218. Sonn JY, Lee J, Sung MK, Ri H, Choi JK, Lim C, et al. Serine metabolism in the brain regulates starvation-induced sleep suppression in *Drosophila melanogaster*. *Proceedings of the National Academy of Sciences.* 2018 Jul 3;115(27):7129–34.
219. Boitard C, Etchamendy N, Sauvant J, Aubert A, Tronel S, Marighetto A, et al. Juvenile, but not adult exposure to high-fat diet impairs relational memory and hippocampal neurogenesis in mice. *Hippocampus.* John Wiley & Sons, Ltd; 2012 Nov 1;22(11):2095–100.
220. Miyamoto T, Slone J, Song X, Amrein H. A Fructose Receptor Functions as a Nutrient Sensor in the *Drosophila* Brain. *Cell.* Elsevier Inc; 2012 Nov 21;151(5):1113–25.
221. Stranahan AM, Norman ED, Lee K, Cutler RG, Telljohann RS, Egan JM, et al. Diet-induced insulin resistance impairs hippocampal synaptic plasticity and cognition in middle-aged rats. *Hippocampus.* John Wiley & Sons, Ltd; 2008;18(11):1085–8.
222. Volkenhoff A, Weiler A, Letzel M, Stehling M, Klämbt C, Schirmeier S. Glial Glycolysis Is Essential for Neuronal Survival in *Drosophila*. *Cell Metabolism.* Elsevier Inc; 2015 Sep 1;22(3):437–47.
223. Thimman MS, Seugnet L, Turk J, Shaw PJ. Identification of Genes Associated with Resilience/Vulnerability to Sleep Deprivation and Starvation in *Drosophila*. *Sleep.* 2015 May 1;38(5):801–14.
224. Routh VH. Glucose-sensing neurons: are they physiologically relevant? *Physiol Behav.* 2002 Jul;76(3):403–13.
225. Burdakov D, Luckman SM, Verkhatsky A. Glucose-sensing neurons of the hypothalamus. *Philos Trans R Soc Lond, B, Biol Sci.* 2005 Dec 29;360(1464):2227–35.
226. Jois T, Howard V, Youngs K, Cowley MA, Sleeman MW. Dietary Macronutrient Composition Directs ChREBP Isoform Expression and Glucose Metabolism in Mice. Guillou H, editor. *PLoS ONE.* Public Library of Science; 2016;11(12):e0168797.
227. Mattila J, Hietakangas V. Regulation of Carbohydrate Energy Metabolism in *Drosophila melanogaster*. *Genetics.* 2017 Dec;207(4):1231–53.